Effects of Changes in Dietary Phosphate on Renal Gene Expression

Dissertation

zur

Erlangung der Naturwissenschaftlichen Doktorwürde

(Dr. sc. nat.)

Vorgelegt der Mathematisch-naturwissenschaftlichen Fakultät

der Universität Zürich

von

Alexander Peter Atanassoff

aus Deutschland

Promotionskomitee:

Prof. Dr. Carsten A. Wagner (Vorsitz)

Prof. Dr. Jürg Biber (Betreuer)

Dr. Natividad Hernando

Dr. Joseph Caverzasio

Zürich, 2011

”*Diese Arbeit widme ich meinen Eltern, Peter und Aurora, für Ihre bedingungslose Liebe und Unterstützung während allen guten und schlechten Zeiten in meinem Leben.“*

"We can't solve problems
by using the same kind of thinking we
used when we created them."
Albert Einstein

Table of Contents

Zusammenfassung

Inorganische Phosphathomöostase und ihre Regulation ist prinzipiell ein Phänomen, das in der Niere kontrolliert wird. Der Natrium-Phosphatkotransporter NaPi-2a, in der apikalen Zellmembran des proximalen Tubulus, wirkt dabei entscheidend mit. Phosphatdefizite stimulieren die Expression des Na/Pi-Kotransporters in der Niere hauptsächlich auf Ebene des Proteins. Dies ist notwendig um normale Phosphatwerte im Plasma wiederherzustellen.

Mit Hilfe von RNA Genexpressionsstudien (Mikroarray Analyse) wurden Gene untersucht, die in der Niere durch verschiedene Phosphatdiäten reguliert werden. Hierzu wurden die Effekte einer fünftägigen und später vierzehnstündigen Spezialdiät mit reduziertem Phosphatgehalt (LPD, 0.1%) relativ zu einer Phosphatüberdosis (HPD, 1.2%) an Wildtypmäusen (C57BL/6) untersucht. Dazu wurden die Nieren entfernt, RNA isoliert und auf Genchips hybridisiert. Anschliessend wurden die Daten ausgewertet und die Genveränderungen zusätzlich mit quantitativer Real Time PCR (RT-qPCR) untersucht. Bisherige Analysen ergaben, dass die Expression vieler Gene, die im Bereich des Energiehaushaltes, wie z. B. Glukosehaushalt und der oxydativen Phosphorylierung, eine Rolle spielen, nach fünf Tagen jedoch nicht nach vierzehn Stunden stark gehemmt wurden.

In der Niere wird die Expression der 1α,25-$(OH)_2$-Vitamin D_3 Hydroxylase (1α-Hydroxylase) durch den Phosphathaushalt im Organismus reguliert. Schon nach wenigen Tagen ist ein Unterschied in 1α-hydroxylase mRNA Mengen zwischen LPD und HPD Mäusen nachweisbar. In dieser Studie war die Menge der 1α-Hydroxylase mRNA nach fünf Tagen LPD im Vergleich zu HPD zehn Mal höher.

Des weiteren wurde in dieser Studie ein neuer SLC Transporter, SLC16A14/MCT14, entdeckt, der durch LPD nach fünf Tagen reguliert wurde. Diese Beobachtung war bis zu diesem Zeitpunkt mit Phosphat nicht in Verbindung gebracht worden.

Da die Wahrscheinlichkeit grösser ist auf Gene zu stossen, die direkt durch frühe Phosphatdefizite beeinflusst werden, wurden verschiedene Zeitpunkte nach einer Phosphatdiät gewählt (4, 8, und 14 Stunden) und Mäusenieren auf RNA-Ebene untersucht. Die mRNA der 1α-Hydroxylase und SLC16A14/MCT14 wurde mit Hilfe

von RT-qPCR quantifiziert. Die Resultate ergaben, dass sich die 1α-Hydroxylase mRNA nach keinem der drei Zeitpunkte signifikant änderte. Für SLC16A14/MCT14 hingegen, wurde nach vierzehn Stunden eine vierfache Hemmung gemessen. Aus diesem Grund wurde eine neue Mikroarrayanalyse nach vierzehn Stunden Phosphatdefizit durchgeführt. Diesmal konnten keine Gene gefunden werden, die Teil der Atmungskette sind, auch solche nicht, die starken Einfluss auf den Energiehaushalt haben. Jedoch wurden drei Gene (PEPCK, SNAT3, Glud1) der Gluconeogenese/Ammoniakgenese identifiziert, die in der Regulierung des Säure-Basen Metabolismus eine wichtige Rolle spielen. Zudem hatte eine vierzehnstündige Phosphatreduzierung eine hemmende Wirkung auf die Gene HMGCS, HMGCR, und Cyp51, die mit der Synthese des Cholesterins in Verbindung gebracht werden. Es ist bekannt, dass der Anteil von Cholesterin in der Zellmembran die Fluidität dieser beeinflusst. Auch gibt es Untersuchungen die beweisen, dass die Funktion von NaPi-2a sowohl direkt als auch indirekt durch Cholesterin beeinflusst wird. Des weiteren wurden Gene gefunden, die beim Zelltod und der Zellalterung (z.B. p53bp2, p21) eine wichtige Rolle spielen, wie auch Gene (z.B. EEA1) die für den frühen endosomalen Transport verantwortlich sind. Auch wurden Gene reguliert, die allerdings schon in anderen Organen identifiziert wurden, aber noch weitgehend unerforscht sind im Zusammenhang mit Phosphathomöostase oder des NaPi-Kotransporters. Einige dieser Gene sind: Cholecystokinin A Rezeptor (CCKAR), Osteomodulin, FK506 binding protein (FK506BP), and Acyl-CoA thioesterase 1 (Acot1). Die Funktion der Proteine vieler dieser Gene ist bisher leider nicht bekannt (z.B. Osteomodulin) und eine Verbindung zur Phosphathomöostase und Pi reabsorption nicht dokumentiert. Die Mehrzahl der Gene die nach fünftägiger Phosphatmangelphase reguliert wurden, konnten nicht nach vierzehn Stunden Phosphatmangels nachgewiesen werden. Dies könnte möglicherweise auf zwei verschiedene Mechanismen deuten, die den Phosphathaushalt während einer Phosphatmangelphase regulieren die zeitlich bestimmt wird.

Der zweite Teil dieser Dissertation befasst sich mit der Charakterisierung des Monocarboxylattransporters SLC16A14/MCT14, der im Gefolge beider Mikroarrayanalysen auffällig war. Dieser Transporter wurde bei Wildtypmäusen

mehrmals auf der Ebene des Proteins und der mRNA untersucht. Erste Resultate ergaben dass durch Phosphatentzug die relative Menge des SLC16A14/MCT14 Proteins und der mRNA in der Niere verändert werden kann. Erste Bestimmungen ergaben, dass SLC16A14/MCT14 im dicken, ausfteigendem Teil der Henle Schleife des Nephrons exprimiert wird und durch Phosphatdiäten nach vierzehn Stunden und fünf Tagen im proximalen Tubulus reguliert wird. SLC16A14/MCT14 wurde durch eine cRNA Injektion in Froscheier (*Xenopus laevis* Oozyten) exprimiert um anschliessend erste Transportstudien durchzuführen. Bisherige Resultate deuten darauf hin, dass SLC16A14/MCT14 Aminosäuren wie L-Alanin, L-Methionin und L-Glutamat transportiert. Weitere Transportstudien wären sinnvoll um die Kinetik des SLC16A14/MCT14 zu entschlüsseln, um dadurch auch den Zusammenhang mit der Phosphathomöostase zu verstehen.

Phosphatdiäten verursachen, wie in dieser Studie untersucht wurde, verschiedene Anpassungsmechanismen in der Niere. Mehrere metabolische Bahnen (Pathways) wurden dabei genauer untersucht, in denen Gene vorkamen, die für die Phosphathomöostase bisher noch keine bekannte Rolle spielten, und womöglich durch diese Studie neues Interesse geweckt haben. Da nach fünf Tagen Phosphatmangels eine grosse Anzahl von Genen in der Atmungskette ein möglicher Hinweis auf Störungen des Energiehaushaltes hinweist, ist es auch weiter wahrscheinlich Gene vorzufinden die nicht von Phosphat direkt beeinflusst wurden. Die meisten Gene die nach einer fünftägigen Phosphatmangelphase beeinflusst wurden, nicht aber nach 14 Stunden, deuten auf eine kurzzeitige Regulierung einiger metabolischer Bahnen (z. B. Cholesterinsynthese, Säure/Basenhausalt). Allerdings wurden einige Gene, die nach beiden Zeitperioden bestimmt wurden, in der vorliegenden Untersuchung auch in gemeinsame metabolische Bahnen eingeteilt werden können. Ob diese Bahnen einen Zusammenhang mit NaPi-2a haben ist noch ausstehend.

Die Konsequenzen einer Phosphatmangelernährung im Organismus wirken sich auf die Expression von bestimmten Genen der Niere aus und sind offenbar zeitbedingt. Die Anzahl und Spezifität der Gene während einer akuten Phophatmangelphase unterscheidet sich dabei wesentlich von einer chronischen Phase. Einen Hinweis für eine Veränderung auf Genexpressionsebene durch Phosphat könnte SLC16a14

sein, da schon frühzeitig und über länger Zeit, eine reduzierte mRNA nachgewiesen wurde die zusätzlich auf Ebene des Proteins bestimmt werden konnte.

Summary

Phosphate (Pi) homeostasis and regulation is mainly realized in the kidney by the proximal tubules. The abundance of sodium Pi cotransporters, in particular NaPi-2a, determines the reabsorption rate of Pi. Therefore, low Pi-diet intake can directly affect the NaPi-2a abundance in the apical membrane of the renal proximal tubule by increasing the presence of the Na/Pi-cotransporter in order to restore normal Pi serum values.

In this study, a change in renal gene expression was investigated upon administering low (LPD) and high Pi-diets (HPD) to mice (C57BL/6). After 5 days ("chronic") Pi-diets, isolated renal RNA was hybridized to mouse whole genome chips, and data was evaluated and analyzed. Results showed, as expected, an increase in 1α,25-$(OH)_2$-Vitamin D_3 hydroxylase (1α-hydroxylase) mRNA levels (10-fold). This compensation is well known to occur after a long term Pi deprivation. Also, an unknown SLC transporter (SLC16A14/MCT14) was found to be down-regulated 4-fold. However, a large number of regulated genes were found to be part of the energy metabolism (respiratory chain, glycolysis) indicating a possible impact on fuel mechanisms that are inhibited by LPD. Eventually, this effect may not be caused directly by LPD but rather by epiphenomenons that influence the energy state of the organism and therefore might lead to false interpretations related to hypophosphatemia. In order to investigate genes that directly act upon dietary Pi restriction, it was suggested to repeat microarray analysis at an earlier time point. Thus, different time points were initially investigated by RT-qPCR for 1α-hydroxylase and SLC16A14/MCT14. Interestingly, no change in RNA levels was detected after 4 and 8 hours for either gene. Also, no change of 1α-hydroxylase was observed 14 hours after administering the LPD, but SLC16A14/MCT14 was down-regulated strongly (4 fold) as observed previously after a "chronic" LPD. Therefore an "acute" time point for the administration of a LPD (in relation to HPD) was set to 14 hours based on SLC16A14/MCT14 regulation and independent of the Vitamin D response. Results obtained by microarray analysis revealed a number of genes grouped in cholesterol biosynthesis and lipid metabolism. Since cholesterol content in the cell

membrane regulates the fluidity of the membrane and is known to directly and indirectly affect the activity of NaPi-2a, it was not further surprising to find various genes involved in this pathway. Other genes were coding for Heat Shock Proteins (HSP), known as intracellular stress responders. These were further found to be involved in regulating p53bp2 and p21 activity that are known to act during apoptosis and senescence. Moreover, a few genes (e.g. EEA1) were grouped in early endosomal trafficking. When microarray data was compared, a number of genes were also found to be significantly regulated during both periods (14 hours and 5 days). However, these genes had not been previously related to dietary Pi changes, nor had they been linked to the regulation of NaPi-2a abundance at the renal brush border membrane (BBM). Among these genes are Cholecystokinin A Receptor (CCKAR), Osteomodulin, FK506 binding protein (FKBP51), and Acyl-CoA thioesterase 1 (Acot1). Unfortunately many of these have not been characterized thoroughly (e.g. Osteomodulin) nor have they been related previously to renal Pi reabsorption or Pi homeostasis. Many genes regulated after a long term (5 days) Pi deprivation were not found to be regulated after 14 hours of LPD intake, indicating two different mechanisms involved during LPD adaptation.

The second half of this thesis focuses on the characterization of the SLC16A14/MCT14 transporter, a member of the monocarboxylate family. It was shown to be a stable dietary Pi responder after a LPD, relative to HPD, administration. A time period of 14 hours and 5 days of LPD, caused a decrease in abundance of the SLC16A14/MCT14 transporter in the kidney on RNA and protein level. A first approach using *in-situ* hybridization studies were not concluding. However, having raised and purified an antibody for SLC16A14/MCT14, and using immunohistochemical approaches on wild type mice (C57BL/6), SLC16A14/MCT14 protein was localized apically in the thick ascending limb (TAL) and the area close to the macula densa. Interestingly, wild type mice that were submitted to a LPD presented, as shortly as 14 hours and thereafter, almost no transporter in the kidney. In contrast, those mice that received a HPD presented the transporter in the proximal tubule and some in the TAL. This was consistent in mice that received a chronic LPD and HPD for 5 days.

A myc-tagged SLC16a14 transporter was expressed in *Xenopus laevis* oocytes and successfully localized at the plasma membrane. Preliminary transport studies using radioactively labeled substrates indicate that SLC16A14/MCT14 carries amino acids (L-Alanine, L-Methionine and L-Glutamate).

Regulatory mechanisms that act in response to dietary Pi are distinct after 14 hours and 5 days. New pathways were studied that included many genes which had not been previously involved in the regulation of renal Pi. Pi homeostasis may harvest more regulatory mechanisms than known to date. This study provides insights into these mechanisms and implicates genes that may play a more important role in the near future than previously assumed. Eventually, this may be important to understand physiological responses in the context of the Na/Pi-cotransport mechanism. It would also be of interest to understand the role of SLC16A14/MCT14 during “acute” and “chronic” adaptation to changes in dietary Pi. Therefore, it would be necessary to understand SLC16A14/MCT14 kinetics. More studies are required to elucidate the mechanisms of adaptation in response to dietary Pi.

The effects of Pi deficiency on renal gene expression differ between an “acute” and a “chronic” phase. This may indicate a change in renal behavior according to time dependent Pi deficiency in the organism. SLC16a14 was shown in this study to respond after a short- and a long-term Pi deficiency and may therefore be considered as a robust indicator of Pi homeostasis.

Introduction

For all organisms, ranging from uni- to pluricellular, phosphorus is a requisite for life. It plays a major role in plasma membrane formation, cell energy metabolism, enzymatic reactions and cell signaling [1]. When the evolutionary step was made towards multicellular complex organisms, phosphorus took over additional functions, such as maintaining acid-base homeostasis and the formation of bone tissue. In mammals, the kidney is a key regulatory organ to maintain constant levels of phosphate in the blood serum.

The Kidney

The kidney, a paired, bean-shaped organ serves three major functions in the living organism: First, it clears the body from toxic metabolic waste products. Second, it plays a central role in regulating fluid status, electrolyte balance and acid-base homeostasis in the blood. Third, it is an endocrine system, involved in releasing hormones to control calcium metabolism (Vitamin D_3), blood flow, blood pressure (renin) and erythropoiesis (erythropoyetin).

Human kidneys, localized behind the peritoneum on each side of the vertebral column, have a weight of approximately 150 g each (Figure 1). A thin, fibrous, non-distensible capsule of connective tissue covers the kidney. In the middle of its concave shape is an opening called hilus. At this point, the renal artery enters and the renal vein and ureter exit. This opening is also shared by the lymphatic vessels and nerves that also pass through. A cross section of the organ reveals a cortex with a granular aspect due to the presence of glomeruli and highly convoluted epithelial structures called tubules. More central, the medulla presents no glomeruli, but rather parallel tubular structures and small blood vessels.

The Renal Blood Flow (RPF) is the amount of blood delivered to the kidney per unit time (in a 70 kg human 1 L/min or 20% of the cardiac output). A high blood flow is necessary for kidney function in order to receive a good supply of oxygen and

nutrients, but especially to form the ultra-filtrate by the glomeruli. Each substance cleared in the kidney has a certain filtration characteristic. Clearance provides information on how well a solute is cleared from the plasma, but this alone cannot provide information on precise sites and mechanisms of the handling of a given solute. Thus, the integration of glomerular filtration, tubular reabsorption, and tubular secretion determines the clearance of a solute. Finally, nutrients and other compounds are reabsorbed into blood. Fine tuning of secretion and reabsorption determines how much of a given metabolite is finally excreted.

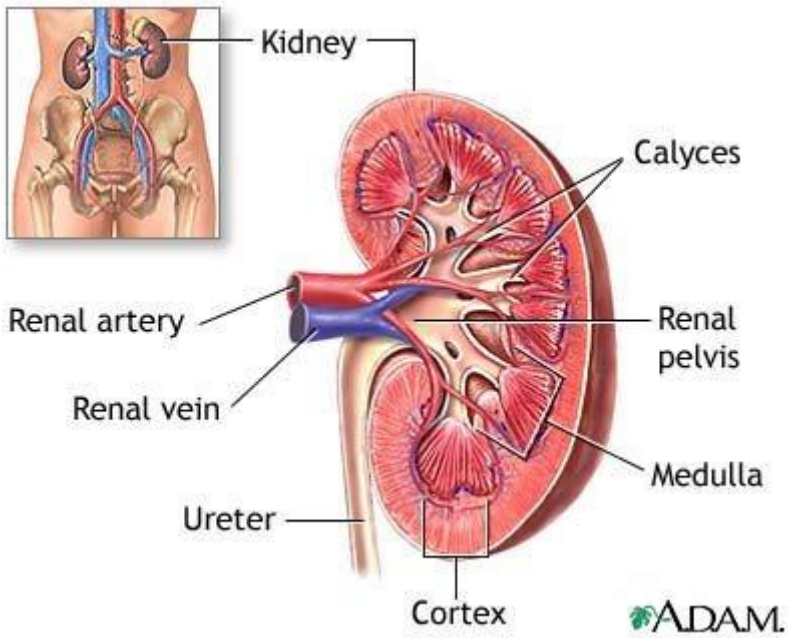

Figure 1. The kidney is localized in the retro-peritoneum. It is subdivided into a cortex and medullary region. These sections have specific functions such as filtration and reabsorption, respectively. The medulla uses an interstitial hyperosmotic condition to form concentrated urine by reabsorbing water. Image taken from www.mdconsult.com.

The Nephron is the functional unit of the kidney

In each human kidney an epithelial unit structure, the nephron, is present about 1 million times. Each nephron is independent until the point where it merges into the collecting tubule (Figure 2).

From a morphological point of view the nephron serves certain functions, depending whether the urinary filtrate passes through juxtamedullary nephrons, situated in the cortex close to the outer medulla, or in cortical nephrons, located in the outer cortex. Juxtamedullary nephrons possess relatively long loops that extend far into the medulla, whereas cortical nephrons have rather short loops. The nephron can be subdivided into various sections (Figure 2); the glomerulus (Glo), the proximal tubule (PT), the loop of Henle (LoH), the thick ascending limb (TAL), the distal tubule and finally the collecting duct (CD), where connecting tubules of various nephrons merge together. It is the integration of all subunits of the nephron that finally determines how a solute is excreted in the urine. The epithelial cells of the tubules are held together by tight junctions, creating a limited trans-epithelial passage. This epithelia becomes tighter the further the tubule extends towards the end of the nephron.

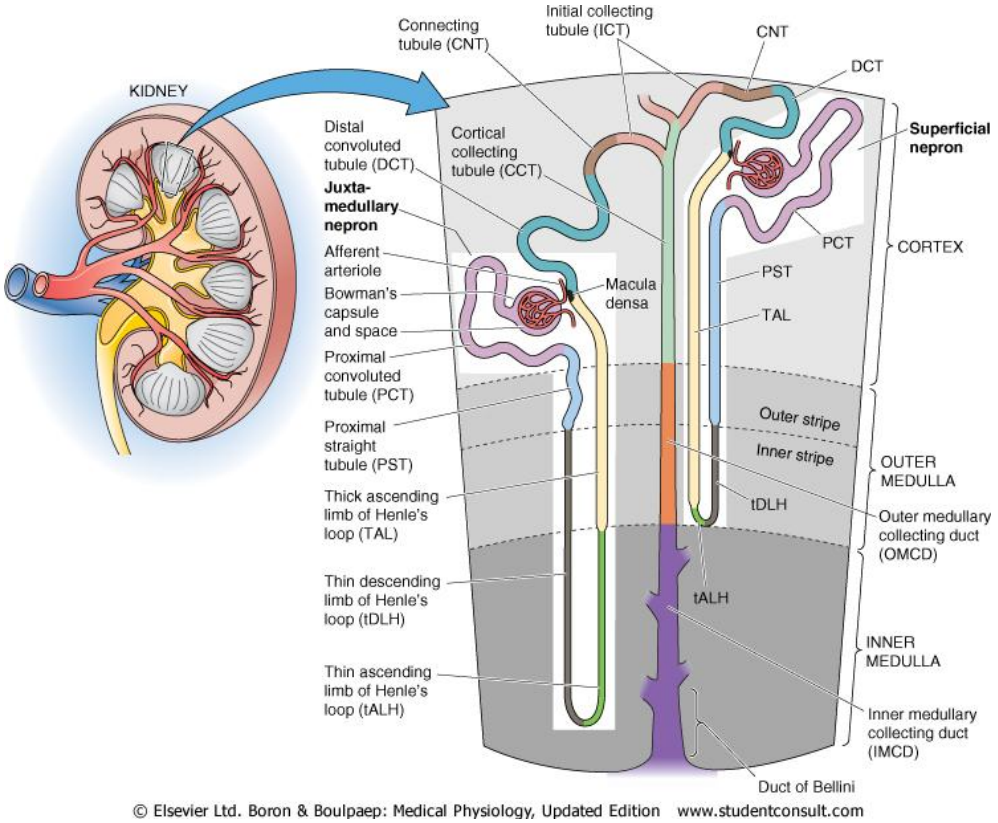

Figure 2. The functional unit of the kidney is the nephron. There are two types of nephrons both localized in the cortex: juxtamedullary nephrons, situated in the cortex at the border of the outer medulla, and superficial nephrons in the cortex, presenting the majority of the nephrons in the kidney. Superficial nephrons can also be identified by their relative short thin loop of Henle and their pronounced length of thick ascending limb when compared to the juxtamedullary nephrons.

The Glomerulus and the juxtaglomerular apparatus

The nephron contains two important functional sites, the glomerulus (Figure 3 A), where blood plasma is filtered, and the tubule, which is lined by epithelia that reabsorb and secrete solutes. As mentioned before, a high renal blood flow allows the nephron to create an ultra-filtrate at the level of the glomerulus. At this point, the capillary tufts that originate from the renal artery, pass into Bowman's capsule. Here, a filtration barrier consisting of capillary endothelium, glomerular basement membrane, and podocyte foot processes allow the blood plasma to pass from the vascular into the tubular system. This barrier is covered with negatively charged proteoglycans and glycoproteins that help to restrict filtration of negatively charged ions and proteins. As blood plasma undergoes the process of ultra-filtration, the

concentration of the primary filtrate of solutes (e.g. amino acids, sugars, and electrolytes) reflects the concentration in the plasma.

Two parameters can affect the process of ultra-filtration, the blood pressure and the filtration barrier. When the blood pressure drops, the process of filtration will reduce itself, unless compensatory mechanisms (e.g. vasoconstriction) occur via the baroreceptors located in the afferent arteriole. The filtration barrier, when damaged, can affect renal handling of metabolites (Figure 3 B).

The juxtaglomerular apparatus (JGA) attaches close to the glomerulus at the height of the TAL. The JGA is formed by the macula densa and the granular cells. The macula densa is a region of specialized epithelial cells of the thick ascending limb (Figure 3 A). Here, the afferent arterioles have specialized smooth muscle cells called granular cells or juxtaglomerular cells. By storing and releasing renin, they control, via a complex feedback mechanism, not only the renal blood flow and filtration rate, but also indirectly sodium balance and systemic blood pressure.

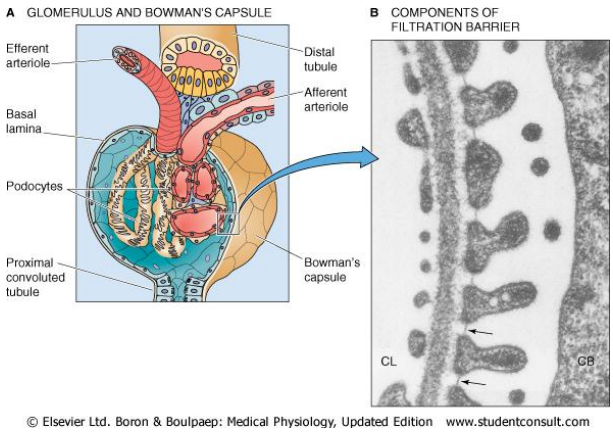

Figure 3. **(A)** Detailed scheme of the glomerulus. It filters the plasma from the afferent arteriole and releases its primary filtrate into Bowman's space. A tight regulation of water balance and blood flow is controlled at the level of the macula densa. Here, renin is released by the granular cells of the smooth muscle. **(B)** The filtration barrier is a structure, where vascular and epithelial components combine to form the site of ultra-filtration provided by a high blood flow. It is a tight filtration membrane composed of capillary endothelium, glomerular basement membrane, and podocyte foot processes.

The Proximal Tubule

The proximal tubule (PT) can be subdivided into two segments, the proximal convoluted tubule (PCT) and the proximal straight tubule (PST) (Figure 4 A & B).

These can also be classified in S1, S2, and S3 segments. The PCT is the S1 segment together with the first half of the S2 section. The PST contains the second half of the S2 section ending in the S3 segment. The PT is the first epithelial structure of the nephron that participates in processing of primary urine. Apart from water, large amounts of solutes (e.g. glucose, Pi, amino acids, and bicarbonate) are reabsorbed along the PT. The apical site of the proximal tubular cell is characterized by numerous microvilli endowed with various transporters. This enlargement of the apical surface correlates with the main function of the nephron segment, namely to reabsorb the bulk of filtered fluid and solutes. At this stage, two thirds of the entire filtered fluid is reabsorbed. Cell complexity progressively declines from S1 to S3 segments, correlating with a gradual decrease of reabsorptive rates along the tubule. On the basolateral side, there are numerous interdigitations that come in close contact with the blood vessels. Various mitochondria are in close contact with the basolateral membrane. The number of mitochondria decreases as cell complexity diminishes from S1 to S3 segment. The lateral membranes of the PT are characterized by various interdigitations.

The Loop of Henle

This structure continues from the last part of the PT further into the medulla of the kidney (Figure 4 C, D & E). The thin descending- and ascending-limbs have a less complex cellular structure than the PT. They contain fewer mitochondria and little cell membrane amplification. They are poorly developed in the superficial nephrons, but they play a more important role in the long loops of juxtamedullary nephrons. The epithelial cells, extending into the thick ascending limb (TAL) up to the macula densa, are characterized by various invaginations containing a large number of mitochondria at their basolateral cell membrane. These physiological adapted cells are responsible for creating a hyperosmotic environment in the renal medullary interstitium.

The Distal Tubule and the Collecting Duct

Based on ultra-structural studies, the “classical distal tubule“, starting at the macula densa, can be distinguished in a distal convoluted tubule (DCT), the connecting tubule (CNT) and the initial collecting tubule (ICT) (Figure 4 F, G, & H).

The DCT has very similar cell structure as the TAL and ends at the transition point to the CNT. The CNT consists of two types of cells which exert specific functions; the connecting tubule cells and the intercalated cells. The two segments that follow are the initial collecting tubule (ICT) and the cortical collecting tubule (CCT) (Figure 4 I), before and after the confluence of two nephrons, respectively. They contain two cell populations; the intercalated and the principal cells. The intercalated cells contribute to acid-base transport (H^+/HCO_3^-) and potassium (K^+) reabsorption. The principal cells, making up two thirds of the cell population in the cortical collecting tubule, secrete K^+, and reabsorb Na^+, Cl^- and water.

Towards the end of the collecting duct, cells become progressively taller and the number of intercalated cells diminishes. In this segment, the cells continue the transport of electrolytes and the hormonally regulated mechanism of water and urea transport. Towards the end of the duct, by the inner medullary collecting duct, the cells join the papillary ducts and become extremely tall (Figure 4 J & K).

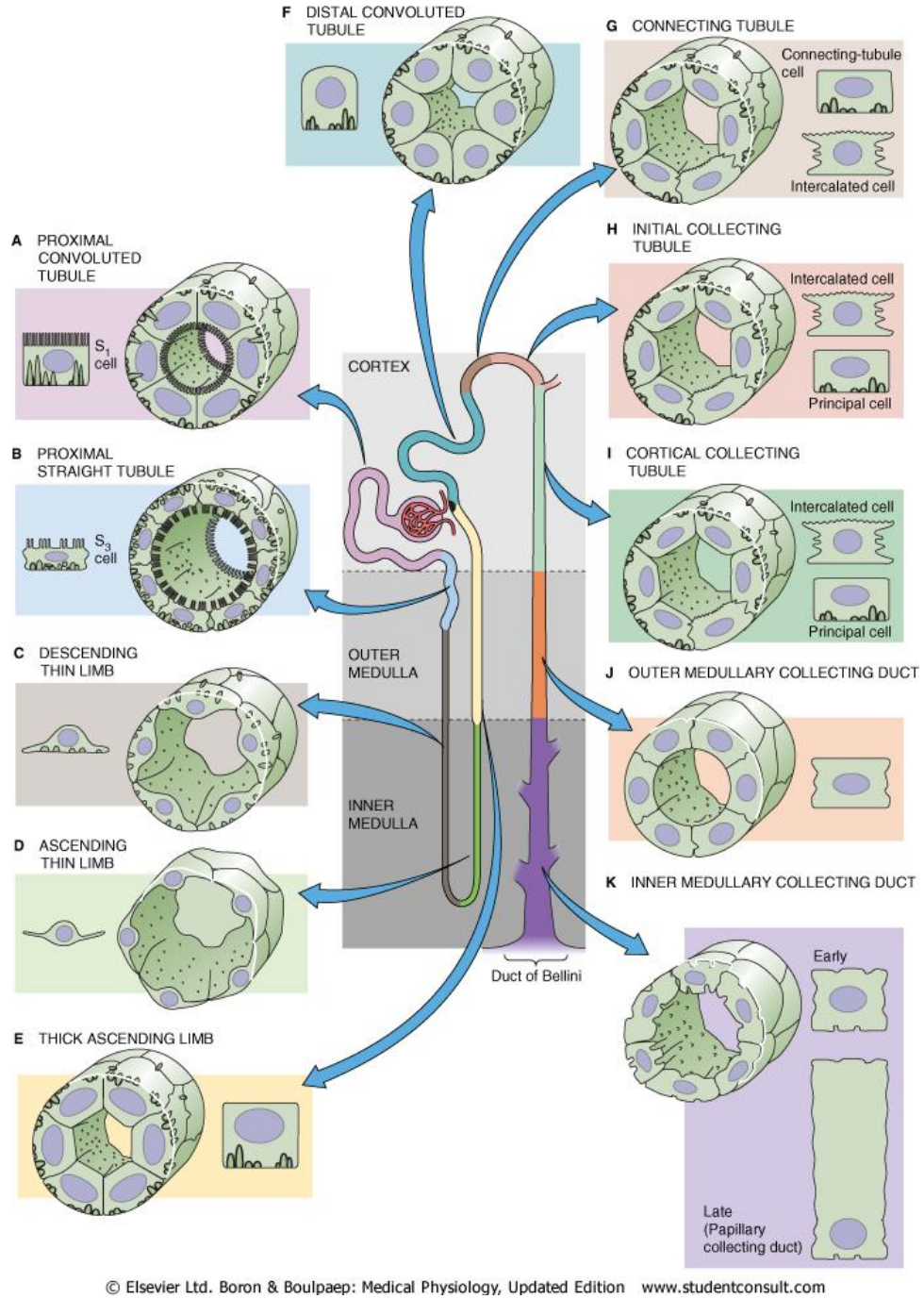

Figure 4. The nephron is a combined structure of different functional cells. The proximal tubule (PT) has a complex brush border membrane (BBM) that starts at the **(A)** proximal convoluted tubule (PCT) and merges into **(B)** the proximal straight tubule (PST). **(C)** The thin descending loop starts at the end of the PST and reaches into the medulla, turning back to the cortex as part of **(D)** the thin ascending loop. The cells of **(E)** the thick ascending limb (TAL) are complex again and specialized at a region called the macula densa, responsible for a negative feedback to control water and salt metabolism. The distal nephron is differentiated into **(F)** the distal convoluted tubule (DCT) and **(G)** the connecting tubule (CNT). The CNT is composed of two types of cells; the principal and the intercalated cells that can also be found in the **(H)** initial collecting tubule (ICT) and the **(I)** cortical collecting tubule (CCT). **(J)** The outer medullary collecting duct (OMCD) and **(K)** the inner medullary collecting duct (IMCD) form the final structures of the nephron, with less complex and more rudimentary cells compared to previous nephron segments.

Phosphate Homeostasis

Many important biological functions are dependent on phosphate (Pi) ($H_2PO_4^-$, HPO_4^{2-}). Pi has been shown to play important roles in energy metabolism [2-3], nucleic acid synthesis [4], cellular signaling [5], muscle function [6-7], cellular membrane integrity [8], enzyme functions [9], bone mineralization [10] and lipid metabolism [11].

Pi can be measured virtually in every body fluid. In human serum, phosphorus is present as inorganic phosphorus or phosphate, lipid phosphorus, or phosphoric ester. Free Pi only represents approximately 50% of the total serum phosphorus and ranges, depending on age (in humans), from 0.83-1.34 mM [1]. The bone is a major reservoir of phosphorus that complexes with calcium as hydroxyapatite mineral, with 10 g of phosphorus per 100 g of dry fat-free bone tissue, whereas in comparison, muscle contains 0.2 g/100 g of fat-free and brain 0.3 g/100 g of fresh tissue [12].

Given such a wide distribution and tight regulation of Pi, it is evident that deviations from normal values can cause clinical diseases (i.e. rhabdomyolysis, muscle weakness, impaired leukocyte function, and altered bone mineralization leading to rickets or osteomalacia [13-15]).

The small intestine and the kidneys both have the ability to regulate Pi availability in the body. The small intestine absorbs Pi from the diet, and the kidneys control the excretion by reabsorption, depending on the needs of the organism [16]. In normal healthy individuals, urinary excretion of Pi reflects intestinal absorption (Figure 5). There are numerous factors that control Pi absorption in the intestine or its reabsorption in the kidney. The most important factor controlling intestinal absorption of Pi is 1α,25-$(OH)_2$-Vitamin D_3 (Vitamin D). Nevertheless, increase of Pi absorption has been observed in various studies lacking the specific vitamin D receptor (VDR) or active Vitamin D_3 [17-22].

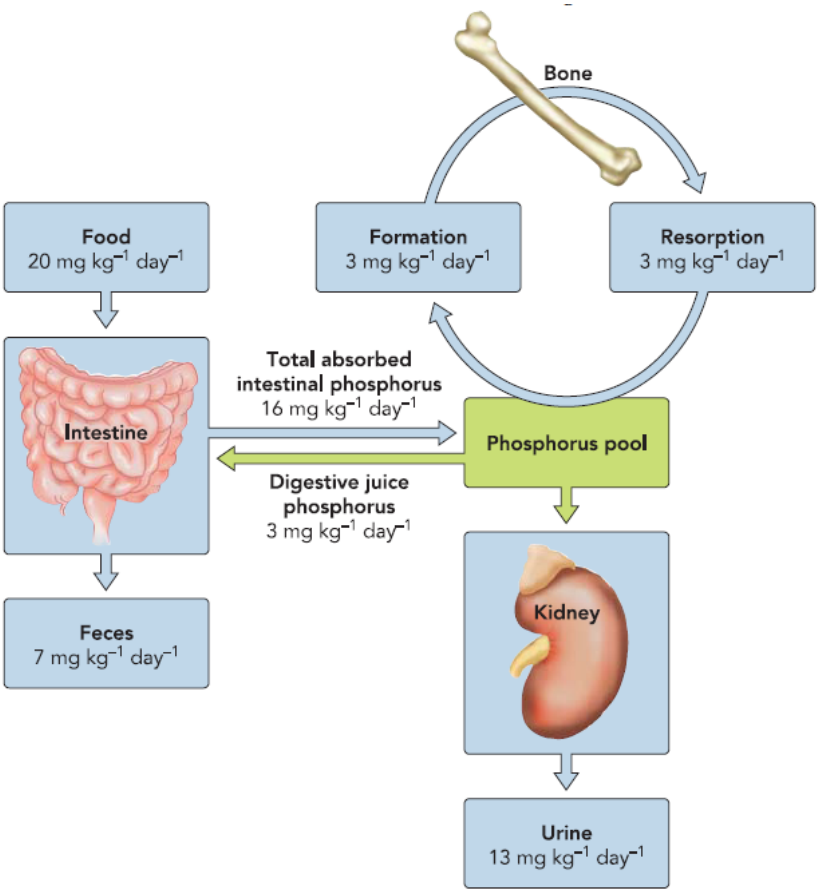

Figure 5. Pi distribution in the body. A constant level of Pi is held in the blood plasma, whereas changes can indicate pathological disturbances due to kidney dysfunction, intestinal malabsorption or bone disease. In healthy individuals, a net excretion in the kidney parallels the net absorption in the gut. The kidneys play a major role in regulating Pi homeostasis by controlling its reabsorption in the proximal tubule. Image taken from [1].

Phosphate reabsorption in proximal tubules

Pi is freely filtered in the glomerulus. The PCT and PST are the major sites for Pi reabsorption; approximately 80% of the filtered Pi is reabsorbed along these nephron segments. Other segments may reabsorb traces of remaining Pi (Figure 6 A), but detailed mechanisms are not known. Under balanced condition, approximately 10% of filtered Pi is excreted in the urine. In the PT, reabsorption of Pi is a transcellular process initiated by Na^+-coupled transporters (Na/Pi-cotransporters) located at the brush border membrane (BBM) [23-25]. Three Na/Pi-cotransporters have been described to be involved in Pi-reabsorption: two members of the SLC34 family (NaPi-2a and NaPi-2c) [26] and one member of the SLC20 family (Pit-2) [27]. Radioactive

phosphorus (^{32}P) studies have revealed sodium dependence for NaPi-2a, NaPi-2c and Pit-2. These transporters have been studied extensively using tracer fluxes in OK cells, oocytes, insect Sf-9 cells, as well as LLC-PK_1 [28-35]. In oocytes, the transport mechanism has also been investigated using electrophysiological techniques (e.g. electrovoltage clamping) [36-41].

There are different transport properties for these three renal Pi carriers. Pit-2 and NaPi-2a mediate electrogenic transport across the plasma membrane [27]. NaPi-2a carries preferentially divalent inorganic Pi with a net positive charge (3 Na^+ with 1 HPO_4^{2-}) [26], whereas Pit-2 carries also a net positive charge (2 Na^+ with 1 $H_2PO_4^-$) using monovalent inorganic Pi. For NaPi-2c, transport is electroneutral (2 Na^+ and 1 HPO_4^{-2}), with a preference for divalent inorganic Pi (Figure 6 B).

Pi reabsorption in the PT depends on NaPi-2a cotransporter abundance in the BBM. NaPi-2c has also been shown to participate, but to a lesser degree than NaPi-2a. Based on NaPi-2a knock out studies, the transporter was shown to be responsible for 70-80% of apical flux of Pi [42], where the remaining 20-30% is probably reabsorbed by NaPi-2c. The latter was also shown to increase up to three times on protein levels in NaPi-2a knock out mice without significant changes in mRNA [43-44].However, in mice, loss of function mutation in the SLC34a3 gene encoding NaPi-2c plasma and renal excretion of Pi were normal [45]. NaPi-2c has also been shown to play a more important role in weaning animals [43].

In-situ hybridization and RT-qPCR studies have shown the presence of NaPi-2a and NaPi-2c mRNA in the renal PT. Protein localization was determined through immunohystochemistry in the PT [46-47]. For NaPi-2a, an inter-nephronal heterogeneity was determined between superficial and juxtamedullary nephrons [46]. Regarding NaPi-2a protein distribution, S3 segments of the juxtamedullary nephrons presented more NaPi-2a at the BBM than the superficial nephrons [46].

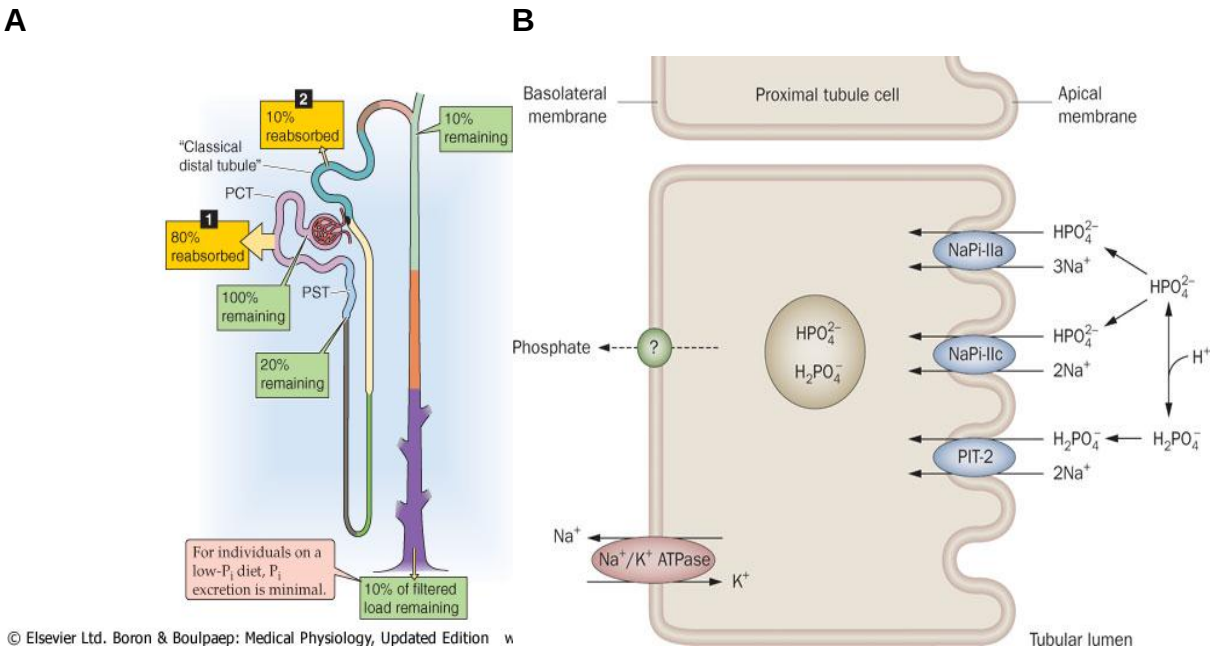

Figure 6. (A) Pi reabsorption along the nephron. The proximal tubule is responsible for up to 80% of Pi reabsorption depending on dietary changes or hormonal regulation. This process is mainly achieved via the transcellular pathway using an active, sodium driven Pi transporter (NaPi-2a). **(B)** The three Na/Pi cotransporters NaPi-2a, NaPi-2c, and Pit-2 are located at the apical membrane of the epithelial cells in the nephron, mainly in the proximal tubule. Image taken from [48].

Using RT-qPCR, heterogeneity for NaPi-2a mRNA was proven to exist between S1 and S3 segments along the juxtamedullary nephrons, but found to be absent in the superficial nephrons [49].

The importance of NaPi-2a is reflected by the effects of minor changes in its expression, causing clinical significant alterations in Pi homeostasis. Homozygous knock-out mice for NaPi-2a presented increased urinary excretion of Pi, hyposphosphatemia, elevated serum concentration of Vitamin D, hypercalcemia, hypercalciuria, and reduced amount of circulating PTH [42]. Even though NaPi-2c is responsible for only 20% of total Pi reabsorption, a mutation of NaPi-2c can lead to Pi wasting, demonstrating its critical involvement in Pi homeostasis [50].

Physiological regulation of phosphate

In order to fulfill an overall Pi homeostasis, it is necessary to control renal excretion of Pi. The main regulatory site is the PT. Regulated reabsorption is achieved by controlling the amount of Na/Pi-cotransporters at the BBM. Pi reabsorption in the kidney is related to a change in maximum velocity (V_{max}) of the Na/Pi-cotransport.

A series of factors (see Table 1) are responsible for the regulation of Pi reabsorption and the abundance of Na/Pi-cotransporters at the proximal tubular BBM. In the following paragraphs, single factors that regulate Pi-reabsorption will be discussed briefly. Two regulators, dietary Pi and parathyroid hormone will be discussed separately in more detail later.

Vitamin D (1α,25-$(OH)_2$-vitamin D_3) has been demonstrated to stimulate proximal tubular Pi reabsorption [51-52]. However, due to interfering factors, it is difficult to discriminate between direct and indirect effects of Vitamin D action, since *in-vivo* it is closely related to changes in PTH and calcium concentrations [53-54]. This will be further discussed later in context of dietary Pi.

Insulin has been shown to stimulate the Na/Pi-cotransport in the BBM, in addition to inhibiting the phosphaturic effect of PTH [55-56]. Some specific binding sites have been discovered for insulin at the basolateral membrane of proximal tubular epithelial cells [57-58].

Growth hormone and insulin like growth factor one (IGF-1), which is locally produced by the kidney, stimulate proximal tubular Pi transport [59-60]. When IGF-1 receptors are stimulated at the basolateral membranes of the PT, the intracellular phospholipase C pathway is triggered [61]. Epidermal growth factor (EGF) has been demonstrated to stimulate Pi reabsorption in perfused PTs, and inhibit Pi transport in OK and LLC-PK1 cells [62-64].

Glucocorticoids decrease Pi reabsorption [65-66]. These effects have been shown to occur *in-vitro* as well as *in-vivo* and can be observed independently of PTH concentrations [67]. It is possible, that during “chronic” metabolic acidosis, high plasma glucocorticoid levels cause a phosphaturic response [65, 68].

Thyroid hormone increases the abundance of NaPi-2a cotransporters in the BBM and thus renal Pi reabsorption [69-70]. In cultured OK cells, thyroid hormone caused

de-novo protein synthesis [71]. Another lipophilic hormone is *β*-estradiol, which has been reported to decrease renal tubular Pi transport [72].

Atrial natriuretic peptide (ANP) inhibits Pi transport. It is still uncertain whether ANP acts directly or not, since ANP receptors were not found in proximal tubular cells [73-74].

Calcitonin can mediate a decrease in Na/Pi-cotransport, independently from PTH and cAMP [75-76]. A possible rise in intracellular calcium could mediate this effect.

Glucagon has the opposite effect on Na/Pi-cotransport than insulin. Administration of this hormone increases phosphaturia. It was suggested that it is an indirect effect of cAMP release from the liver when pharmacological doses of glucagon were given [77].

Phosphatonins have been recently described in tumour induced osteomalacia (TIO) and other diseases associated with bone resorption and phosphaturia [16, 40, 78]. Renal Pi wasting had been directly linked to serum factors affecting Na/Pi-cotransport in the kidney, while also inhibiting the Vitamin D responsive pathway [40]. The most studied phosphatonins are: Fibroblast growth factor 23 (FGF-23), frizzled related protein-4 (sFRP-4), fibroblast growth factor 7 (FGF-7) and matrix extracellular phosphoglycoprotein (MEPE). The latter two were shown to inhibit Pi transport *in-vitro* (renal epithelial cells) and *in-vivo* (rat), without blocking compensational increase in serum Vitamin D levels, or direct inhibition of 1α-hydroxylase activity seen in other hypophosphatemic cases [16, 79-85].

Prostaglandins (e.g. PGE_2) are produced in the kidney and PGE_2 has been shown to antagonize the effect of PTH under physiological conditions [86]. Whether the cAMP signaling cascade is involved, is not known.

Dopamine acts during “acute” renal denervation by increasing renal Pi excretion independently of the action of PTH levels in plasma. Both, the precursor L-dopa and dopamine reduce the expression of NaPi-2a and thus Pi transport, as has been demonstrated in isolated rabbit proximal tubules and OK cells [87-91].

Fasting has been correlated with phosphaturia. Why Pi is excreted in fasting rats is not known. It may be a hormonal interaction (e.g. glucagon) that is involved during fasting [92-93].

Plasma calcium changes can lead to direct changes in PTH levels that can act on Pi reabsorption in the kidney [94-95]. *In-vitro* however, extracellular calcium was shown to affect NaPi-2a in the proximal tubular BBM [96]. Perfused proximal tubules have demonstrated an increase in Na/Pi-cotransport in response to high Ca^{2+} concentrations [97]. In contrast, OK cells *in-vitro* increased Na/Pi-cotransport when exposed to low calcium concentrations [98]. It is suggested that the calcium receptor is involved in mediating this effect.

Acid-Base disturbances can affect Pi reabsorption in the PT. An alkaline intratubular pH leads to stimulation of the NaPi-cotransporter while acidic conditions inhibit the cotransporter [99-100]. This may be due to protons competing with sodium ions for the binding site of the cotransporter. “Chronic” metabolic acidosis decreases Pi reabsorption while “acute” metabolic acidosis does not. Some data suggests that the elevation of glucocorticoids during “chronic” metabolic acidosis may be responsible for phosphaturia. Respiratory alkalosis stimulates Pi reabsorption and respiratory acidosis causes Pi excretion [65-66, 68, 101].

Volume expansion causes Pi excretion in the urine and reduction of NaPi-2a abundance in the BBM. It has been questioned whether the effect of volume expansion on NaPi-2a is either directly or indirectly related to the action of humoral factors (i.e. ANP, dopamine) [102].

Decreased Pi transport	Increased Pi transport
High Pi-diet	Low Pi-diet
PTH and related peptide PTHrP	Growth hormone
Glucocorticoids	Insuline
Chronic metabolic acidosis	Thyroid hormone
Acute respiratory acidosis	1,25α$(OH)_2$Vitamin D_3
Aging	Chronic metabolic alkalosis
Phosphatonins	High potassium diet
ANP	High calcium diet
Fasting	Stanniocalcin
Hypokalemia	
Hypercalcemia	
Diuretics	
Calcitonin	

Table 1. Hormonal and non-hormonal factors play a role in proximal tubular Pi reabsorption. PTH, Vitamin D, and Pi-diets are included under the most studied factors modulating Na/Pi-cotransport at the BBM. Phosphatonins have recently been described to be involved in renal Pi wasting.

Regulation of phosphate excretion by parathyroid hormone

In humans, there are four parathyroid glands located on the posterior surface of the left lobe of the thyroid and additional two on the right. In total, the glands weigh approximately 500 mg and consist mainly of chief cells (parathyroid cells) which are specialized gland cells that secrete parathyroid hormone (PTH). The main regulator of PTH secretion is serum calcium concentration, acting via a negative feedback mechanism. This involves calcium-sensing receptors located in the chief cells that are activated by low calcium concentrations. Vitamin D and Pi have also been observed to act on PTH secretion [103].

Renal Pi cotransporter NaPi-2a is greatly decreased upon PTH stimulation with consequent phosphaturia. Rodents that had been injected with PTH presented within minutes later lower NaPi-2a abundance at their renal proximal tubular BBM compared to their controls [104]. During prolonged increase of PTH, a reduction in mRNA content of NaPi-2a was observed in the PT [104]. In addition, *in-vitro* studies with OK cells showed a decrease of intrinsic and transfected rat NaPi-2a

cotransporter [105-106]. A rapid recovery of NaPi-2a follows after PTH inhibition. In OK cells, this recovery has been shown to be dependent on protein synthesis [107-108]. The effect of PTH on NaPi-2a is three times faster than on NaPi-2c which also appears to be modulated by dietary Pi, growth, and FGF-23 [19, 109-112]. For Pit-2, the only regulators that have been identified to date are dietary Pi and potassium depletion [113-114].

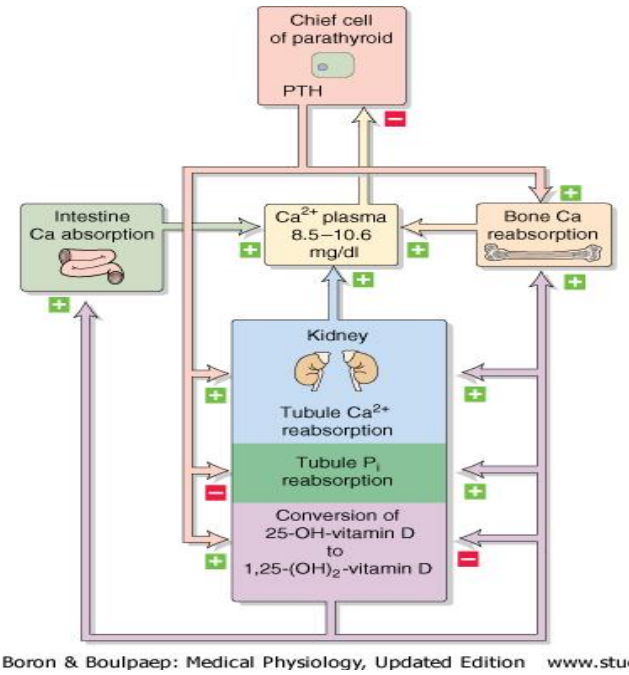

Figure 7. PTH controls serum Pi and calcium levels in the organism. The PT is the main site of PTH action by regulating the abundance of Na/Pi-cotransporters in the apical membrane. PTH stimulates Pi excretion and calcium retention as well as Vitamin D synthesis.

Parathyroidectomized (PTX) animals have shown up-regulation of NaPi-2a in absence of any changes in mRNA levels [104]. PTH receptors have been localized to the apical and basolateral membranes of the PT and OK cells [115-117]. Experiments realized with cultured cell lines and renal proximal tubular preparations indicated that PTH regulation of NaPi-2a occurs through receptor dependent increase of cAMP, diacylglycerol (DAG), and inositol triphosphate (IP_3) [118-122]. These messengers, acting through several kinases including protein kinase A (PKA) and C (PKC), lead to the inhibition of apical brush border Na/Pi-cotransport. This is

due to lower abundance of NaPi-2a, and thus, a reduction in V_{max} value [118, 123-124].

Recent studies have revealed that associated membrane proteins may be involved in trafficking of NaPi-2a [125]. PDZ containing proteins (Postsynaptic protein PSD95, *Drosophila* protein dlg (discs large)-A and tight junction protein ZO-1) such as PDZK1 and Na^+/H^+ exchanger regulatory factor (NHERF1) interact and colocalize with NaPi-2a and are assumed to play an important role in the apical distribution of NaPi-2a at the membrane [126-129]. When kinase cascades are activated in response to PTH, NaPi-2a is retrieved and internalized into subapical vesicles [130-132]. Interestingly, it is not NaPi-2a that is subjected to phosphorylation, but rather its binding protein NHERF-1 [133-134]. NHERF-1 contains two PDZ domains that interact with specific sequences in C-terminal ends of target proteins [135-136]. NHERF-1 has also been demonstrated to bind through its C-terminal end to cytoskeletal interacting proteins MERM family, (moesin, ezrin, radixin, and merlin) [137]. The first PDZ domain, which interacts with NaPi-2a contains a Ser^{77} that is subjected to phosphorylation in response to PTH (and dopamine), leading to the dissociation of the NaPi-2a/NHERF-1 complex [132, 134]. The separation of NaPi-2a from NHERF-1 is important for correct removal of NaPi-2a from the apical BBM and for entering into the endocytic pathway [138]. It may be, that NHERF-1 functions as a NaPi-2a retention signal and when NHERF-1 is absent, it limits NaPi-2a abundance at the surface of the membrane [128-129]. Once NaPi-2a internalization is completed, the cotransporter is degraded in the lysosomes [108, 116, 139].

Regulation by dietary phosphate

Dietary intake of Pi influences its reabsorption and excretion in the urine. When a high Pi-diet (HPD) is administered, Pi excretion increases while a low Pi-diet (LPD) decreases Pi excretion [140-141]. Abundances of NaPi-2a, NaPi-2c and Pit-2 are altered by changes of dietary Pi intake, independent of PTH and other factors [23, 47, 116-117, 142-143]. Dietary Pi restriction (5 days, “chronic”) has been shown to increase the expression of NaPi-2a in S1-S3 segments without changes in the mRNA

distribution profile. This suggests that NaPi-2a adaptation to Pi imbalances is not due to changes in mRNA levels. Overall, an axial heterogeneity is more pronounced in HPD treated animals than in LPD animals [49]. During Pi deprivation, a resistance has been documented to the phosphaturic effect of PTH [144-146]. This may be due to the reduced dopamine synthesis in the nephron during Pi deficiency. Administration of PTH to LPD animals, followed by dopamine injection, were shown to overcome phosphaturia [147]. Moreover, micro puncture studies demonstrated in acutely thyro-parathyroidectomized (TPTX) rats, that the response to changes in Pi adaptation is mainly reflected by changes in Pi reabsorption by superficial nephrons [148], and to a lesser extent by the distal nephron. The response to Pi diets in the brush border membrane vesicles (BBMV) is specific for Pi. Other Na^+-coupled transporters, such as Na^+-dependent L-proline or D-glucose transport, are not affected by changes in dietary Pi. Kinetics for Pi transport, demonstrate an increase in V_{max} in LPD animals without any changes in the apparent affinity (K_m).

Renal adaptation to dietary Pi deprivation can be classified in an early and a “chronic” phase. The early phase is imminent, and can be detected in the BBM within hours (2 - 4 h) [149-151]. It is characterized by a fall in serum Pi concentration and is PTH independent. Some evidence suggests, that decreased synthesis of dopamine in the nephron may be involved in the response of the early renal adaptation to dietary Pi restriction [147]. A shuttle mechanism for the cotransporter has been proposed and confirmed for the rapid phase adaptation at the BBM. This would explain the post-transcriptional regulation of NaPi-2a without any changes in its mRNA levels [142, 151-153]. An opposite adaptation to Pi has been shown after phosphate infusion; where 40 min thereafter a diminished sodium dependent uptake was detected [154]. When OK cells were incubated in the presence of a Pi transport inhibitor (PFA), followed by its removal, NaPi-2a abundance increased rapidly [152, 155]. Even in presence of RNA or protein synthesis inhibitors, increase in amount of NaPi-2a occurred. This suggests that the mechanism for Na/Pi-cotransport may be controlled by the availability of subapical pools of NaPi-2a cotransporter proteins that are recruited to the membrane upon LPD stimulation. Adaptation to “chronic” dietary Pi restriction involves *de-novo* synthesis of Na/Pi-cotransporter protein that is completed after several days [156-158]. This process is fundamental for Pi homeostasis.

"Chronic" adaptation can be inhibited with the administration of actinomycin D to LPD animals [159].

Experiments with rats under fasting conditions have demonstrated that reabsorption of Pi is not as pronounced as after LPD [92, 160-162]. When compared to normal Pi-diet (NPD) rats, fractional excretion of Pi ($U_{Pi}V$) was lower in animals deprived of food, but significantly higher than in LPD rats. Tracer studies with BBM preparations of these animals showed higher Pi uptake for LPD than for NPD rats. However, uptake of fasted rats was just below that of NPD rats [160]. The reason why total fasting does not correlate with the increased Pi uptake of animals on LPD is still unknown. An explanation would be that during starvation metabolic acidosis accounts for a higher phosphaturia. In addition, supply of metabolic energy is reduced, which is required for proximal tubular function and the expression of the NaPi-2a cotransporter in the BBM.

The role of Vitamin D in response to dietary phosphate

The Vitamin D axis is known to respond to dietary Pi changes in the organism. Thus, after a LPD ingestion, an increase in renal expression of 1α-hydroxylase (Cyp27B1) with consequent action of Vitamin D can be detected [1]. Renal expression of the Cyp27B1 gene generates the enzyme 1α-hydroxylase [163]. A specific mechanism involving the epithelial cell surface receptors megalin/cubulin is known for the 25-OH-D_3/DBP complex uptake at the apical BBM of the renal PT cell. Knock-out (KO) mice for megalin show a reduced Vitamin D metabolite level and a clear vitamin D deficiency. Hypophosphatemia is an important regulator for 1α-hydroxylase [164-167]. The increase of Vitamin D levels in serum in response to LPD has been shown to be independent of PTH levels. However, after performing hypophysectomy, the response of Vitamin D was completely abolished [164, 168]. Even though serum Pi levels have not been associated with changes in growth hormone (GH) secretion [168], it is suggested that the pituitary GH-IGF-I axis may be a mediator of 1α-hydroxylase synthesis in response to hypophosphatemia [169-171].

Hypophysectomized (HPX) rats set on LPD restored 1α-hydroxylase activity after the administration of GH [169-172].

A time course for isolated mitochondrial 1α-hydroxylase activity was determined in LPD and HPD animals, but no increase of activity was observed after the first day of LPD [173]. On the second day of LPD, a linear increase which became more pronounced until reaching the highest expression on the 8th day was attained. Similar data was collected using RT-qPCR methods with no increase in 1α-hydroxylase gene expression level until the second day [173]. Moreover, different LPDs were tested to investigate the degree of stimulation necessary to reach the highest activity of 1α-hydroxylase. A significant increase was determined with 0.02% of Pi, reaching an 8 fold increase with 0.2% and no change with 0.6% compared to control diet (1%). RT-qPCR data confirmed this activity for gene expression level as well [173].

Phosphate sensors and an intestine-kidney axis responsible for Pi homeostasis

Individual cells have the ability to sense Pi in their environment and to respond accordingly to maintain homeostasis. Unicellular organisms have developed “phosphate sensors” [174-176] that allow them to sense their external media by generally changing the phosphorylation state of intracellular proteins that in turn affect the transcription level of nuclear proteins. Mammals have biologically inherited this sensing mechanism by which Pi is held constant intracellularly. Several studies have revealed evidence for Pi signaling mechanisms residing in the gastrointestinal tract and in the parathyroid gland of rodents [177], but the exact mechanism of action still remains unknown to date. Rats, after a duodenal Pi infusion, had a change in fractional excretion of Pi within 10 min without any changes in serum Pi values [178]. This was also confirmed in TPTX rats, where Pi excretion was imminent upon duodenal Pi loading, indicating an independent mechanism of PTH action. Also, no significant changes in concentration of phosphaturic peptides (e.g. FGF-23, sFRP-4) in normal and in PTX rats were determined after duodenal Pi loading. Moreover, this data suggests a Pi sensor in the intestine, that controls renal excretion of Pi within a

short time period after sensing it in the intestinal mucosa [178]. The phosphaturic response of the kidney is not mediated by any of the known agents that have been classified to stimulate Pi excretion. Renal denervation excluded the nervous system to be involved in this mechanism. After intraduodenal infusion of Pi in rats, a homogenate was prepared from the intestinal mucosa of these rats, and after isolating the proteins they were infused into a new group of rats which caused consequent Pi excretion in the animal. This experiment indicated a factor present in the intestine responsible for the phosphaturic action in the kidney [178]. More studies need to be performed to confirm and elucidate the mechanisms behind these actions.

Aim of the Study

Several observations indicated in the past that intake of a diet of low phosphate content alters various renal functions. Some of these changes occur without altered gene expressions, but other effects were shown to be based on regulated gene expressions. For example, altered gene expression has been observed in the case of the regulation by low Pi-diet of renal 1α-hydroxylase or the Na/Pi-cotransporter NaPi-2c. Besides these examples, little is known about other genes that are regulated in the kidney by altered dietary intake of phosphate.

The aim of this work was to analyse the impact of dietary content of phosphate on renal gene expression in general and, in particular, on the expression of genes that may be involved in the renal handling of Pi and consequently in body Pi homeostasis.

Materials and Methods

Animals and collection of organs and blood

For all animal studies performed in this work, male C57BL/6 mice of age between 10 and 13 weeks were used (purchased either from the Institute für Labortierkunde (University of Zürich) or from Harlan (Animal research laboratory). All animal handlings were carried out in accordance with the Swiss Animal Welfare Laws and approval of the local veterinary authority (Kantonales Veterinäramt). Mice were kept in a temperature and humidity controlled atmosphere, with a 12 hour light and dark cycle.

At the end of each experimental period, animals were anesthetized intraperitoneally using ketamine (4 mg/mouse) in combination with xylazine (0.8 mg/mouse). Venous blood was collected from each mouse and centrifuged in the presence of heparin (8000 r.p.m. for 3 min) to separate blood cells from plasma. Plasma was snap frozen in liquid nitrogen and stored at -80°C. After extraction of the kidneys, capsules were removed and kidneys were snap frozen in liquid nitrogen and stored at -80°C.

Experimental Setups

Phosphate diets

Diets, containing different amounts of phosphorus, were purchased from Provimi Kliba AG (CH-4303 Kaiseraugst). The phosphorus content of the diets used was either 1.2% (high Pi-diet; HPD) or 0.1 % (low Pi-diet; LPD). Both diets contained the same amount of calcium.

“Chronic” (5 days) adaptation to different Pi-diets:

After arrival, animals were adapted to facility conditions for a few days, and afterwards separated in two groups (routinely 6 animals per group). One group received a HPD while the other group received a LPD for 5 days. Water and food were supplied *ad-libitum.*

“Acute” adaptation to different Pi-diets:

In order to investigate short term effects of different Pi-diets, mice were trained to eat the HPD for 5 days during a 3 hour period (6 pm-9 pm), and on the 6th day they were separated into two groups. HPD and LPD, respectively, were given at 6 pm and removed at 9 pm. Mice were sacrificed after different time points (4, 8 and 14 h), followed by the collection of blood and kidneys.
In a second set of experiments, mice were trained to eat the HPD for 3 hours (6 to 9 pm) in normal cages for 3 days. On the 4th day they were placed in metabolic cages (Tecniplast 3600M021, Buguggiate, Italy). Urine was collected in 24 h intervals and water consumption was measured every 24 h. They continued to receive HPD for the following 2 days during the 3 h evening period. On the 3rd day in metabolic cages, the experimental group (6 mice) was changed to LPD while the control group continued to eat the HPD. The following morning (8 am), 14h after receiving LPD and HPD, animals were sacrificed after collecting blood and kidneys.

RNA related methods

Total RNA isolation and quality control

Total RNA was extracted from whole kidney tissue (RNeasy Mini extraction kit, Qiagen, Cat. No. 74104). 20 to 30 mg of renal tissue was homogenized on ice with

the help of a glas-teflon potter (B.Braun, Melsungen AG) in 600 µl RLT buffer™ (Qiagen, Germany) supplemented with 1% *β*-mercaptoethanol (Sigma, USA). The resulting homogenate was further processed according to the protocol of the manufacturer, and final total RNA was eluted with RNAse free water.
The concentration of total RNA was determined spectrophotometrically (NanoDrop ND-1000 Spectrophotometer, Deleware, USA). Quality of total RNA was analyzed by the RNA 6000 Nano LabChip (Agilent technology, Cat. No. 5065-4476) and the 2100 Bioanalyzer (Agilent technology, Waldbronn, Germany). Quality was based on the 260 nm/280 nm ratio and the RIN (RNA Integration) number.

Hybridization of total renal RNA to whole mouse genome microrarray chips

All hybridization experiments were done in and by the Functional Genomics Center Zürich (FGCZ). Only samples of total RNA with a 260 nm/280 nm ratio between 1.8 and 2.1, a 28S/18S ratio between 1.5 and 2, and a RIN greater than 8 were used for hybridization to microarray chips. Total RNA samples (2 µg) were reverse-transcribed into double-stranded cDNA and then *in-vitro* transcribed in the presence of biotin-labeled nucleotides using an IVT Labeling Kit (Affymetrix Inc., P/N 900449, Santa Clara, CA). Following purification and quantification using BioRobot Gene Exp – cRNA Target Prep (Qiagen AG, Switzerland), the quality of labeled cRNA was determined using Bioanalyzer 2100. Before hybridization to GeneChip® Mouse Genome 430 2.0 arrays (Affymetrix) (16 h at 45°C), biotin-labeled cRNA samples (15 µg) were fragmented randomly into 35–200 bp at 94°C using fragmentation buffer (Affymetrix Inc., P/N 900371, Santa Clara, CA). This was finally mixed in 300 µl of hybridization mix (Affymetrix Inc., P/N 900720, Santa Clara, CA) containing hybridization controls and control oligonucleotide B2 (Affymetrix Inc., P/N 900454, Santa Clara, CA). After GeneChip® hybridization, arrays were washed using an Affymetrix Fluidics Station 450 FS450_0001 protocol. In order to determine the

fluorescent intensities emitted by the labeled targets, an Affymetrix GeneChip Scanner 3000 (Affymetrix Inc., Santa Clara, CA) was used.

Obtained data were processed using the software GCOS 1.4 (Affymetrix Inc., Santa Clara, CA). By means of the MAS5 algorithm [179], probe cell intensities were calculated and summarized for the respective probe sets. Global scaling was performed to compare the expression values of the genes from chip to chip, which resulted in the normalization of the trimmed mean of each chip to target intensity (TGT value) of 500, as detailed in the statistical algorithms description document of Affymetrix (2002). Before performing the statistical analysis, quality control measures were considered. These included adequate scaling factors (between 1 and 3 for all samples) and appropriate numbers of present calls calculated by application of a signedrank call algorithm [180]. Using the following parameters the efficiency of the labeling reaction and the hybridization performance was controlled: Present calls and optimal 3'/5' hybridization ratios (around 1) for the housekeeping genes (GAPDH and ACO7), for the poly A spike in controls and the prokaryotic control (BIOB, BIOC, CREX, BIODN). A simplified schematic presentation of a microarray chip can be seen in Figure 8.

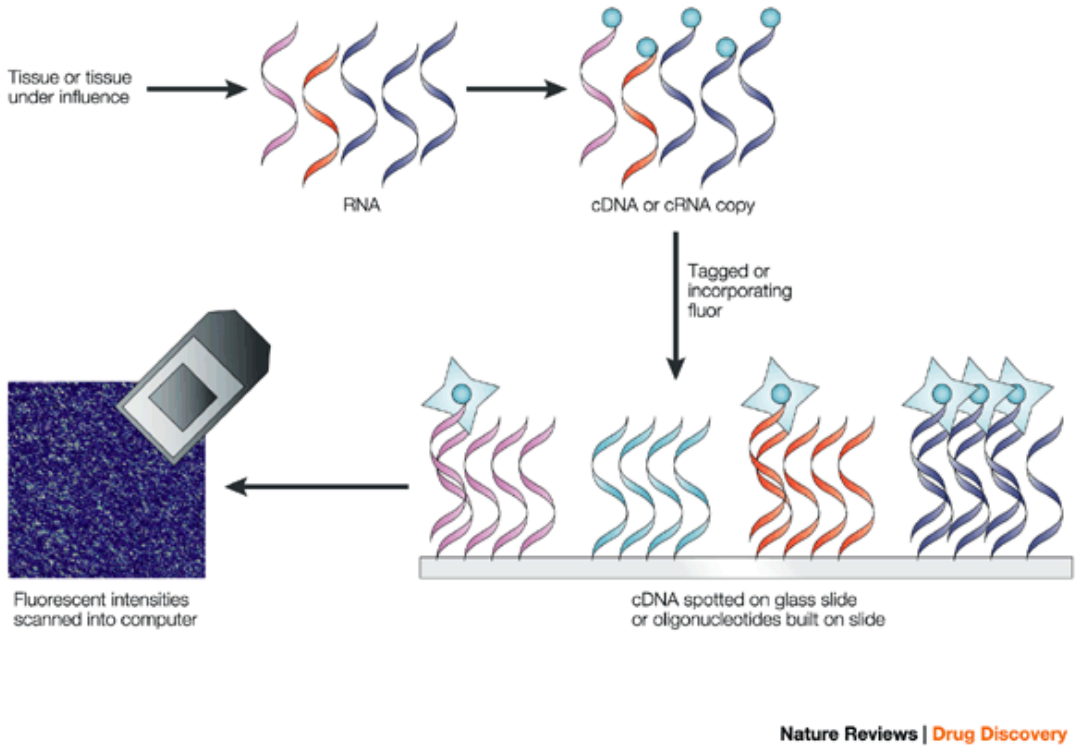

Figure 8. Scheme of a microarray analysis experimental process. Image taken from [181].

Analysis of Microarray data and Pathway toolkits

Microarray gene lists obtained were analyzed using Rosetta Resolver® (CeibaSolutions, MA, USA) provided by the FGCZ of the University of Zürich. Unpaired student *t*-test ($p < 0.05$, $n = 4$) was applied for statistical analysis for each experimental group (HPD and LPD). Gene expression profiles were compared intrinsically within each group before evaluating gene expression sets between groups.

- Web based gene set analysis toolkit (WEBGESTALT) is one of many programs that is freely accessible on the internet and that is currently used for gene data obtained from humans and mice. By incorporating different public resources it enables scientists to integrate large data sets to obtain pathways and gene patterns that would not be detected otherwise. The program was originally designed for functional genomics and large scale genetic studies, from which high amount of data are continuously produced. It is necessary to be registered on the webpage http://bioinfo.vanderbilt.edu/webgestalt/ and it is recommended not to rely on the program for permanent data storage.
- G-Profiler (http://biit.cs.ut.ee/gprofiler/) is another high throughput genetic profiling program. It is provided by the University of Tartu in Estonia and uses a number of analysis systems (g:GOst, g:Cocoa, g:Convert, g:Sorter, g:Orth) that can be chosen separately on the webpage depending on the type of grouping between genes that is desired (e.g. expression similarity, orthology search, etc.).
- Gene Ontology Enrichment Analysis Software Toolkit (GOEAST) (http://omicslab.genetics.ac.cn/GOEAST) also belongs to a web based analysis toolkit that integrates input data, especially from microarray hybridization experiments, to visualize it comprehensively. WEBGESTALT, G-Profiler, and GOEAST all use information from the Kyoto Encyclopedia of Genes and Genomes (KEGG).

Real time RT-qPCR

Purified total RNA was reverse transcribed (TaqMan® Reverse Transcription Kit, Applied Biosystems) in the presence of 2.5 µM random hexamere primers. Reverse transcription was performed using the Robocycler 40 (Stratagene) with the following parameters: 10 min at 25°C, 60 min at 42°C, 5min at 95°C, and kept at 4°C until further use. Following cDNA synthesis, real time RT-qPCR was performed in 96-well plates (Applied Biosystems, USA). 0.75 µl (~18 ng) of cDNA was combined with either 0.75 µl of Taq Man® Gene Expression Assay buffer containing a mix of pre-designed primers and corresponding probes (www.appliedbiosystems.com), or designed primers (5 µM) and probes (1 µM) (Supplementary Table S1). Designed probes (obtained from Microsynth, Balgach, Switzerland) were labeled with the reporter dye FAM at the 5' end whereas the quencher dye, TAMRA, was attached at the 3' end. Expression Assays™ (Applied Biosystems, USA) contained just the reporter dye FAM, no quencher. Ribosomal 18 S RNA (18 S rRNA), used as a "Housekeeping" gene, had VIC as a reporter and TAMRA as a quencher. To the primer and probe mixture, Taq Man® Universal PCR master mix (Applied Biosystems, USA) was added to give a final volume of 15 µl. The 96-well plate was put into a centrifuge (Eppendorf centrifuge 5804) to spin down all contents. Finally, RT-qPCR was performed using the 7500 Fast Real Time PCR System (Applied Biosystems, USA). Standard thermal cycles (up to 40) were set as follows: 2 min at 50°C, 10 min at 95°C, 40 cycles of 15 s at 95°C and 1 min at 60°C. Data were analyzed using the 7500 Fast Real-Time PCR System Sequence Detection Software v1.4 (Applied Biosystems, USA). Automatic threshold and baseline were calculated by the program. Each sample was run in triplicates, except for the negative control, and the mean Ct value used for evaluation. Abundance of a gene was calculated in relation to "housekeeping" genes (*β*-actin or 18 S rRNA). These values were determined by assuming an efficiency value of 2, which presents the fold-increase in input mRNA required to decrease the cycle number by 1. The relative expression ratios were then calculated as $R = 2^{(Ct(control)-Ct(experiment))}$.

Isolation of nephron segments for RNA extraction

Mice were anesthetized as described above. Perfusion was performed through the left ventricle with a solution containing 3 ml of Ham's F-12 medium (GIBCO BRL), 10 mM (HEPES)-NaOH (pH 7.4), and 1 mg/ml of collagenase type I (Sigma, USA). Kidneys were removed and placed in RNA*later*® (Ambion). 20 proximal tubules and 20 thick ascending limbs were isolated from the cortex region and placed in Eppendorf tubes containing 50 µl RLT buffer™ (Qiagen, Germany) supplemented with 1% *β*-mercaptoethanol (Sigma, USA). After vortexing for 30 s, tubes were either shock frozen in liquid nitrogen and stored at -80°C, or directly processed for RNA isolation according to the protocol of the manufacturer using the RNeasy® Micro kit (Qiagen, Germany, Cat. No. 74004).

In-situ hybridization of SLC16A14/MCT14

Mice were anesthetized as described above. After removing capsules, kidneys were placed in small baskets made of nylon mesh. All pre- and post-hybridization procedures, including paraffin embedding, were carried out using a BioLane HTI *in-situ* hybridization machine (Holle & Hütter AG, Tübingen, Germany). The baskets containing the kidneys were placed in ice cold phosphate-buffered saline (PBS). A fixative solution of 4% paraformaldehyde (PFA) (Aldrich, USA) was prepared in PBS and then used for kidney incubation at 4°C for at least 3 days. Afterwards, kidneys were cut into thin longitudinal and transversal sections and placed in 50% ethanol (diluted in H_2O) for 2 h, followed by 60% ethanol for 2 h. Further dehydration steps before paraffin embedding were as follows: 2 h in 70% ethanol, 2 h in 80% ethanol, 2 h in 90% ethanol, twice for 1 h in 96% ethanol, twice for 1 h in anhydrous (≥ 99.5%) ethanol (Sigma, USA), twice for 1 h in xylol, and 3 times paraffin embedding for 1 h. Next, kidneys were cut into 5 µm thin slices using a microtome (Leica RM2235) and placed onto poly-lysine coated glass slides (O. Kindler GmbH & Co., Freiburg, Germany). Copeland jars were used for incubating slides with a volume of 200 ml for

several steps. First, slides were immersed twice for 10 min in xylol followed by one wash in xylol/ethanol (1:1) for 2 min, followed by incubation in anhydrous ethanol (twice for 10 min each). Several ethanol solutions (diluted in PBS) with decreasing concentration were then applied for 1 min each: 96%, 90%, 70%, and finally 50%. Rehydration was completed by immersing the slides twice in PBS for 5 min. Proteinase K (Gibco, Roche Cat. No. 15401011) digestion was done at 37°C for 5 min with a pre-warmed working solution of 10 mg/ml proteinase K in 0.1 M Tris-HCl (pH 8), 0.2% glycine in freshly prepared PBS solution. This reaction was stopped by two washes (5 min each) with PBS. Tissue was fixed for 20 min in 4% PFA / 0.2% glutaraldehyde (Sigma, USA) made in PBS. Again, slices were washed for 5 min with PBS. Slides were taken out of PBS and placed vertically over paper towels to remove excess solution. Tissue was encircled using the “ImmEdge” pen (Vector laboratories, USA, H-4000). This procedure was done quickly to avoid the slices from drying. Finally, they were placed back into Copeland jars with PBS for 5 min.

The following hybridization buffer was prepared (for 50 ml solution): 25 ml formamide (50% final concentration), 12.5 ml 20xSSC (3 M NaCl, 0.3 M Na-citrate pH 7 in DEPC water and autoclaved), 3 ml blocking solution containing 500 mg blocking reagent (Roche, Switzerland, Cat. No. 11096176001), 500 µl of 0.5 M EDTA, 50 µl of Tween-20 (Sigma-Aldrich, USA, P5927), 500 µl of 10% CHAPS (Sigma-Aldrich, USA, Cat. No. C3023-1G), 1 ml heparin solution (Sigma-Aldrich, USA, Cat. No. H3393-50KU), and 5 ml of 10 mg/ml yeast t-RNA (Invitrogen, USA, Cat. No. 15401011).

The pre-hybridization buffer contained 95 µl of hybridization buffer and 5 µl of sterile dH_2O while for the hybridization buffer, instead of dH_2O, the DIG- labeled probe RNA at a concentration of 1 µg/ml was added. Before using the hybridization buffer with the labeled probe, it was pre-heated to 100°C for 5 min and then quenched on ice.

Sense and anti-sense probes for SLC16A14/MCT14 were synthesized using Sp6 and T7 RNA polymerases respectively. The myc tagged SLC16A14/MCT14 (see later section “creating a myc-SLC16A14/MCT14”) served as a template for RNA synthesis. The control probes (sense and anti-sense) for SLC5a2 and SLC12a1 were provided by the research group of Prof. Carsten A. Wagner of the Institute of Physiology, University of Zürich. 2.5 µl of DIG-labeled nucleotide mix were added to 2.5 µl of 10x buffer followed by 2.5 µl (Sp6 or T7) polymerase (Roche, Basel,

Switzerland). Finally, 1 µg of cDNA was dissolved in 25 µl of dH_2O. Incubation was performed for 4 h at 37°C. Probes were kept on ice until hybridization, or snap frozen in liquid nitrogen followed by storage at -80°C.

Slides were taken out of PBS and placed into rectangular boxes (Nunc™ boxes, Denmark) previously covered with paper towels soaked in 50% formamide / 2x SSC (approximately 50 ml per box). Pre-hybridization buffer (30-100 µl) was added to the kidney sections. Nunc™ boxes were closed and the slides were incubated at least 1 h at 70°C. Pre-hybridization buffer was removed and replaced with hybridization buffer, containing sense or anti-sense probes. The incubation step was repeated using a large box covered with soaked solution where the smaller boxes were placed inside. The box was wrapped in aluminum foil to prevent excessive evaporation during overnight incubation at 70°C.

Slides were rinsed with 2xSSC pH 7 and incubated twice for 20 min at 65°C in 50% formamide / 2xSSC pH 7 in Copeland jars. They were washed for 5 min in PBS-tween (3 times). Blocking buffer (B-Block) was prepared as follows: to 90 ml of PBS (at 95°C) 2 g of blocking reagent (Roche, Basel, Switzerland) were added. Solution was cooled and 100 µl of Tween-20 and 10 µl of goat serum (Vector laboratories, USA, S-1000) were added. B-Block was warmed to RT, pipetted on the slides (20 to 30 µl) and incubated for 30 min at room temperature using the Nunc™ box. This was followed by incubation with anti-DIG alkaline phosphatase at a dilution of 1:5000 in B-block (before use mixed for 30 min at RT). Incubation followed overnight at 4°C in a closed box containing water soaked paper towels. Next day, slides were washed 3 times for 5 min in PBS-tween on the shaker. Slides were washed in NTN-tween solution (100 mM tris pH 9.5, 100 mM NaCl, 50 mM $MgCl_2$, 0.05% Tween-20) for 5 min. Slides were then incubated again at 4°C overnight with BMPurple AP substrate precipitation (Roche, Switzerland, Cat. No. 11442074001) in a box with water soaked paper towels and covered with aluminum foil to prevent light contamination. Next day, slides were washed in PBS and postfixed in 4% PFA (Sigma, USA) in Copeland jars for at least 1 hour. Finally they were washed for 5 min (two times) and mounted with cover slips (Menzel Gläser, Germany) using Mowiol® (Sigma, USA, Cat. No. 81381-50G). Visualization and imaging was realized by light microscopy (Eclipse TE 300, Nikon Japan).

DNA related methods

Myc-tagging SLC16A14/MCT14

E. coli transformed with *Mus musculus* SLC16A14/MCT14 cDNA (inserted in pCMV-Sport6) was purchased from imaGenes (Germany, Berlin). Bacteria were grown on agar plates containing 100 µg/ml of ampicillin. Overnight growth at 37°C resulted in colonies that were picked and grown overnight in liquid LB (Luria-Bertani) medium containing 100 µg/ml of ampicillin. A plasmid extraction kit (QIAprep® Spin Miniprep kit, Qiagen, Germany, Cat. No. 27106) was used to isolate plasmid DNA. SLC16A14/MCT14 was subcloned into a modified pSD-Easy vector (pSPOK-G obtained from S. Gisler). Besides containing a myc coding sequence (ATG-GAA-CAA-AAA-CTC-ATC-TCA-GAA-GAG-GAT-CTG), pSPOK-G also contained a KOZAK consensus sequence and a poly-A tail sequence required for mRNA translation and stability. In order to insert the SLC16A14/MCT14 into the pSPOK-G vector, primers were ordered from Microsynth (CH-9436 Balgach) and *Sac*I/*Xho*I restriction sites were created at the end terminals of SLC16A14/MCT14 gene upon PCR amplification (Figure 9 & 10). After *Sac*I/*Xho*I digestion, SLC16A14/MCT14 was subcloned into pSPOK-G down-stream of the myc sequence (C-terminus). The chosen restriction sites had to fulfil various conditions: first, they were only allowed to exist once in the pSPOK-G vector for linearization containing the complementary ends of *Sac*I (5’ end) and the *Xho*I (3’ end). Second, restriction sites for *Sac*I and *Xho*I needed to be absent in the SLC16A14/MCT14 sequence except the added sequences for insertion to the pSPOK-G vector. Third, insertion of the *Sac*I/*Xho*I digested SLC16A14/MCT14 gene needed to follow the myc tag sequence as close as possible without frame shifts. Fourth, the restriction site for linearization of pSPOK-G containing SLC16A14/MCT14 needed to be down-stream of the poly-A tail. For confirmation plasmids were sequenced at Microsynth® (CH-9436 Balgach) and additionally confirmed by enzymatic digestion.

```
agactgggagccgagtgagatcttagcctctcgggctgcgtgcaaaaaccttagaaaatg
R  L  G  A  E  -  D  L  S  L  S  G  C  V  Q  K  P  -  K  M
tatacgagtcatgaagatatcgggtatgaccttgaagacgaccgaaaggctaagaataag
Y  T  S  H  E  D  I  G  Y  D  L  E  D  D  R  K  A  K  N  K
aagacgctgaagccccacccagatatcgatggcgggtgggcctggatgatggtcctctcg
K  T  L  K  P  H  P  D  I  D  G  G  W  A  W  M  M  V  L  S
tccttctttgttcacatcctcatcatgggctcacagatggccctaggagtcctcaacgtg
S  F  F  V  H  I  L  I  M  G  S  Q  M  A  L  G  V  L  N  V
gagtggcttgaagagtttcaccagagccgcggcctgaccgcctgggtcagctccctgagc
E  W  L  E  E  F  H  Q  S  R  G  L  T  A  W  V  S  S  L  S
atgggcatcaccttgatcgtgggacctttcatcggcttgttcattaacacctgcgggtgc
M  G  I  T  L  I  V  G  P  F  I  G  L  F  I  N  T  C  G  C
cgccagacagcaatcattggaggcctggtgaactccctcggctgggtgttgagcgcctat
R  Q  T  A  I  I  G  G  L  V  N  S  L  G  W  V  L  S  A  Y
gcagccaatgtgcagtctctctttattacctttggagtggcagcaggccttggcagtggg
A  A  N  V  Q  S  L  F  I  T  F  G  V  A  A  G  L  G  S  G
atggcttacctacctgcagtggtcatggtgggaaggtactttcagaagagacgagccctg
M  A  Y  L  P  A  V  V  M  V  G  R  Y  F  Q  K  R  R  A  L
gcccagggcctcagtaccacggggacaggatttgggacgttcctgatgaccgtgttgctg
A  Q  G  L  S  T  T  G  T  G  F  G  T  F  L  M  T  V  L  L
aaatacctgtgcgcagaatatggctggcggaatgctatgttcatccaaggtgctctgtcc
K  Y  L  C  A  E  Y  G  W  R  N  A  M  F  I  Q  G  A  L  S
ctgaacctgtgtgtctgtggggcgctcatgaggcccctctctcccgagaagttagaaaac
L  N  L  C  V  C  G  A  L  M  R  P  L  S  P  E  K  L  E  N
tgcccagaagcggaagagccgtgtgctctcccagcttactccactgaatctgttaagtct
C  P  E  A  E  E  P  C  A  L  P  A  Y  S  T  E  S  V  K  S
ggaggaccactgggcatggctgaagaacaggacagaaggcccgggaatgaggagatggtg
G  G  P  L  G  M  A  E  E  Q  D  R  R  P  G  N  E  E  M  V
tgtgaccttcaaacacaggagtgtcaaggtcaaacccatccgaggaagaatgtgtgtgcc
C  D  L  Q  T  Q  E  C  Q  G  Q  T  H  P  R  K  N  V  C  A
ttccgggttctgaagacagtgagccagctcactgtgcaagtccggaggggctttagggac
F  R  V  L  K  T  V  S  Q  L  T  V  Q  V  R  R  G  F  R  D
tggcactcaggctattttgggacggcttcactcttcaccaaccgcatgtttgtagccttt
W  H  S  G  Y  F  G  T  A  S  L  F  T  N  R  M  F  V  A  F
attttctgggctctgttcgcatacagcagctttgtcatccctttcatccacctgcccgaa
I  F  W  A  L  F  A  Y  S  S  F  V  I  P  F  I  H  L  P  E
atcgtcagtttgtataacttgtcagagcaaaatgacacattccctctgacctcgattata
I  V  S  L  Y  N  L  S  E  Q  N  D  T  F  P  L  T  S  I  I
gcaatacttcacatcttcgggaaggtgatcttgggggccgtggccgacctcccctgtatc
A  I  L  H  I  F  G  K  V  I  L  G  A  V  A  D  L  P  C  I
agcgtctggaatgtcttcctcatcgctaacttcaccctcgtcctcagcatcttccttctg
S  V  W  N  V  F  L  I  A  N  F  T  L  V  L  S  I  F  L  L
cctctgatgcacacctacgcgagtctggctgtcatttgtgccctaattgggttttctagc
P  L  M  H  T  Y  A  S  L  A  V  I  C  A  L  I  G  F  S  S
gggtatttctccctcatgcctgtggtgacagaggacctggttggcactgagcacttggcc
G  Y  F  S  L  M  P  V  V  T  E  D  L  V  G  T  E  H  L  A
aatgcctacggcatcatcatctgcgccaatggcatctcagccttactaggaccaccattc
N  A  Y  G  I  I  I  C  A  N  G  I  S  A  L  L  G  P  P  F
gcaggatggatctttgacatcacccaaaaatatgacttttccttttatatatgtggtttg
A  G  W  I  F  D  I  T  Q  K  Y  D  F  S  F  Y  I  C  G  L
ctttacatggtagggatactctttttgctcattcaaccgtgtattcagatgatagatcaa
L  Y  M  V  G  I  L  F  L  L  I  Q  P  C  I  Q  M  I  D  Q
tccagaaggaagtgcatagagggtgcacatgtttagtgtcctgtaacgtttcctgtgggt
S  R  R  K  C  I  E  G  A  H  V  -  C  P  V  T  F  P  V  G
```

Figure 9. SLC16A14/MCT14 cDNA (without Myc sequence, see results for myc-SLC16A14/MCT14 construct) and protein sequence in red. Added restriction sites are marked in blue. Green represents the stop codon. Yellow marked letters are the first and the last amino acids respectively of the coding sequence.

Primers for PCR with annealing restriction sites for *Sac*I and *Xho*I

*Sac*I
Forward Primer: 5' AAAAGAGCTCTATACGAGTCATGAAG 3'
Length: 16b
38% CG
35,5°C = Tm

*Xho*I stop
Reverse Primer: 5' AAAACTCGAGCTAAACATGTGCACC 3'
Length: 15b
47% CG
39,7°C = Tm

pSPOK-G (restriction sites for *Sac*I and *Xho*I)
5'Myc...GAGCTCGCCCCCCTCGAG.....3'
3' ...CTCGAGCGGGGGGAGCTC.....5'

Figure 10: Primers designed for modification of the 3' and 5' ends of SLC16A14/MCT14 sequence. *Sac*I and *Xho*I were chosen as restriction sites, since these sites were absent in the SLC16A14/MCT14 sequence and present only once in the pSPOK-G vector.

Reverse transcription of myc-SLC16a14/MCT

SLC16A14/MCT14 cDNA (2 µg) was linearized with *Pvu*II at the 3' end down stream the poly-A tail. The product was purified using the QIAquick gel extraction kit (Qiagen, Germany, Cat. No. 28704). cDNA was eluted in 25 µl of dH_2O. cRNA was synthesized using the mMessage mMachine® kit (Ambion, USA). To 1 µg of purified template (12 µl), 3 µl of 10x buffer, 12 µl NTPs/Cap mixture and 2 µl of enzyme mix containing Sp6 RNA polymerase were added to a final volume of 30 µl. The mixture was incubated at 37°C for 5 h. RNA synthesis was then stopped on ice with 20 µl of RNAse free water and 40 µl lithium solution kept at -20°C for at least 1 h. Precipitated cRNA was recovered by centrifugation (13'000 r.p.m. for 20min at 4°C) and the resulting pellet was washed with ice cold 70% ethanol. The tube was centrifuged for 10 min (4°C), ethanol was removed as much as possible and traces of ethanol were left to evaporate for 1 h. Final cRNA was dissolved in 25 µl of RNAse free dH_2O and its concentration determined. RNA was finally stored at -80°C until further use.

Xenopus laevis oocyte expression studies

Frogs (*Xenopus laevis*) were anesthetized using tricaine mesylate (MS222) (Sigma, USA, Cat. No. A5040) and oocytes were collected by surgery. Ovaries were cut into small pieces, pulled apart with forceps and washed several times (in 50 ml Falcon tubes) in calcium free Barth's solution (Table 2) using a rotator (Model 151, Level 2, Bender + Hobein, Switzerland). After several washes, liquid was removed and collagenase containing solution [20 ml calcium free Barth's solution, 4 mg trypsin inhibitor (Sigma Aldrich, USA), 40 mg collagenase type 1A (Sigma, USA)] was added in a ratio 3:1 (15 ml of collagenase containing solution to approximately 5 ml of oocytes (measured in a Falcon tube)). Collagenase digestion was performed for 30-35 minutes (at RT). Collagenase was removed by several washing steps with calcium free Barth's solution. Finally oocytes were washed twice with calcium containing Barth's solution and stored at 16°C. Final Barth's solution contained 5 mg doxycyclin (Fluka, USA, Cat. No. 44577) and 5 mg gentamicin (Fluka, USA, Cat. No. 48760) per liter.

Table 2. *Barth's solution*

Barth's Solution	
NaCl	88 mM
KCl	1 mM
$CaCl_2$	0.41 mM
$MgSO_4$	0.82 mM
$NaHCO_3$	2.5 mM
$Ca(NO_3)_2$	2 mM
HEPES	7.5 mM

pH was adjusted to 7.5 with 1M TRIS → autoclaved → antibiotics added before use → stored at 4°C

RNA was synthesized as described above and 25 ng in 50 nl were injected per oocyte using the Nanoject II (Drummond Scientific Company, USA). Ooocytes were incubated at 16°C for 3 days before uptake studies were conducted. Confirmation for

correct expression of the myc-Scl16a14 construct was realized by running a Western blot using oocyte homogenates (see oocyte homogenate preparation below).

Uptake Studies

Transport experiments with oocytes were performed either in the presence or the absence of Na^+ - ions (Table 3).

Table 3. *Uptake solutions for transport experiments with Xenopus laevis*

	ND100		**ND0**
NaCl	100 mM	Choline-Cl	100 mM
KCl	2 mM	KCl	2 mM
$CaCl_2$	1.8 mM	$CaCl_2$	1.8 mM
$MgCl_2$	1 mM	$MgCl_2$	1 mM

pH was adjusted to the desired pH (see results) using 1 M HEPES and 1 M Tris base.

Stock solutions of amino acids were prepared in uptake solutions or dH_2O, depending on the concentration required and the solubility of each amino acid. Radioactively labeled amino acids were added in quantities depending on their specific radioactivity. Uptake buffers containing a single substrate were supplemented with ^{3}H-labelled substrates (2 µCi/100 µl) or ^{14}C–labelled substrates (0.4 µCi/100 µl).

For each uptake, 10 oocytes (injected or non-injected) were used. Oocytes were added to a test tube and Barth's solution was removed carefully. 100 µl of uptake solution containing test substrate were added and incubation was performed at RT for 15 min. Uptake buffer was removed and oocytes were washed (3 to 4 times) with ice cold ND0 solution. Oocytes were transferred individually into single scintillation vials containing 200 µl of 4% SDS and put on a shaker for 30 min. Each vial was

filled with 3 ml scintillation liquid (Emulsifier-Safe™, Perkin Elmer, USA) and analyzed by liquid scintillation (Packard Tri-Carb 2900TR).

Protein related methods

Kidney homogenate and brush border membrane isolation

Pieces of frozen kidneys were added to 800 µl of homogenization buffer (300 mM D-mannitol, 5 mM EGTA, 12 mM Tris-base; adjusted with concentrated HCl to pH 7.1; buffer A). Protease inhibitor, Phenyl-methane-sulfonylfluoride (PMSF) (Sigma, USA), previously dissolved in isopropanol, was added to give a final concentration of 0.5 mM. The amount of tissue (wet weight) did not exceed 10% of the total volume of the homogenization buffer. Homogenization was performed with a Polytron homogenizer (Model 2100, about 15'000 r.p.m.) for 90 s on ice. The homogenate was shock frozen and stored at -80°C until further analysis.

Proximal tubular brush border membranes (BBMV) were isolated as described [182]. To the homogenate of kidney tissue (see above), 1 ml of water and 1 M $MgCl_2$ (to give a final 12 mM solution) were added. This mixture was kept on ice for 15 min followed by centrifugation (Sorvall® RC-5B) at 4'500 r.p.m. (3'000 g_{av}) with a SS34 rotor (Sorvall®) at 4°C. The formed supernatant was removed and centrifuged at 16'000 r.p.m. for 30 min at 4°C. The pellet was resuspended in 500 µl diluted (1:1) buffer A. Tubes were again centrifuged at 16'000 r.p.m. for 30 min and the final pellet resuspended in a small amount of diluted (1:1) buffer A using a 25 G needle mounted on a 1 ml tuberculin syringe. Purified BBMV's were shock frozen and kept at -80°C until further use.

Oocyte homogenate

Three oocytes were pooled in a 1.5 ml Eppendorf tube. Barth's solution was removed and 60 µl of homogenization buffer (20 mM Tris-HCl pH 7.6, 100 mM NaCl, 5 mM EDTA) were added. To prevent protein degradation, 1 µl of protease inhibitor cocktail (PIC) (Sigma, USA) was added to 5 ml of homogenization buffer. Oocytes were ruptured by pipetting (yellow tip) up and down until an even homogenate was formed. Following homogenization, Eppendorf tubes were vortexed for 20 s and placed on ice. Centrifugation was performed at 17'000 r.p.m. (Sorvall® RP45-A rotor) for 3 min at 22°C and resulted in two separate layers and a pellet. Below the surface layer, cellular proteins can be collected with the homogenization buffer. In order to remove the homogenization buffer containing the proteins, a 200 µl pipette penetrated the surface and the solution below was extracted.

Determination of protein concentration

Protein concentrations were determined by the Bio-Rad D_c Protein Assay (BioRad, USA). Measurements were done in triplicates (in 96-well plates) and a standard curve was included using BSA (10 mg/ml stock solution). Homogenates and BBMV solutions were diluted 1:20 and 1:5 respectively and 5 µl were used for each determination. The reaction was performed according to the protocol of the manufacturer and after 15 min absorption was determined at 595 nm (Analyzer *µ*Quant, Biotek®).

Western blots

Proteins were separated by SDS-polyacrylamide gel electrophoresis (SDS-PAGE). Minigels were prepared as described in Table 4.

Table 4. *SDS-PAGE Protocol*

Gel %:	9%	10%	15%.	stacker
Water	3.21 ml	2.75 ml	0.50 ml	3.75 ml
Tris/HCl, pH 8.8 (1.5 M)	2.50 ml	2.50 ml	2.50 ml	--------
Acrylamide stock (22%)	4.10 ml	4.55 ml	6.80 ml	1.70 ml
Tris/HCl,pH 6.8 (0.5 M)	----------	----------	---------	1.90 ml
SDS 20%	0.05 ml	0.05 ml	0.05 ml	0.04 ml
Am.-persulfate (10%)	0.10 ml	0.10 ml	0.10 ml	0.07 ml
Before pouring gel add: TMED (Sigma)	4 µl	4 µl	4 µl	5 µl

Homogenate and BBM samples were thawed on ice prior to use. 6 mg of DL-dithiotreitol (DTT) (Fluka, USA) were added to 100 µl concentrated 4x Laemmli buffer (4x LB; 8% SDS, 40% glycerol, 20% 2-mercaptoethanol, 0.008% bromophenol blue, 0.25 M Tris-HCl with final pH 6.8, aliquoted and stored at -20°C). 50 µg homogenate or 15 µg BBM, were made up to a volume of 10 µl using dH_2O. 4 µl of LB containing DTT were added, and samples boiled for 2 min at 95°C followed by quenching on ice. Electrophoresis was performed at 12-15 mAmp/gel in 25 mM Tris, 190 mM Glycine, and 0.1% of SDS .

Separated proteins were transferred onto nitrocellulose membranes (Whatman® Schleicher & Schuell Protran BA 83 0,2 µm) in 25 mM Tris, 190 mM glycine and 20% methanol (100 V for 80 min). After transfer, nitrocellulose membranes were washed in TBS (150 mM NaCl, 25 mM Tris-HCl, pH 7.4) and incubated for 1 h in blocking buffer (TBS containing 5% of low fat milk powder (Coop-Switzerland) adjusted to pH 7.4). Incubation with primary antibodies was performed in blocking buffer overnight at 4°C (see supplementary table S2 listed at the end of “Materials and Methods”). On the next day, membranes were washed 3 times in TBS for 10 min each, followed by incubation in blocking buffer for 1 h. Secondary antibodies (coupled to horse radish peroxidase; GE Healthcare, UK) were added and incubation was continued for another 2 h. Blots were washed at least 3 times with TBS and incubated for 3 min in chemiluminescent substrate (SuperSignal®, West Pico, USA). Chemiluminescence was recorded with an image analyzer (LAS-4000, Fujifilm).

Immunohistochemistry

Kidney tissue was fixed *in situ* with a fixative solution made from the the following stock solutions:

- **Fixative 1:** 0.1 M cacodylate buffer: 10.71 g of sodium-cacodylate (Sigma, USA, Cat. No. CO250-250G) together with 17.12 g of sucrose were dissolved in 500 ml of dH_2O and adjusted with HCl to a pH of 7.4. This solution was checked for an osmolarity of 300 mOsm.
- **Fixative 2:** 0.1 M of phosphate buffer: (1) 0.2 M NaH_2PO_4 (Sigma, USA) (stored at 4°C). (2) 0.2 M Na_2HPO_4 (Sigma, USA) (stored at RT). (3) 0.1 M $CaCl_2$ (Sigma, USA) (stored at 4°C). For use: 95 ml of (1) mixed with 405 ml of (2), 2.3 ml of (3), 450 ml of dH_2O, pH adjusted to 7.4, and final volume corrected to 1000 ml.
- Caco-HAES or phosphate buffer-HAES: 0.33 g of $MgCl_26H_2O$ together with 0.5 g picric acid were added to 200 ml 10% hydroxyethyl starch in isotonic NaCl (HAES) (Fresenius Kabi, Germany GmbH) and 300 ml of 0.1 M cacodylate buffer or 0.1 M phosphate buffer (see above) was added.
- 33% PFA: 15 g of PFA (Aldrich, USA, Cat. No. 16005) were added to 45 ml H_2O (pre-heated to 70°C). 10 N NaOH was added dropwise until the solution became clear.

To obtain a working fixative solution, Caco-HAES buffer was mixed with 45 ml 33% PFA solution to a volume of 500 ml to obtain a 3% PFA fixative solution. The pH of the solution was adjusted to 7.4 (with HCl or NaOH) and filtered (Whatman®, Schleicher & Schuell, 0.2 µm). The final solution was used directly or stored at -20°C for up to one year.

Perfusion of kidneys:

In-situ perfusion of kidneys was performed via the left ventricle. Perfusion was started with 5 ml PBS followed by approximately 50 ml of final fixative solution. Kidneys were removed, cut in 2 pieces, and incubated for two hours in fixative solution followed by

washing steps (5 times) with PBS. Thin kidney slices were placed on cork pieces together with a small drop of Kryostat® (Medite, Nunningen, Switzerland) for tissue embedding. Tissue was snap frozen in liquid propane and stored at -80°C.

A cryostat microtome (Leica CM1850) was used to cut kidney slices of 4-5 µm thickness that were fixed onto poly-lysine coated glass slides (O. Kindler GmbH & Co., Freiburg, Germany). Serial cuts were fixed and oriented on the same slide. Single tissue slices were encircled with the "ImmEdge" pen (Vector laboratories, USA, H-4000). Glass slides were placed in PBS and washed 3 times (10 min each). Finally, tissue slices were washed and incubated in PBS (at 4°C) overnight. Tissue sections were incubated (at RT) with blocking buffer (1% BSA and 0.02% Na^+-azide in PBS) for 15 min in a humid chamber. Antibodies (see Supplementary table S2) were diluted in blocking buffer, and 50-100 µl were added to the slices followed by an incubation of 60 to 90 min. Slides were washed 3 times (10 min each) in PBS. The secondary antibody, donkey Alexa Fluor® 488 anti rabbit IgG (H+L) (2 mg/ml) (Molecular Tecnologies® Invitrogen, USA) was diluted in blocking buffer 1:1000 and applied to the slices for 60 min (humid chamber under dark conditions). Finally, slides were washed 3 times (10 min each) in PBS. Processed tissue slices were mounted in Glycero Gel mounting medium (DakoCytomation, Denmark) and left to dry for 30 min. Immunofluorescence was detected with a fluorescent microscope (Eclipse TE 300 Nikon, Japan) and images were recorded with the NIS-Elements F3.0 software (Nikon, Japan).

Urine and Blood Analysis

Creatinine determination

Urinary content of creatinine was determined according to the method of Jaffé [183-184]. The following solutions were used:

- Reagent A: 4.4 g of NaOH dissolved in 400 ml dH_2O. Then 9.5 g trisodium phosphate ($Na_3PO_412H_2O$) and 9.5 g sodium tetraborate ($Na_2B_4O_710H_2O$) were added. After solutes where dissolved, pH was checked to be above 10 and if necessary adjusted with 10 M NaOH. Water was added to a volume of 500 ml and the solution was stored at 4°C (up to 3 months).
- Reagent B: 5% sodium dodecyl sulfate (SDS) (Calbiochem® Merck, Darmstadt, Germany) in dH_2O solution was prepared and kept at RT.
- Reagent C: 7 g of moist picric acid was added to 500 ml of distilled water and mixed overnight at 37°C. The solution was filtered and stored light protected at room temperature. The reagent was stable for up to one year.
- A creatinine (Sigma, USA) standard solution (1 mg/ml) was prepared in 0.1 M HCl.

Sample solutions were prediluted 1:5 (10 µl urine + 40 µl dH_2O) before measurements. The working reagent was made up with equal volumes of reagent A, B, and C. 10 µl of each sample or standard solution were added to a 96 well plate (Nunclon™ Surface, Denmark). 150 µl of working reagent was added, mixed and plates were incubated for 30 min at RT. Absorption was measured at 505 nm. 10 µl of 30% acetic acid were added and after 5 min at RT, absorbance at 505 nm was measured again. The second OD_{505} was subtracted from the first one and creatinine concentration was calculated.

Phosphate determinations

Pi concentrations in plasma and urine were determined according to Fiske and Subbarow [185]. The following solutions were used:

- 20% trichloroacetic acid (TCA)
- 1.25 g Ammonium molybdate in 100 ml of 2.5 N H_2SO_4
- 1 g of Fiske & Subbarrow reducer (Sigma, USA, Cat. No. F5428-25G) per 6.3 ml of dH_2O

- Phosphate standard solution was purchased from Randox® Laboratories (United Kingdom)

Before measurements, urine samples from the HPD group animals were diluted 1:10. Serum Pi was determined without prior dilution of samples. Samples or standards (10 µl) were mixed with 90 µl of 20% TCA and vortexed for 10 s. 900 µl of dH_2O were added and tubes were vortexed again for 10 s. Samples were left on ice for 10 min followed by centrifugation for 20 min at 13'000 r.p.m. at 4°C. 250µl of supernatants were added to a 96-well plate (Nunclon™ Surface, Denmark) and 50 µl of ammonium molybdate solution was added followed by the addition of 12.5 µl of Fiske & Subbarrow reducer solution. The plate was rotated gently and left at room temperature for 15-20 min. Absorption was determined at 620 nm.

Ion chromatography and NH_3/NH_4^+ determination

Urine samples of LPD and HPD mice were analyzed for K^+, Na^+, Mg^{2+}, Ca^{2+}, and Cl^- using ion exchange chromatography (Metrohm ion chromatography, Herisau, Switzerland). Urinary content of ammonium was measured according to the protocol of Berthelot [186].

Following reagents were prepared:

- Phenol Reagent (Sigma, USA, Cat. No. 242322) (for 100 ml) containing 5 g together with 0.025 g of Sodium nitroprusside ($Na_2[Fe(CN)_5NO]2H_2O$) (Sigma, USA, Cat. No. S0501)
- Alkaline Reagent (for 100ml) containing 2.5 g NaOH and 2.82 ml Sodium hypochlorite (Sigma, USA, Cat. No. 425044)
- Ammonium standard solution (50 mM of NH_4^+) with 33 mg ammonium sulphate (Sigma, USA, Cat. No. A4418) made up to 100 ml.

Urine dilution was 1:10. A Standard curve was obtained using the ammonium stock solution. For control anaylsis, phenol reagent was used as a negative control (blank). To 20 µl of each urine sample, 1 ml of phenol reagent was added in an Eppendorf and vortexed briefly. 1 ml of alkaline reagent was added and vortexed again. Tubes were left incubated for 40 min at RT. 300 µl of each sample were added to a 96 well plate (Nunc™, Denmark) and analyzed at 623 nm.

Statistics

All experimental results (microarray analysis (see above), real time RT-qPCR, oocyte uptakes, quantification of immunoblots) are expressed as means ±SEM. The 2D graphical and statistical software GraphPad Prism® was used for data handling. Data evaluation analysis for statistical significance was done by unpaired student *t*-test. The levels of significance were defined as follows; highly significant ($^{***}p < 0.001$), very significant ($^{**}p < 0.01$), and significant ($^{*}p < 0.05$).

Supplementary

Supplementary table S1a. *Designed primers and probes used for RT-qPCR*

Gene	Acc. N.	Primers	Probe (reporter : FAM, quencher TAMRA)
SLC38a3 (SNAT3)	NM_023805	F: 5'-CGAATCATGCCCACTGACAA-3' (1651-1670) R: 5'-AACCGCAGCGAAACAAAGG -3' (1704-1722)	5‘-AGCCTGCAAGATCCACCCCTAAAATCCT -3' (1673-1700)
PEPCK	NM_028994	F: 5’-GTGGGCGATGACATTGCC-3’ (1062-1079) R: 5’-ACTGAGGTGCCAGGAGCAAC-3’ (1143-1162)	5’-CCCAAGGCAACTTAAGGGCTATCAACCC-3’ (1096-1123)
SLC34a1 (NaPi-2a)	NM_011392	F: 5'-TGATCACCAGCATTGCCG-3' (907-924) R: 5'-GTGTTTGCAAGGCTGCCG-3' (1022-1039)	5'-CCAGACACAACAGAGGCTTCCACTTCTATGTC-3' (975-1006)
SLC34a3 (NaPi-2c)	NM_080854	F: 5'-TAATCTTCGCAGTTCAGGTTGCT-3' (1399-1421) R: 5'-CAGTGGAATTGGCAGTCTCAAG-3' (1478-1499)	5'-CCACTTCTTCTTCAACCTGGCTGGCATACT-3' (1427-1456)
β-actin	NM_007393	F: 5'-GACAGGATGCAGAAGGAGATTACTG-3' (1010-1034) R: 5'-CCACCGATCCACACAGAGTACTT-3' (1085-1107)	5'-AGGAGGAGCAATGATCTTGATCTTCATGG-3'

Supplementary Table S1b. *Expression Assays® (AppliedBiosystems) for RT-qPCR*

Gene	Acc. N.	Assay ID
SLC7a12	NM_080852	Mm00499866_m1
SLC39a14	NM_001135151	Mm00522700_m1
SLC16A14/MCT14	NM_027921	Mm01272722_m1
Abcb1a	NM_011076	Mm00440761_m1
Glud1	NM_008133	Mm00492353_m1
Acot1	NM_012006	Mm01622471_s1
Acot11	NM_025590	Mm00452633_m1
Cyp51	NM_020010	Mm00490968_m1
Car4	NM_007607	Mm00483021_m1
Cyp27B1	NM_010009	Mm01165921_g1
18 S rRNA	NM_022551	Hs99999901_s1
Omd	NM_012050	Mm00449589_m1
FKBP51	NM_020009	Mm00444968_m1
Gphn	NM_172952	Mm00556895_m1

Supplementary Table S2. *Primary Antibodies used for Immunohistochemistry and Western Blots*

Antibody for:	Type	Raised against (peptide sequence)	Dilution		Source	Reference
			Western Blot	Immunohisto-chemistry		
ROMK (mouse, rat)	Rabbit (polyclonal)	Commercial (intracellular C-terminus)		1 : 200	Alomone Labs (Jerusalem, Israel), provided by Prof. Loffing (Institute of Anatomy, UZH)	
MCT14 (mouse)	Rabbit (polyclonal)	NH_2-KSGGPLGMAEEQDRRPGNEEMVC-COOH (affinity purified)	1 : 4'000	1 : 200	Pineda Ab-Production (Berlin, Germany)	
NKCC2 (mouse)	Rabbit (polyclonal)	NH_2-CEYYRNTGSVSGPKVNRPSLQE-COOH		1 : 20'000	Provided by Prof. Loffing (Anatomical Institute, Universtiy of Zürich)	[187]
NaPi-2a (mouse)	Rabbit (polyclonal)	Synthetic 12-mer C-terminal and N-terminal NaPi-2a peptides	1 : 4'000	1 : 500	Physiological Institute, University of Zürich (Prof. Murer's Lab)	[31, 46]
NaPi-2c (mouse)	Rabbit (polyclonal)	NH_2-CYENPQVIASQQL-COOH (affinity purified)	1 : 1'000		Physiological Institute, University of Zürich	[100]
β-actin (mouse)	Mouse (monoclonal)	Commercial	1 : 30'000		Sigma, USA	

Abbreviations

LPD	Low phosphate diet
HPD	High phosphate diet
RT	Room temperature
DEPC	Diethylpyrocarbonate
RIN	RNA integration number
FGCZ	Functional Genomics Center University Zürich
HEPES	4-(2-hydroxyethyl)-1-piperazineethanesulfonic acid
PBS	Phosphate buffered saline
CHAPS	3-[(3-Cholamidopropyl) dimethylammonio]-1-propanesulfonate
EDTA	Ethylene diamine tetraacetic acid
DIG	Digoxigenin
PFA	Paraformaldehyde
SDS	Sodium dodecyl sulphate
EGTA	Ethylene glycol tetraacetic acid
PMSF	Phenyl-methane-sulfonylfluoride
BBMV	Brush border membrane vesicles
PIC	Protease inhibitor cocktail
BSA	Bovine serum albumin
TCA	Trichloroacetic acid
DTT	Dithiotreitol
TBS	Tris buffered saline
HAES	Hydroxyethyl starch
SEM	Standard error of the mean
RT-qPCR	Real Time Quantitative PCR

RESULTS

Microarray analysis after 5 days ("chronic") of LPD and HPD administration

In a first attempt to determine if altered intake of dietary Pi changes renal gene expression, mice were fed either a HPD or LPD for 5 days ("chronic" adaptation). Animals were sacrificed in the morning at 8 am of the 6th day, and kidneys and blood were harvested. The effect of different Pi-diets was controlled by a determination of plasma Pi-concentration and by analysis of the amount of the Na/Pi-cotransporter NaPi-2a. As illustrated in Figure 11 A, mice fed a LPD showed reduced Pi serum concentration levels compared to mice fed a HPD. Only traces of Pi were deteted in the urine of LPD mice while phosphaturia was observed in mice fed a HPD (data not shown). The pH values of the urine were determined as well, and a significant difference between both groups was assessed. There was a clearly acidic urine in the HPD group when compared to the LPD group, which was rather scattered and partly basic (Figure 11 B). In agreement with published results [23, 142], the amount of NaPi-2a protein was higher in kidneys of mice fed a LPD compared to mice fed a HPD (Figure 11 C).

Total renal RNA was extracted and analyzed by RT-qPCR for contents of NaPi-2a and NaPi-2c mRNAs. As illustrated in Figure 12, no significant change for NaPi-2a mRNA, but a 2-fold difference in the NaPi-2c mRNA content was observed between the LPD and HPD groups; these data were in agreement with published data [49]. Of note, content of NaPi-2a mRNA was approximetely 100-fold higher than NaPi-2c mRNA reflecting the relative importance of the two Na/Pi-cotransporters in renal Pi handling [188].

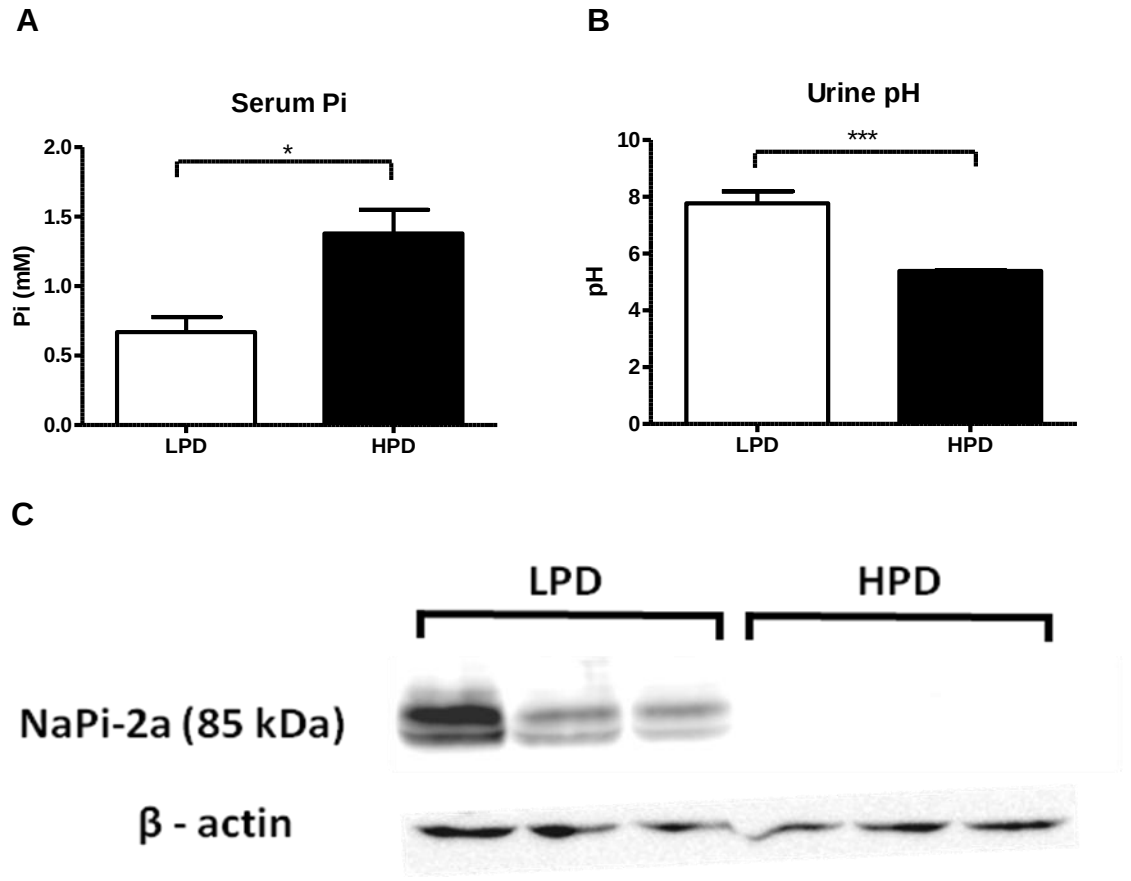

Figure 11. "Chronic" adaptation (5 days) of mice to low (LPD) and high (HPD) Pi-diets. **(A)** Serum Pi concentration. **(B)** Comparison of urine pH between mice that received LPD and a HPD. **(C)** Western blot analysis for NaPi-2a in kidney homogenates. Immunoblot was stripped and reprobed with an antibody against *β*-actin for control of equal loading. Data with ± SEM; $n = 6$; *$p < 0.05$, ***$p < 0.001$.

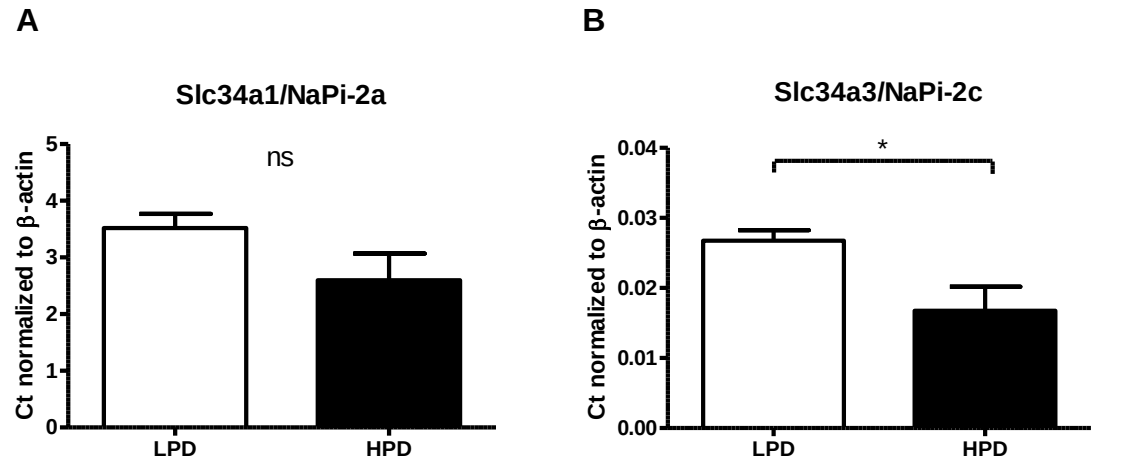

Figure 12. RT-qPCR for Na/Pi-cotransporters after "chronic" (5 days) feeding of mice with LPD and HPD. **(A)** NaPi-2a mRNA shows no significant (ns) difference between LPD and HPD **(B)** NaPi-2c mRNA was significantly up-regulated by LPD compared to HPD. Data with ± SEM; $n = 6$; *$p < 0.05$.

Before total RNA samples were processed for microarray analysis, they were analyzed by electrophoresis for quality using the 2100 Bioanalyzer (Agilent technology, Waldbronn, Germany) (Figure 13). In all samples the ratio 260/280 nm was 2.15 to 2.25 and with a RIN of at least 9 (a RIN of 8 was required for microarray analysis). Best 4 total RNA samples of each group were processed and analyzed by hybridization onto GeneChip® Mouse Genome 430 2.0 arrays (Affymetrix).

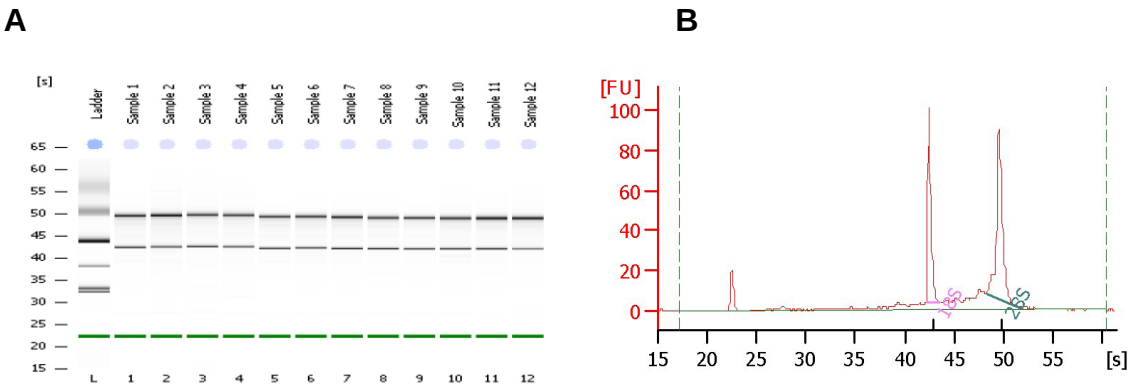

Figure 13. Quality analysis of total kidney RNA. Samples 1-6 were from LPD animals and samples 7-12 were from mice that have been given a HPD. **(A)** Virtual gel of RNA samples integrated from the information obtained in (**B)** that shows the peaks of ribosomal 18 S and 28 S RNA. Quality is determined by the RIN (RNA integration number) which is obtained by integrating the area beneath the peaks obtained from the ribosomal RNAs.

Of the 8 samples hybridized to the chip containing approximately 34'000 protein coding genes with over 39'000 transcripts, 12'934 genes were detected representing 38% of the total number that were present on the array. 3833 genes were detected to be changed significantly ($p < 0.05$) in response to LPD versus HPD feeding (see Supplementary table S3 on CD). Of those, 1892 were detected to be up-regulated (1259 genes with a fold change ≥ 1.5) and 1762 genes were down-regulated (631 with a fold change ≤ 0.67). Only genes with a fold change of 50% and higher were considered for further analysis. Genes whose expression was affected mostly (microarray fold change (mFC) ≥ 50%, $p < 0.01$) by LPD vs. HPD diet are listed in Table 5 a & b.

Table 5a. *Genes down-regulated after 5 days of LPD (p < 0.01)*

Gene Symbol	Gene Name	Fold Change	GeneBank Acc. No.
Ccl28	Chemokine (C-C motif) ligand 28	0.08	NM_020279
Ces1	Carboxylesterase 1	0.12	NM_021456
Odc1	Ornithine decarboxylase, structural 1	0.19	NM_002539
SLC16A14/MCT14	Solute carrier family 16, member 14	0.21	NM_027921
Frzb(SFRP3)	Small frizzled related protein 3	0.40	NM_011356
Trp53bp	Transformation related protein 53 binding protein 2	0.42	NM_173378
Lpl	Lipoprotein lipase	0.42	NM_008509
PEPCK	Phosphoenolpyruvate carboxykinase 1, cytosolic	0.43	NM_011044
SLC39A14	Solute carrier family 39, member 14 (zinc transporter)	0.48	NM_001135151
CCKAR	Cholecystokinin A receptor	0.50	NM_009827
AACS	Acetoacetyl-CoA synthetase	0.56	NM_030210

Table 5b. Genes *up-regulated after 5 days of LPD (p < 0.01)*

Gene Symbol	Gene Name	Fold Change	GeneBank Acc. No.
Cyp27B1	Cytochrome P450, family 27, subfamily b	10	NM_010009
Abtb2	Ankyrin repeat and BTB(POZ) domain containing 2	7.7	NM_178890
ABC1a	ATP binding cassette sufamily B (MDR/TAP) member 1A	4.3	NM_011076
Olfm3	Olfactomedin 3	4.2	NM_153458
Pik3ca	Phosphatidylinositol 3-kinase, catalytic	4.2	NM_008839
Acot3	Acyl-CoA thioesterase 3	3.7	NM_134246
Acot1	Acyl-CoA thioesterase 1	3.5	NM_012006
Lrat	Lecithin-retinol acyltransferase	3.5	NM_023624
SLC25A36	Solute carrier family 25, member 36	2.7	NM_138756
Jub	Ajuba	2.0	NM_010590

List of selected genes that were down- and up-regulated after a LPD (vs. HPD). For each gene, the symbol, gene name, fold change, and GeneBank accession number is given.

Some genes were selected and analyzed by RT-qPCR (Figure 14) chosen either randomly (e.g. Slc7A12, Supplementary table S3) or selectively (e.g. Cyp27B1, Table 5b) to confirm changes observed on the GeneChip. Another solute carrier, SLC7A12, a cationic amino acid transporter, was shown by RT-qPCR to be up-regulated after a LPD, confirming microarray data (mFC = 3.5). The aromatic amino acid transporter SLC16A10/TAT1 (mFC = 3.6) was not significantly changed when tested using RT-

qPCR. Amplification of gephyrin, a protein involved in sorting, did not agree with the data on the chip (mFC = 2). The zinc transporter SLC39A14/ZIP14 (mFC = 0.5) also showed lower expression in the LPD group when compared to the HPD group based on the data collected by RT-qPCR. The Abcb1a transporter was not significantly changed, even though a difference of mRNA content between both diet groups was detected on the chip (mFC = 1.8). Cyp27B1 (1α-hydroxylase), the enzyme responsible for the activation of Vitamin D, was strongly up-regulated as expected [173], in LPD when compared to HPD group (mFC = 10). This was also confirmed by RT-qPCR. SLC16A14/MCT14, a member of the monocarboxylate transporter family with unknown function (See below “Characterization of SLC16A14/MCT14”), was strongly down-regulated in the LPD group based on the chip data (mFC = 0.2). This was also supported by RT-qPCR experiments. Overall, for most genes tested, fold-changes, as observed by microarray chip analysis, could be reproduced by RT-qPCR using total kidney RNA obtained from independent experiments (Figure 15).

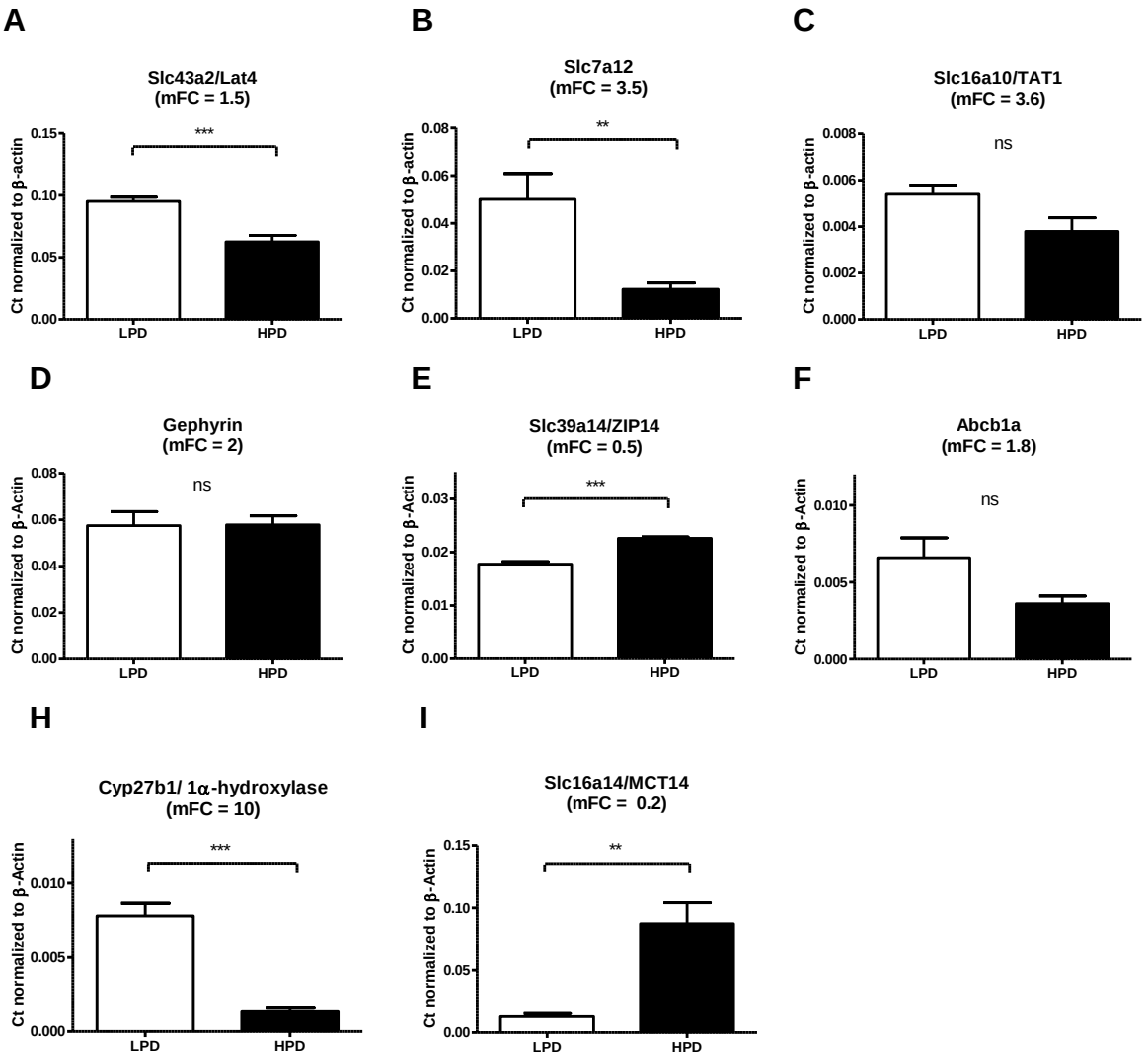

Figure 14. RT-qPCR confirmation of gene transcripts from microarray data. Below the gene name, in paranthesis, the fold change (mFC) obtained from microarray data is presented. For confirmation, genes have either been randomly **(A-F)** chosen from the gene list obtained (See Supplementary table S3), or selectively based on known responsive actions to Pi, such as **(H)** 1α-hydroxylase, or for classification of a new dietary Pi responder, such as **(I)** SLC16A14/MCT14. Data with ± SEM. $n = 6$, ns: not significant $^{**}p \leq 0.01$,$^{***}p \leq 0.001$.

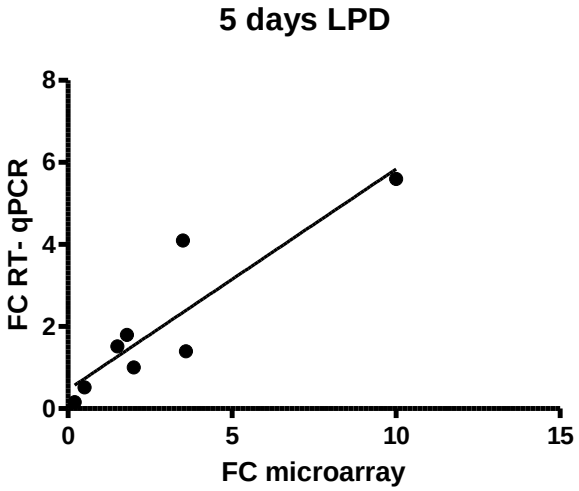

Figure 15. Linear regression after 5 days of LPD between fold changes (FC) of selected genes analyzed by RT-qPCR and micorarray analysis. $n = 8$, $R^2 = 0.803$.

Pathway Analysis

Web based pathway analysis toolkits (e.g. WebGestalt, G-profiler) indicated that most of the genes affected by “chronic” (5 days) intake of a LPD were involved in oxidative phosphorylation and energy metabolism. Other pathways affected were lipid metabolism, skeletogenesis, adipogenesis, and Wnt signalling (see Discussion Table 10 a & b). Nine solute carrier transporters (SLC) responded to dietary Pi depletion (3 down- and 6 up-regulated, See Table 6). Of the monocarboxylate transporter family (SLC16), two members were found to be changed; the amino acid transporter Tat1 (SLC16A10) and the SLC16A14/MCT14, of unknown function, with a fold change of 2.6 and 0.2 respectively.

As expected, Cyp27B1/1α-hydroxylase, was up-regulated (mFC = 10) in response to LPD (see also Discussion). In addition, phosphoenolpyruvate carboxykinase (PEPCK), a key enzyme in gluconeogenesis, was found to be regulated as well (mFC = 0.4). Interestingly, altered expression levels of PEPCK have also been observed in response to acid loading in mice [189]. Also, the small frizzled related protein sFRP3 was down-regulated (mFC = 0.4) in LPD mice. sFRP3 has been demonstrated to regulate limb skeletogenesis, triggering hip osteoarthritis [190], cell growth, apoptosis

and differentiation of specific cell types [191]. It was previously shown that small frizzled related protein 4 (sFRP4) has phosphaturic effects by selectively inhibiting the Na/Pi-cotransport in the kidney [79] as well as acting as a soluble modulator in the Wnt signalling pathway [192]. Whether sFRP3 has a similar inhibiting or antagonizing effect on Na/Pi-cotransport as sFRP4 remains to be elucidated. Surprisingly, both factors, sFRP3 and sFRP4 have been shown to modulate cell apoptosis when acting through the Wnt signalling pathway [192].

Table 6. *Solute carriers affected by dietary Pi ($p < 0.01$)*

Gene Symbol	Solute Carrier	Fold Change	GeneBank Acc. No.
SLC16A14/MCT14	Monocarboxylate transporter, unknown	0.2	NM_027921
SLC39A14	Zinc transporter, widespread	0.5	NM_001135151
SLC37A2	Glycerol 3-phosphate exchanger, widespread	0.6	NM_020258
SLC43A2	Lat4, neutral amino (aa) acid transporter, kidney	1.5	NM_173388
SLC6A8	Na^+/Cl^-/creatine cotransporter, ubiquitous	1.6	NM_133987
SLC35E3	Nucleoside/sugar transporter family member, unknown	1.7	NM_029875
SLC16A10	TAT1, Aromatic aa transporter, kidney (basolateral)	2.1	NM_028247
SLC25A36	Mitochondrial carrier, unknown	2.7	NM_138756
SLC7A12	Cationic aa transporter/glycoprotein family member, unknown	3.4	NM_080852

In summary, the profile of renal gene expression after “chronic” (5 days) feeding with a LPD (versus HPD) showed that many genes involved in energy metabolism were affected (see discussion for details). This may be an obvious finding at first glance,, as intracellular Pi is directly involved in the generation of ATP. Therefore, disturbances of energy metabolism may affect in a more pleiotropic way various other cellular functions as manifested by the high number of genes, the expression of which was affected by “chronic” LPD. In order to find genes that are possibly more directly influenced by LPD, the period of intake of LPD was therefore shortened in a new experimental setup.

Investigating an early time point for responses to different Pi-diets

Intake of different Pi-diets (under trained conditions) results, within a few hours, in an altered abundance of the Na/Pi-cotransporter NaPi-2a [149-151]. This effect, however, is not associated with altered expression of NaPi-2a mRNA. In order to establish a time point suitable to investigate early effects of altered Pi-diet on renal gene expression, mice were trained to eat for 5 days between 6 and 9 pm. On the day of experiment, mice were fed for 3 hours (h) (6 to 9 pm) with high (control) or low Pi-diets and kidneys and blood were harvested 4, 8 and 14 h after the onset (6 pm) of the different Pi-diets. As shown in Figure 16, hypophosphatemia was detected after 4 h and was not altered after 8 h. Interestingly, after 14 h of LPD, serum Pi was elevated again accounting for a significant increase from 8 to 14 h.

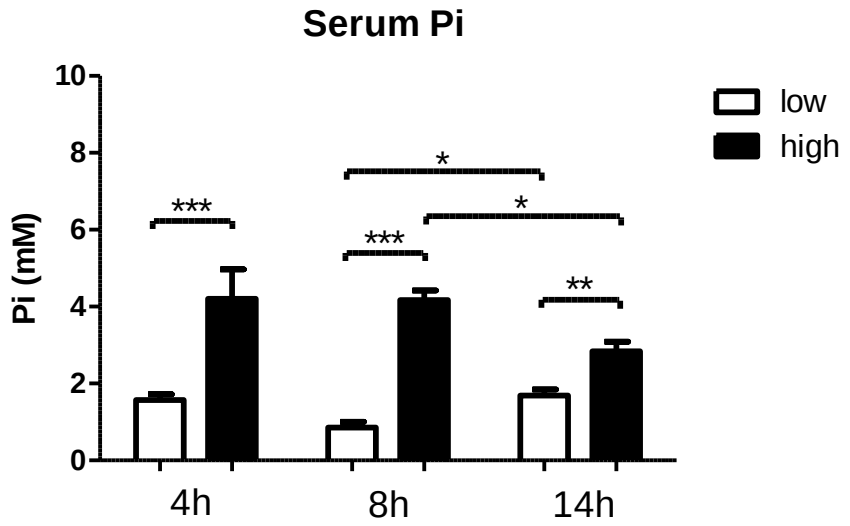

Figure 16. Serum Pi of mice given a LPD and a HPD over different time points. After 4 h, a significant decrease in serum Pi concentration of mice with LPD intake can be observed. This difference is further observed after 8 h which then increases in the LPD group significantly after 14 h. Data with ± SEM; *n* = 3-6; **p* < 0.05, ***p* < 0.01, ****p* < *0.001.*

From kidneys harvested after the different time points, BBM were isolated and analyzed for abundance of the Na/Pi-cotransporter NaPi-2a by immunoblot. As illustrated in Figure 17**,** NaPi-2a abundance was increased after 4 and 8 h of LPD as

expected. Similar changes of NaPi-2a abundance were observed after 14 h (data not shown).

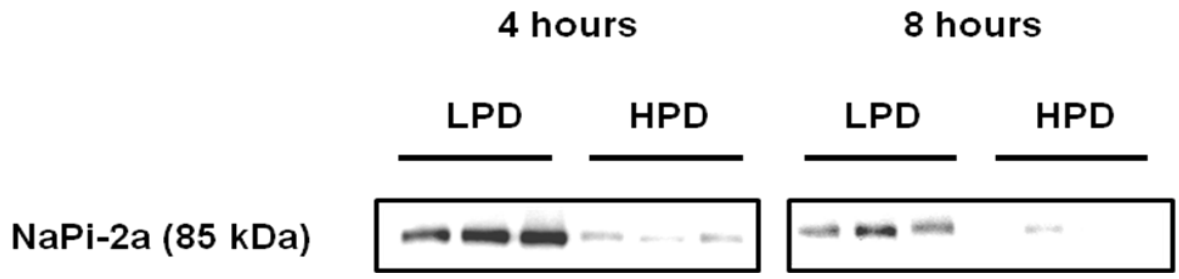

Figure 17. Western Blot of NaPi-2a. Regulation of NaPi-2a abundance in the BBM of the proximal tubule after 4 h and 8 h of LPD in comparison to HPD.

RT-qPCR for selected genes was performed on total renal RNA isolated after 4, 8 and 14 h of feeding periods. These genes were found to be regulated during “chronic” adaptation to LPD (compared to HPD). For expression of selected genes, most significant differences between the two Pi-diets were observed after 14 h, whereas no significant changes were observed after 4 and 8 h (data not shown). As illustrated in Figure 18, expression of the SLC16A14/MCT14 gene was similarly affected (0.2 fold) by LPD as observed after “chronic” (5 days) adaptation. Cyp27B1 did not respond at any of the three periods, which agrees with data previously published [173]. After 14 h, altered expression of PEPCK and Acot1 were observed as well. Based on this data, a 14 h period (referred thereafter as “acute” adaptation) was selected for further investigations.

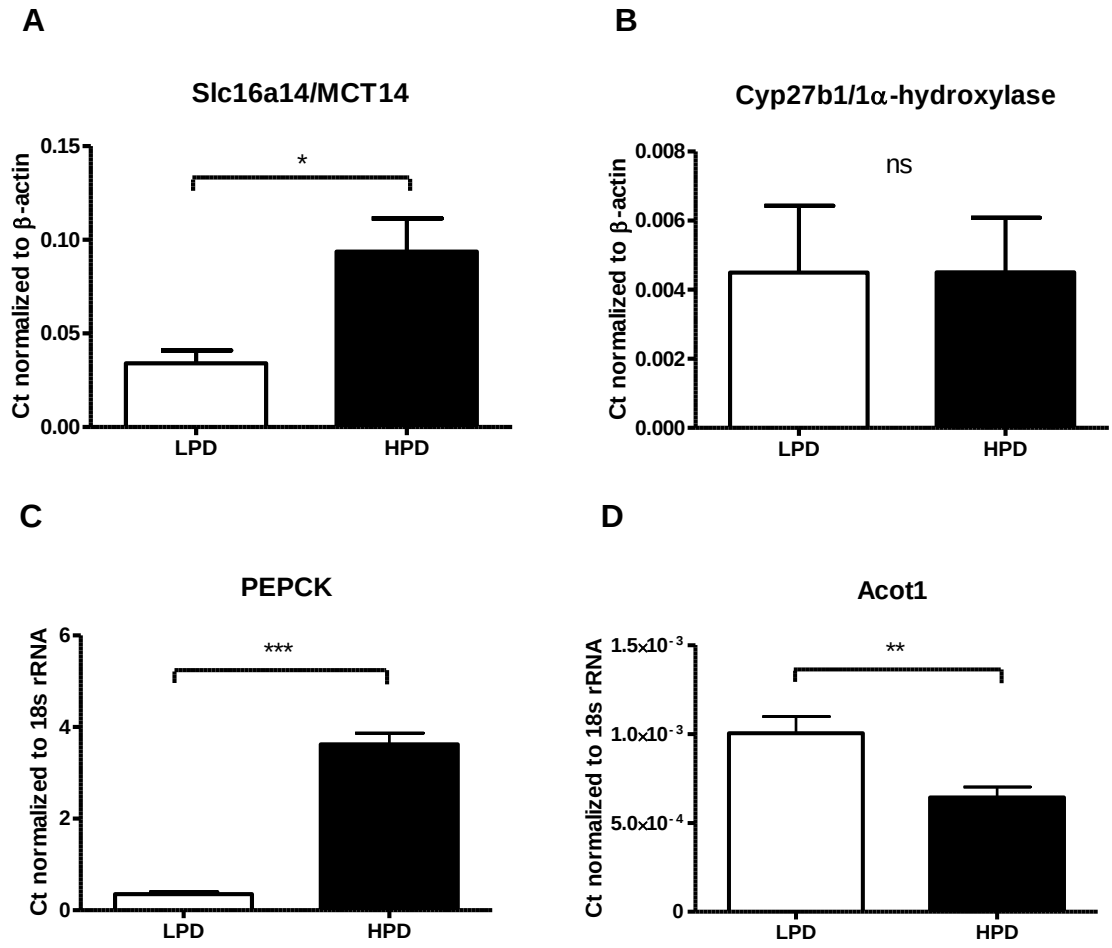

Figure 18. RT-qPCR of selected genes regulated 14 h after the onset of LPD and HPD. Genes were selected based on their regulation after 5 days of LPD and HPD administration. **(A)** SLC16A14/MCT14 changed significantly while (**B)** 1α-hydroxylase was not regulated after 14 h LPD. **(C)** PEPCK mRNA expression levels were very significantly decreased in the LPD group while **(D)** Acot1 mRNA was up-regulated in LPD animals. ns: not significant. Data with ±SEM, $n = 6$, *$p < 0.05$, **$p < 0.01$, ***$p < 0.001$.

Urinary analysis after 14 hours ("acute") LPD and HPD

Mice (n = 12), after being trained to eat between 6 and 9 pm, were exposed to HPD for a 3 h feeding period. Three days before sacrifice they were individually placed in metabolic cages with 3 h HPD administration in the evenings. On the last evening, the experimental group (n = 6) received a LPD for 3 h while the control group continued to eat the HPD. Overnight (14 h) urine was collected before blood and kidneys were harvested. Urine was analyzed for the content of several components. As shown in Table 7, no significant differences were observed for urinary excretion of

Cl^-, SO_4^{2-}, Na^+, K^+, Ca^{2+}, and Mg^{2+}. Excretion of Pi and NH_3/NH_4^+ was significantly decreased in LPD animals when compared to HPD animals. Similarly as observed after “chronic” (5 days) adaptation, urinary pH of the HPD mice was more acidic than the urine collected from LPD mice. All other parameters; food and water intake, body weight, and urine volume did not differ significantly between the two diet groups. Control of food intake was of particular importance, as mice could have eaten less of the low Pi-diet and therefore the energy balance could have been disturbed.

Table 7. *Summary of urine analysis*

	HPD (1.2%)	LPD (0.01%)
pH	5.79±0.070	6.16±0.100*
Creatinine (mg/dl)	29.50±7.530	35.50±10.800ns
Pi (mM)/crea (mg/dl)	6.47±0.940	0.79±0.240‡
Cl^- (mM)/crea (mg/dl)	3.64±0.720	3.75±0.800ns
SO_4^{2-} (mM)/crea (mg/dl)	0.43±0.140	1.33±0.490ns
NH_3/NH_4^+ (mM)/crea (mg/dl)	7.41±1.060	1.49±0.350‡
Na^+ (mM)/crea (mg/dl)	3.26±0.760	2.37±0.440ns
K^+ (mM)/crea (mg/dl)	6.89±1.080	4.36±1.020ns
Ca^{2+} (mM)/crea (mg/dl)	0.11±0.050	0.37±0.110ns
Mg^{2+} (mM)/crea (mg/dl)	0.44±0.060	0.61±0.170ns
Urine volume (ml)	1.30±0.200	1.10±0.200ns
Urine volume/BW	0.06±0.010	0.05±0.001ns
Body weight (g)	20.40±0.590	21.00±0.380ns
Water intake ml/ BW	0.20±0.020	0.18±0.010ns
Food intake g/ BW	0.08±0.001	0.09±0.001ns

Urine values summarized from mice receiving a low (0.1%) Pi and a high (1.2%) Pi-diet during a 3 h feeding period and sacrificed 14 h after receiving their diets. Urine was collected from the beginning of the feeding period (6 pm) and values normalized against creatinine (crea). n = 6 per group; BW, body weight; ns, not significant. *p < 0.05, ‡p < 0.001.

Microarray analysis after 14 hours ("acute") LPD and HPD administration

RNA was extracted from kidneys and tested for quality. Samples had a 260nm/280nm ratio of 2.2 and RIN between 8 and 9 (Figure 19). At the FGCZ, best 8 samples (4 of each group) were processed for hybridization to GeneChip® Mouse Genome 430 2.0 arrays (Affymetrix). Approximately 40% (12'893 protein coding genes) of total genes that were present on the array were detected. 210 transcripts were changed significantly ($p < 0.05$) after a 14 LPD vs. HPD. Of those, 156 were down-regulated (93 with a fold change < 0.67) and 54 up-regulated (50 with a fold change > 1.5). (see Supplementary table S4 on CD). Again, only genes with a 50%-fold change and more were considered.

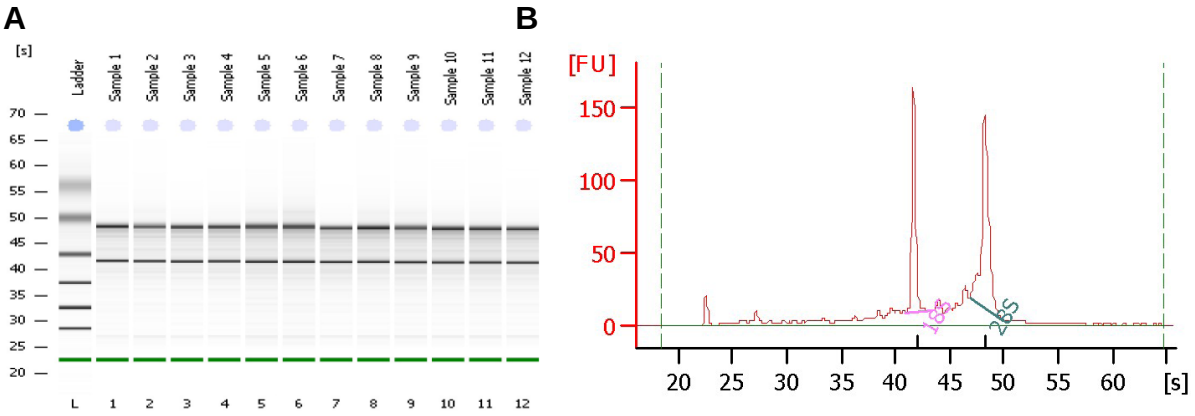

Figure 19. Summary of quality measurement of mouse kidney mRNA after 14 h LPD and HPD. **(A)** Virtual gel of RNA samples. Bands represent the 18 S and 28 S rRNA. This can also be demonstrated in graphic **(B)** where the integrated areas below the peaks represent the RNA integration number (RIN) by which RNA purity is determined.

Analysis of "acute" GeneChip data

Analysis of the microchip data revealed that numerous genes affected by 14 h of Pi depletion are involved in metabolic activities. However, pathway grouping was more difficult than with the data obtained after "chronic" Pi restriction. This was mainly due to fewer genes that could be grouped in single pathways (only 2-3 genes) and

therefore no direct conclusion was possible from these analyses. PEPCK is a main regulator of gluconeogenesis and was down-regulated after 14 h and 5 days of LPD. Down-regulation of PEPCK had been previously confirmed with RT-qPCR after 14 h of LPD (Figure 18 C). Also, after an "acute" Pi feeding period, ammoniagenesis was significantly changed as indicated by altered excretion of NH_3/NH_4^+ (see Table 7). Several genes previously found to be regulated in acidotic conditions [189] did also respond to dietary Pi changes (Table 8a). These are: the solute carrier SLC38a3 (SNAT3), a basolateral Na^+-coupled glutamine transporter; glutamate dehydrogenase 1 (Glud1), an enzyme responsible for releasing an NH_4^+ ion from glutamate when converting to α-ketoglutarate; and PEPCK, responsible for converting oxaloacetate into phosphoenolpyruvate and carbon dioxide. SLC16A14/MCT14 is an orphan transporter belonging to the monocarboxylate transporter family, also shown to be changed during acidotic conditions [189]. It was also detected through gene chip analysis after 14 h of LPD as previously expected from RT-qPCR experiments. Of the genes that had been up-regulated, many are of unknown function or have not been throughly characterized. A number of selected genes are represented in Table 8.

Selected genes obtained from micorarray analysis table (supplementary S4) were subjected to RT-qPCR to confirm altered expression levels (Figure 20). Fortunately, all of the genes selected were shown to agree with the approximate fold changes observed during microarray analysis as demonstrated by linear regression in Figure 21.

Many genes regulated after 14 h of LPD were shown to be altered after "chronic" Pi deprivation (see Table 11), such as: PEPCK, Glud1, and SLC38a3/SNAT3 showed a strong regulation after 14 h of LPD. Osteomodulin and cholecystokinin A receptor (CCKAR) mRNA levels also showed significant difference. Osteomodulin (FC 3-fold), an extracellular matrix keratan sulphate proteoglycan, had been previously published to be involved in osteoclastic activity during bone resorption [193]. This may well be an indicator of an early Pi demineralising signal to the bone as short as 14 h after Pi deprivation. If osteomodulin directly acts on Na/Pi-cotransport is unknown (see discussion). CCKAR, a member of the G-protein coupled receptors (GPCR) that binds CCK, is a major physiological regulator of pancreatic secretion and smooth muscle contraction of gall bladder and stomach [194]. The receptor regulates satiety

in the central and peripheral nervous system [194]. How this factor interferes with Pi homeostasis or Na/Pi-cotransport mechanisms is not known. It is possible that by regulating the secretion of dopamine [195] this receptor may be indirectly involved (see Discussion).

SLC16A14/MCT14 (MCT14) appeared to be a robust responder after 14 h and 5 days of “chronic” dietary Pi changes. Based on gene clustering and homology analysis, this transporter belongs to the members of the monocarboxylic acid transporters (MCTs) [196]. Neither its function nor its renal localization has been determined to date.

Table 8a. *Genes down-regulated after 14 hours of LPD (p < 0.01)*

Gene Symbol	Gene Name	Fold Change	GeneBank Acc. No.
PEPCK	Phosphoenolpyruvate carboxykinase 1, cytosolic	0.16	NM_011044.2
SLC16A14/MCT14	Solute carrier family 16, member 14	0.23	NM_027921
SLC38A3	Solute carrier family 38, member 3	0.38	NM_0203805.2
SLC13A2	Solute carrier family 13, member 2	0.40	NM_022411.3
AACS	Acetoacetyl-CoA synthetase	0.45	NM_030210.1
CCKAR	Cholecystokinin A receptor	0.45	NM_009827.2
Glud1	Glutamate dehydrogenase 1	0.51	NM_008133.4
PpaRα	Peroxisome proliferator activated receptor alpha	0.58	NM_011144.6
ENPP2	Ectonucleotide pyrophosphatase/phosphodiesterase 2	0.60	NM_015744.6
Trp53bp	Transformation related protein 53, binding protein 2	0.61	NM_173378.2
Thyms	Thymidylate synthase	0.63	NM_021288.3

Table 8b. *Genes up-regulated after 14 hours of LPD (p < 0.01)*

Gene Symbol	Gene Name	Fold Change	GeneBank Acc. No.
Omd	Osteomodulin	3.2	NM_012050.2
Acot11	Acyl-CoA thioesterase 11	2.1	NM_025590.4
Tln2	Talin 2	1.9	NM_027458.1
SLC25A36	Solute carrier family 25, member 36	1.9	NM_138756.4
Jub	Ajuba	1.8	NM_010590.4
Acot1	Acyl-CoA thioesterase 1	1.8	NM_012006.2
Olfm3	Olfactomedin 3	1.7	NM_153458.2
Lrat	Lecithin-retinol acyltransferase	1.6	NM_023624.4
Itgb6	Integrin beta 6	1.6	NM_021359.3
Spsb4	SplA/ryanodine receptor domain containing SOCS box	1.6	NM_145134.3

Listed are a number of selected genes that responded to ”acute” (14 h) LPD.

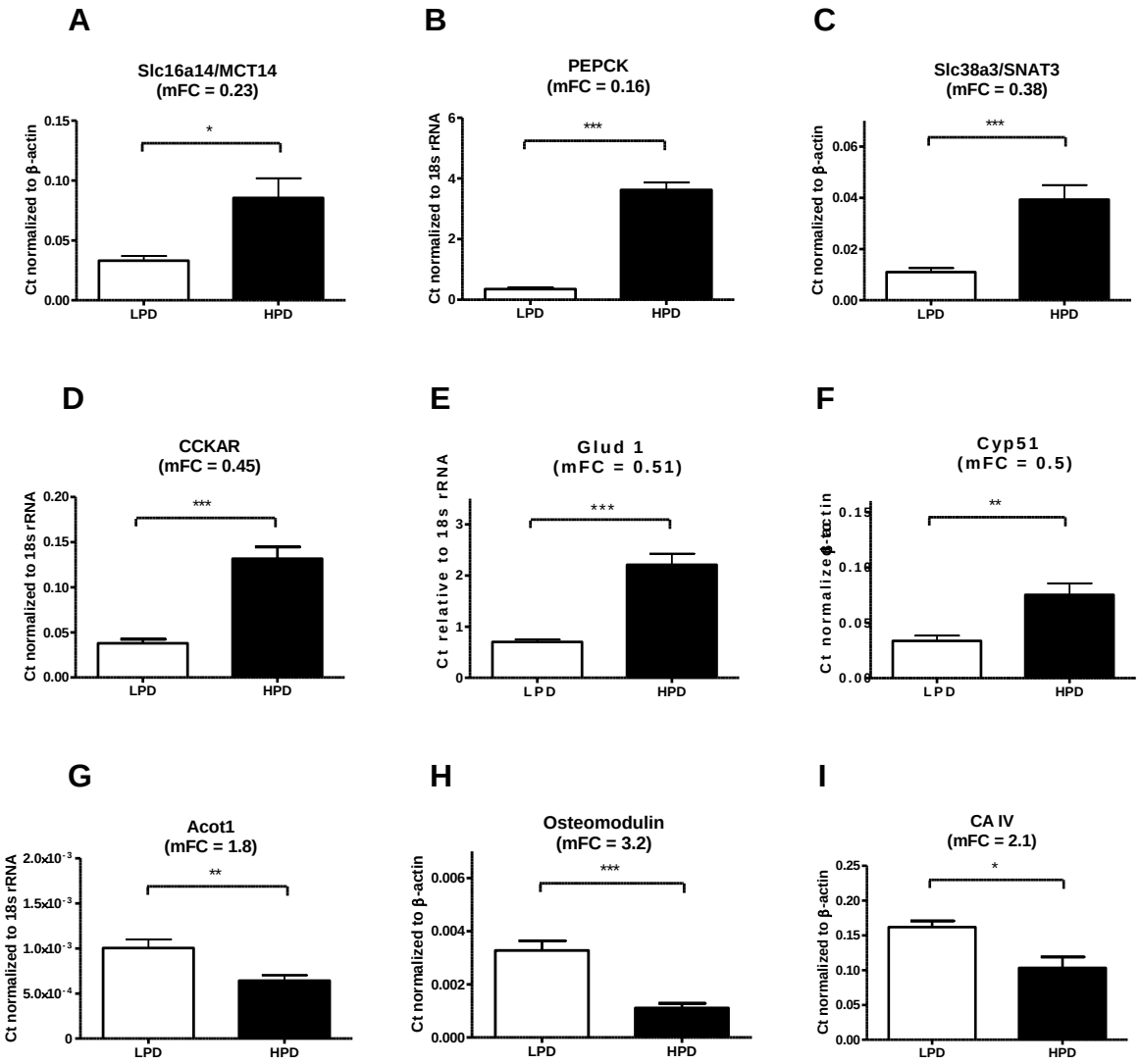

Figure 20. RT-qPCR of some selected transcripts (supplementary table S4) based on microarray analysis after 14 h of LPD. **(A)** SLC16A14/MCT14 changed significantly in agreement with fold changes observed from microarray data. **(B)** Pepck, an enzyme involved in gluconeogenesis, was strongly down-regulated in the LPD group. **(C)** Na^+- dependent glutamine transporter (SNAT3) was down-regulated in LPD as well as **(D)** cholecystokinin A receptor, **(E)** Glutamate dehydrogenase (Glud) and **(F)** Cyp51. **(G)** Acot1, **(H)** Osteomodulin, and **(I)** Carbonic anhydrase IV had an increased expression level in response to LPD. Data with ±SEM, $n = 6$, *$p < 0.05$, **$p < 0.01$, ***$p < 0.001$.

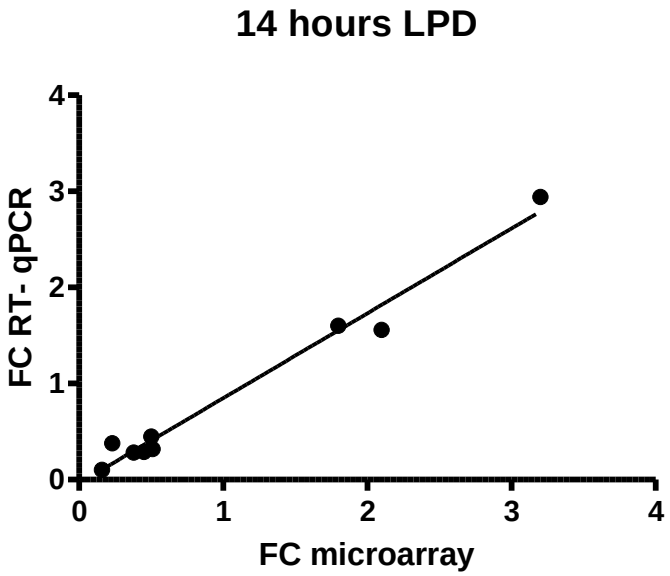

Figure 21. Linear Regression after 14 h LPD between fold changes of selected genes analyzed by RT- qPCR and micorarray analysis. n = 9, R^2 = 0.979.

Characterization of SLC16A14/MCT14

Renal expression of SLC16A14/MCT14, a member of the monocarboxylate transporter family SLC16 [196], was affected by intake of a low Pi-diet after “chronic” (5 days) and “acute” (14 h) conditions. Therefore SLC16A14/MCT14 was regarded as a new gene whose expression is influenced by dietary Pi. Thus far, SLC16A14/MCT14 has not been localized in the kidney and its function has not been described. In the following experiments, the renal localization and a possible function of SLC16A14/MCT14 were investigated.

Tissue distribution of SLC16A14/MCT14

A variety of tissues from one wild type C57BL/6 mouse fed with standard chow was collected, total RNA extracted and analyzed by RT-qPCR. Among the tissues tested, the kidney showed the highest expression level of SLC16A14/MCT14 mRNA. Less pronounced expression was found in the pancreas and testis. Only very low expression was observed in the epididymis, salivary and vesicular glands. The stomach, intestine, colon, spleen and thyroid gland were also tested and did not present any detectable SLC16A14/MCT14 mRNA levels (Figure 22).

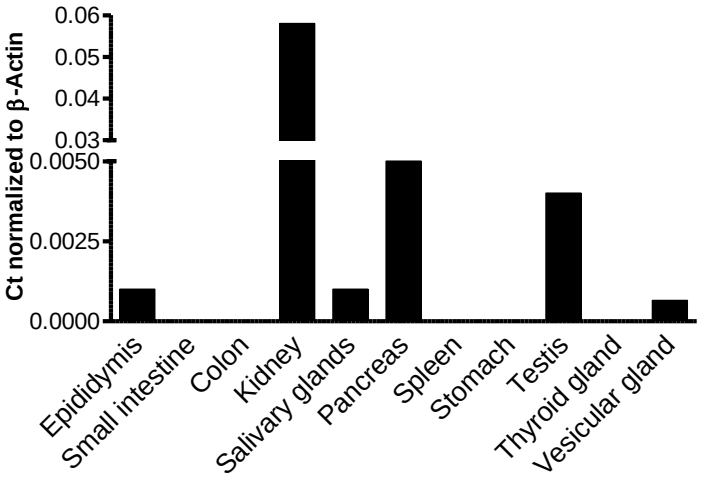

Figure 22. Tissue distribution of SLC16A14/MCT14 mRNA using RT-qPCR. Data normalized against β-actin. (*n* = 1)

Renal localization of SLC16A14/MCT14

Expression of SLC16A14/MCT14 mRNA in kidney tissue was first assessed by *in-situ* hybridization (ISH) in wild type mice (C57BL/6) that were fed a standard diet. With the results obtained and presented in Figure 23, the localization of SLC16A14/MCT14 mRNA could not be determined. No signal for SLC16A14/MCT14 could be detected (Figure 23 A & B). Anti-sense sequences for SLC12a5 and SLC5a2 were used as controls for the experimental procedure (Figure 23 C & D).

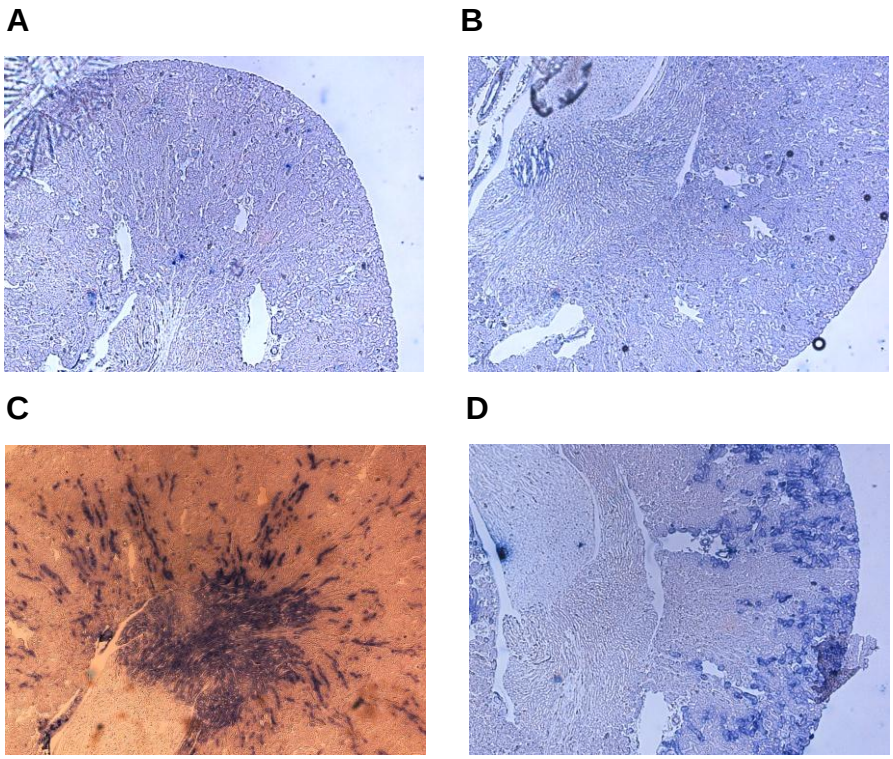

Figure 23. *In-situ* hybridization of SLC16A14/MCT14 in kidneys of wild type C57BL/6 mice fed with standard diet. **(A)** No visible signal after hybridization of the SLC16A14/MCT14 anti-sense sequence. **(B)** SLC16A14/MCT14 sense sequence used for negative control. For the control of experimental procedure anti-sense sequences of **(C)** SLC12a5 and **(D)** SLC5a2 were used.

Localization of SLC16A14/MCT14 by immunohistochemistry

An antibody was raised against a synthetic peptide of SLC16A14/MCT14 (Supplementary Table S2 at the end of Methods) and used to determine renal localization of SLC16A14/MCT14 by immunohistochemistry.

From two immunized rabbits, sera were collected after 60, 90, and 105 days. Sera of both rabbits after 90 days of injection resulted in visible stainings when applied to sections prepared from kidneys (wild type mice fed with standard diet) fixed with 4% PFA. All following stainings were performed with serum from rabbit 1 (serum 1). First stainings indicated signals in the PTs and the outer medulla, most likely in the TAL (Figure 24). Based on these results, serum 1 from 105 days was used to affinity purify SLC16A14/MCT14 antibodies.

After obtaining the purified antibody, new immunostainings were performed in kidneys from wild type mice that were fed standard diet. In order to determine the

exact localization of SLC16A14/MCT14, a number of serial cuts were performed on PFA fixed kidneys that were stained for SLC16A14/MCT14 as well as for NaPi-2a (as a marker for PT), NKCC2, and ROMK (as markers for the TAL). Comparison of the pattern of expression of SLC16A14/MCT14 (Figure 25 A) and NaPi-2a (Figure 25 B) indicates that both proteins are not expressed in the same tubular segments, ruling out the presence of SLC16A14/MCT14 in the PT. In contrast, SLC16A14/MCT14 (Figure 25 C) was detected in tubular structures also stained with NKCC2 (Figure 25 D) and ROMK (Figure 25 E). Together, these results indicate that SLC16A14/MCT14 protein is expressed in the TAL, whereas no stainings in the PT were observed using the affinity purified antibody.

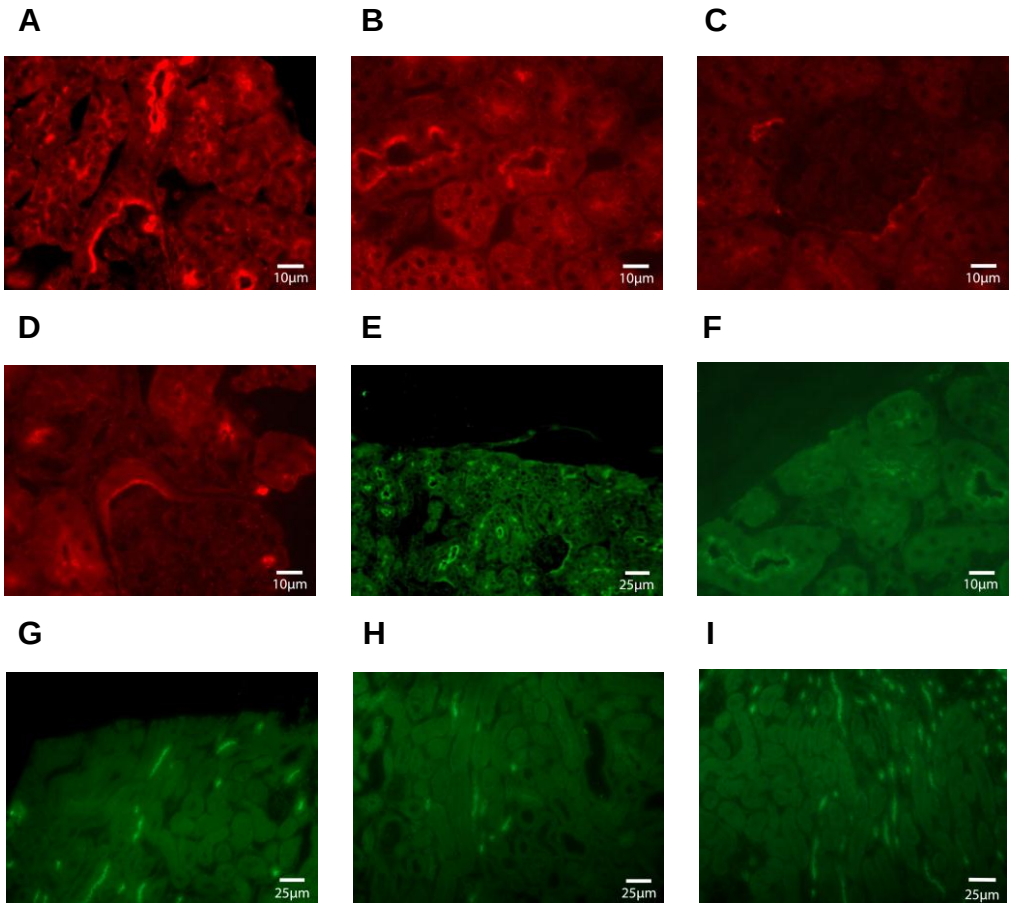

Figure 24. Serum from rabbit 1 (not purified) after 105 days of SLC16A14/MCT14 peptide injection applied to kidney sections of C56BL/6 wild type mice fed standard chow. Stainings in the PT were detected as well as TAL like structures. **(A)** A glomerulus with its PT. **(B)** Convoluted tubular structures which present SLC16A14/MCT14 in the PT of the cortex. **(C)** The urinary pole of a glomerulus shows staining in the PT. Also, the tubule attached to the glomerulus, which is the macula densa region of the TAL, is stained. **(D)** PT with its glomerulus. **(E)** Lower magnification of the cortex region revealing various PTs stained for SLC16A14/MCT14. **(F)** Detailed visualization of the BBM system of the PT in the cortex. **(G & H)** Signal for SLC16A14/MCT14 in the TAL. **(I)** Outer medullary staining of SLC16A14/MCT14 reaching into the cortex. Magnification: A-D, F: x60 ; E, G-I: x20

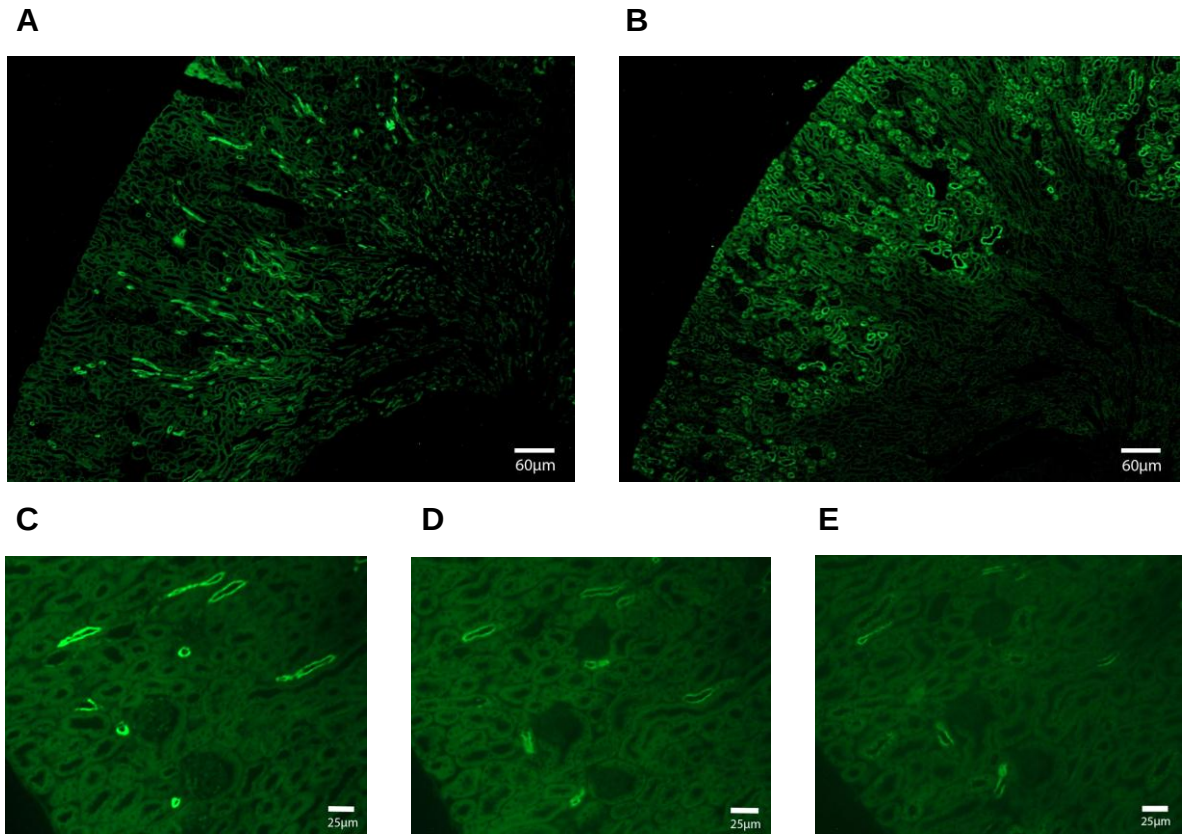

Figure 25. Localization of SLC16A14/MCT14 in kidneys from standard diet fed wild type mice using affinity purified antibody. **(A)** Cross section of the whole mouse kidney reveals an outer medullary distribution of SLC16A14/MCT14 reaching into the cortex. **(B)** Staining in the cortex of the PT shows the distribution of NaPi-2a. Serial sections of mouse kidney show stainings for **(C)** SLC16A14/MCT14 that overlaps with the localization of **(D)** NKCC2 and the localization of **(E)** ROMK, which are all present in the TAL. Magnification: A & B: x4 ; C-E: x20.

The cellular distribution of SLC16A14/MCT14 was confined to the apical side (Figure 26 A). Moreover, when kidney sections were observed under higher magnification (x60), some SLC16A14/MCT14 signals of the CCD basolateral membrane most likely of principal cells were detected (Figure 26 B). In addition, affinity purified antibody specificity was confirmed by peptide blocking (Figure 26 C & D).

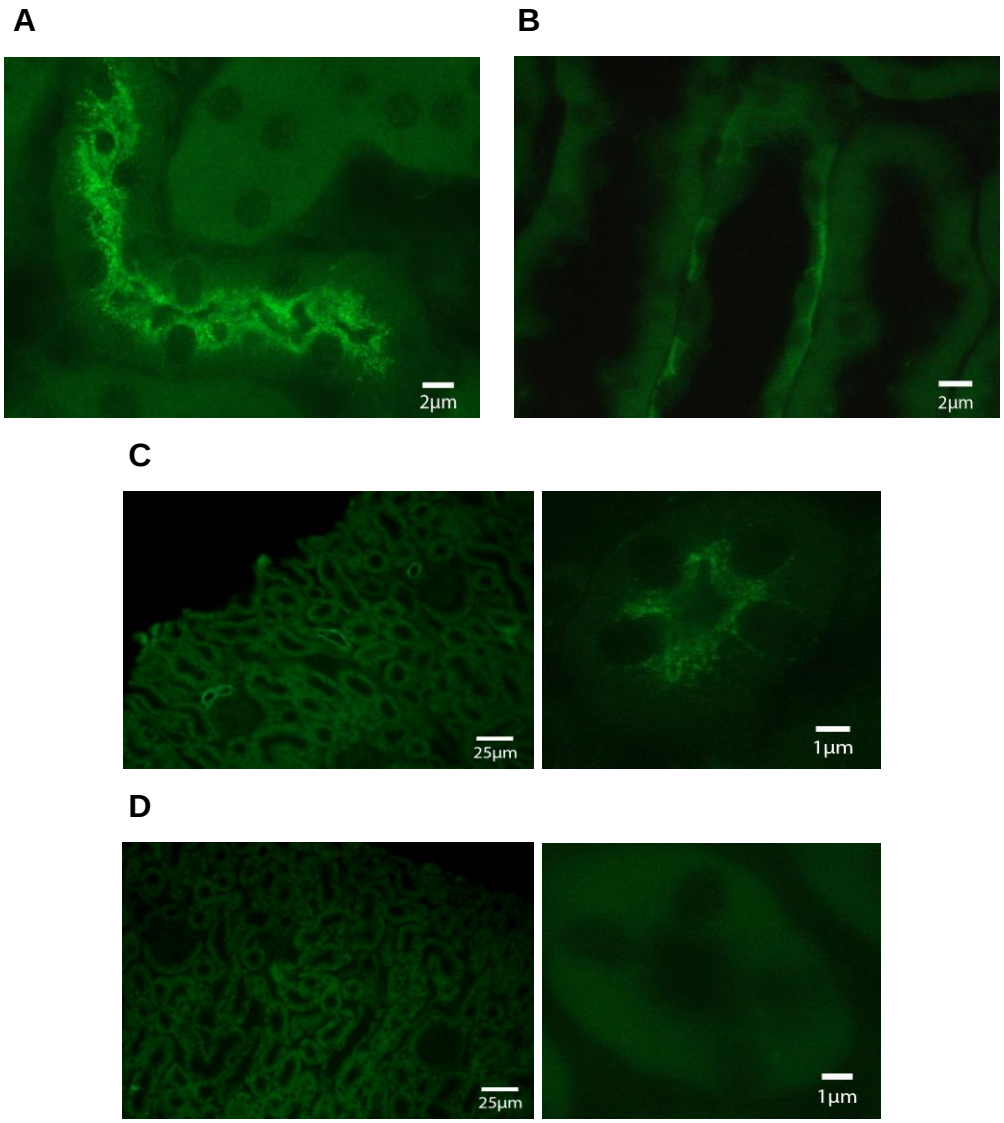

Figure 26. (A) SLC16A14/MCT14 staining in the apical membrane of a TAL and **(B)** the basolateral membrane of principal or intercalated cells in the CCD. **(C)** SLC16A14/MCT14 in the TAL without peptide block and (**D)** Pre-incubation of anti-SLC16A14/MCT14 antibody with target directed peptide. Magnification: A & B: x60(oil) ; C & D: x20 & x80(oil) respectively.

RT-qPCR analysis of SLC16A14/MCT14 in isolated nephron segments

In order to confirm the observations made by immunofluorescence, it was necessary to determine SLC16A14/MCT14 mRNA in micro-dissected nephron segments. These segments (PT and TAL) were isolated from a freshly removed kidney of a wild type C57BL/6 mouse fed a standard diet and RT-qPCR was performed for

SLC16A14/MCT14. As shown in Figure 27, the expression level of SLC16A14/MCT14 mRNA abundance was very low in the TAL and even lower in the proximal straight tubule (PST). This low expression may explain the (almost) negative result obtained by *in-situ* hybridization. As controls, RT-qPCR for NaPi-2a (marker for PT) and NKCC2 (marker for TAL) were performed as well.

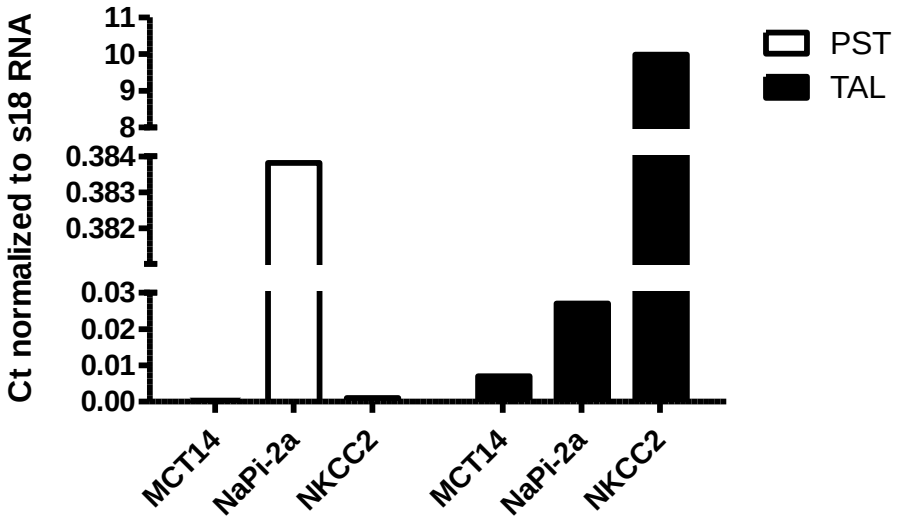

Figure 27. RT-qPCR performed for SLC16A14/MCT14 in the nephron segments of the PST and the TAL from one standard diet wild type mouse kidney. NaPi-2a served as a positive control in the PST and as a negative control in the TAL while NKCC2 served as a negative control in the PST and as a postivie in the TAL. mRNA was obtained from 20 tubuli of each segment. Data was normalized against 18 S rRNA. *n = 1.*

Regulation of SLC16A14/MCT14 protein by dietary intake of Pi

Kidney homogenates and BBMs were tested by Western blot analysis in order to determine whether the abundance of SLC16A14/MCT14 protein is regulated in response to dietary intake of Pi. Animals were sacrificed after 3 h, 14 h, and 5 days of special diets. Western blots were performed either with homogenates or isolated BBMs. As seen in Figure 28 A & D, no difference of SLC16A14/MCT14 abundance was detected in kidney homogenates after 3 h of LPD ingestion (compared to HPD), even though abundance of NaPi-2a was already strongly upregulated in the LPD group after 3 h. After 14 h, a significant difference of SLC16A14/MCT14 abundance

was observed between LPD and HPD in kidney homogenates and BBM fractions (Figure 28 B & D). Again, NaPi-2a abundance was strongly up-regulated in BBM and homogenates after 14 h LPD. Similar as after 14 h, abundance of SLC16A14/MCT14 was reduced by LPD intake after 5 days (Figure 28 C & D). As a control for the antibody that was raised against a specific synthetic peptide, an antibody-peptide block was performed using three different amount of homogenate loadings as seen in Figure 28 E.

Taken together, Western blot analysis indicated that LPD decreased the abundance of SLC16A14/MCT14 after 14 hours and 5 days of Pi depletion. However, and in contrast to NaPi-2a, no change of SLC16A14/MCT14 abundance was observed after 3 hours. This indicates that even though regulation of SLC16A14/MCT14 by dietary intake of Pi occurs already after 14 hours, the mechanism might differ from that involved in the rapid regulation of NaPi-2a protein.

A

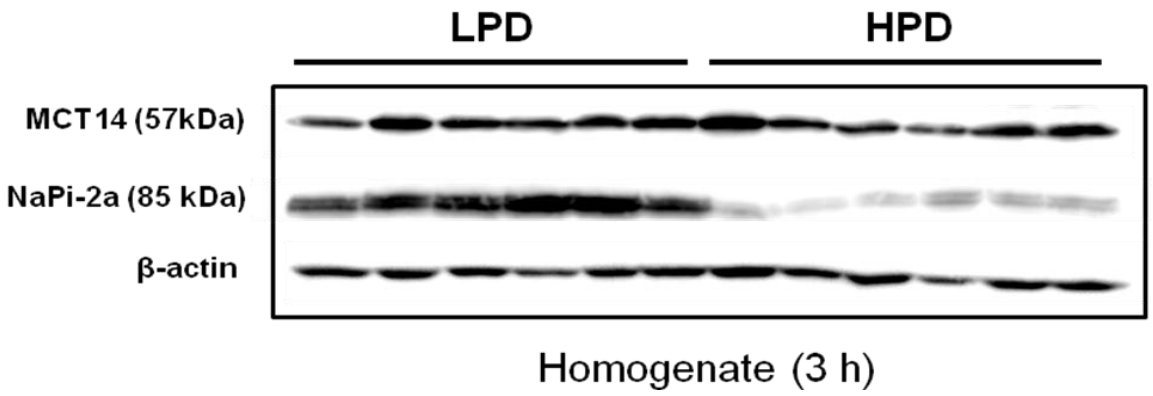

Homogenate (3 h)

B

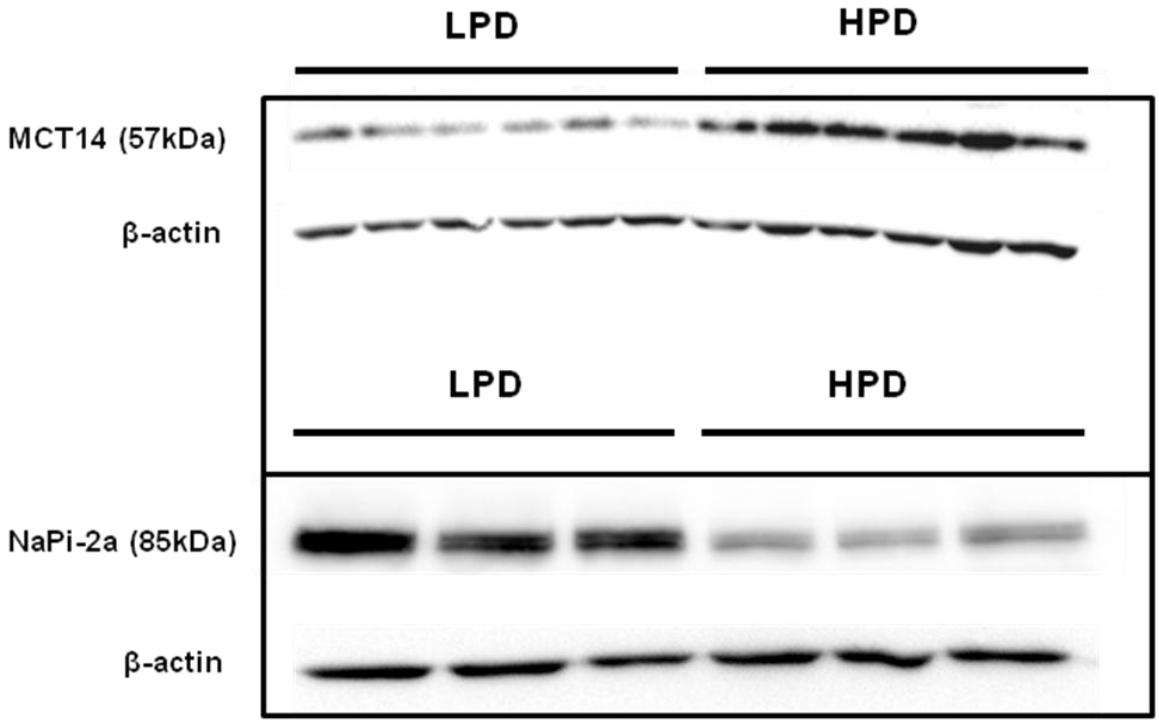

Homogenate (14 h)

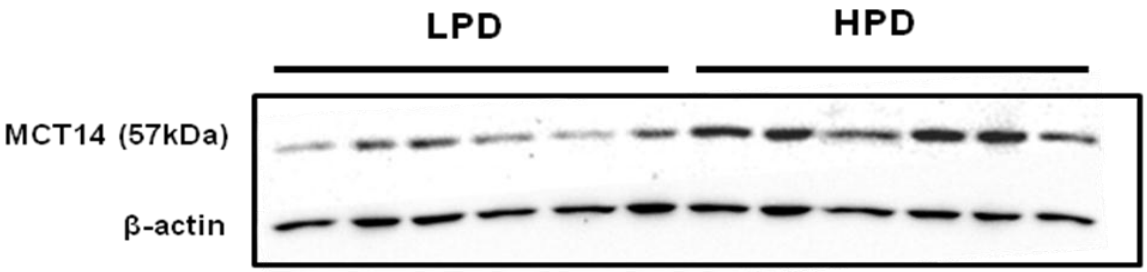

BBMV (14 h)

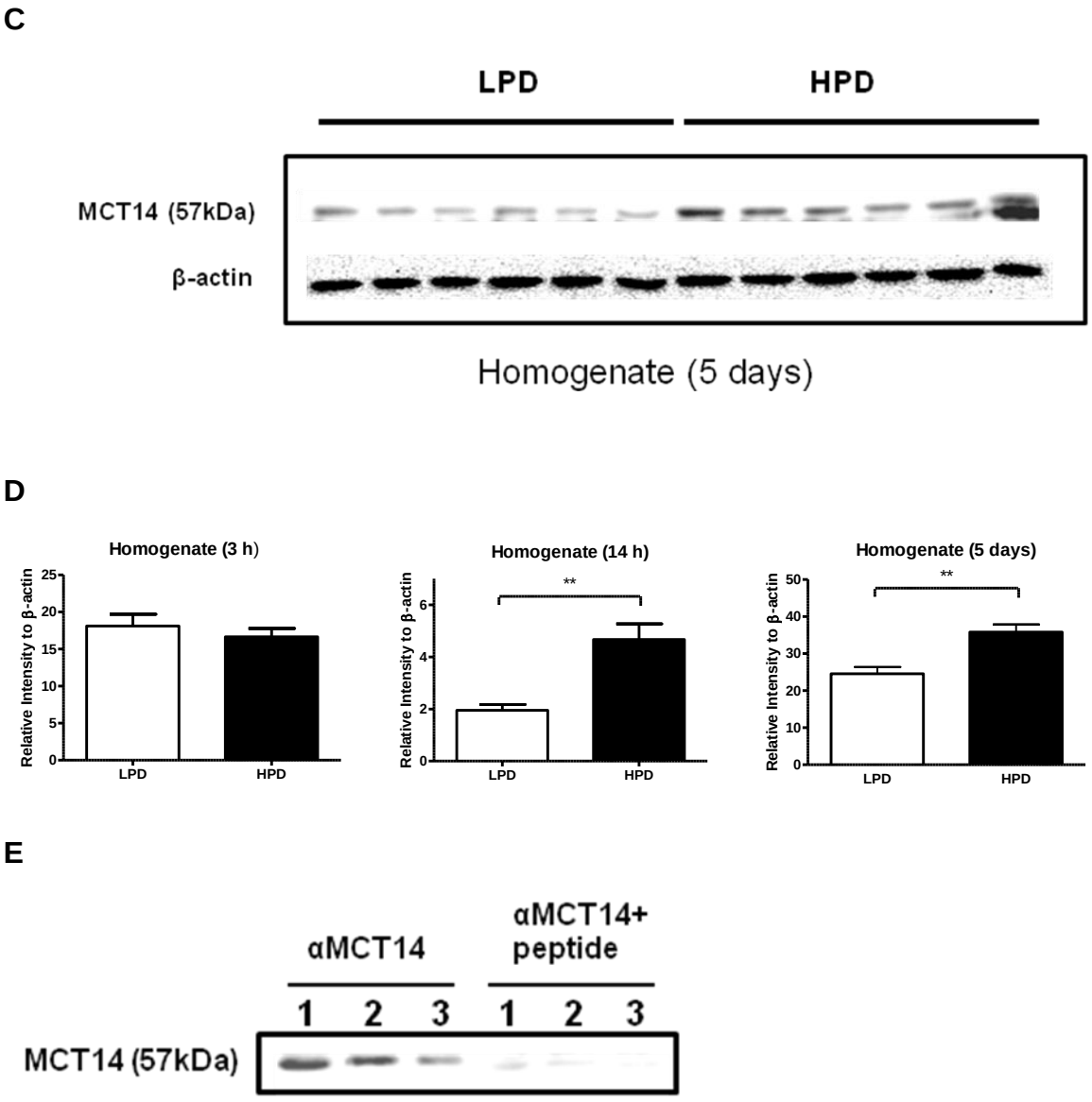

Figure 28. Western blot anaylsis of SLC16A14/MCT14 in the kidney of wild type mice after different time periods upon LPD and HPD administration. **(A)** No change was observed after 3 h of LPD (**B)** Significant difference beween LPD and HPD after 14 h of food administration. The abundance of SLC16A14/MCT14 in BBM was also shown to be regulated after 14 h of LPD and HPD. **(C)** Homogenates of "chronic" (5 days) treated LPD and HPD animals show significant reduction of SLC16A14/MCT14 in the LPD groups. **(D)** Bar graphs summarize the data from immunoblots with homogenates for SLC16A14/MCT14. **(E)** Standard test for antibody specificity after affinity purification using three different homogenate concentrations (1: 70µg, 2: 50µg, 3: 30µg) from a standard fed wild type mouse while peptide concentration remained the same. Membranes were stripped and reprobed for *β*-actin. BBMV: Brush border membrane vesicles; αMCT14: anti-SLC16A14/MCT14 antibody. All data were normalized against *β*-actin. Data with ±SEM, $n = 6$ per group, $*p < 0.05$, $**p < 0.01$.

Regulation of SLC16A14/MCT14 abundance was additionally investigated by immunofluorescence. Kidneys were fixed with PFA as described (see Methods). Expression of SLC16A14/MCT14 was first investigated under "acute" (14 h) dietary

conditions. When kidneys of “acute” HPD mice were stained for SLC16A14/MCT14, the transporter was localized in the BBM of PTs (Figure 29 A). However, immunostainings of kidneys from LPD fed animals did not show clear SLC16A14/MCT14 presence in the BBM (Figure 29 B). Instead, SLC16A14/MCT14 appears in subapical compartments of the cell. This may suggest possible regulation of apical SLC16A14/MCT14 triggered by changes in dietary Pi. Interestingly, no significant presence of SLC16A14/MCT14 was detected in the TAL of these mice as previously shown in NPD mice.

Additional experiments focused on renal SLC16A14/MCT14 distribution after “chronic” HPD and LPD adaptation. Mice treated for 5 days with HPD presented SLC16A14/MCT14 protein in PTs and randomly in the TALs (Figure 30 A). Nevertheless, after 5 days of LPD feeding, SLC16A14/MCT14 was detected apically in the TAL cells and in the cytosol of some PT and TAL cells. (Figure 30 B). Overall, it cannot be ruled out that the distribution of SLC16A14/MCT14 in the nephron is regulated by other mechanisms different to the response caused by dietary Pi.

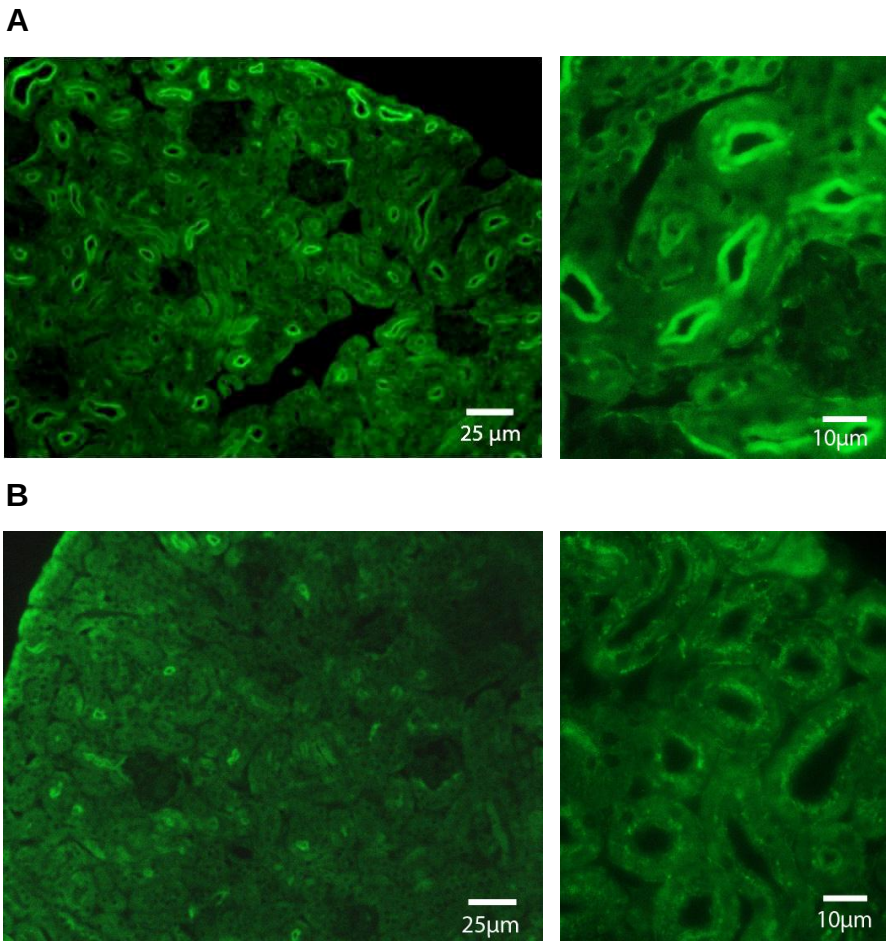

Figure 29. Expression of SLC16A14/MCT14 in the wild type mouse kidney cortex 14 h after the administration of LPD and HPD. **(A)** Mice after a HPD administration expressed SLC16A14/MCT14 in the renal cortex. Seen in more detail under higher magnification (right) **(B)** When given a LPD, the expression of SLC16A14/MCT14 in the cortex is reduced. Under higher magnification (right), the tubules reveal a subapical staining for SLC16A14/MCT14, suggesting a possible internalization of SLC16A14/MCT14 14 hours upon LPD ingestion. Under higher magnification (right side) SLC16A14/MCT14 signal is determined in the BBM of the PTs. Magnification: left: x20 ; right: x60 (oil).

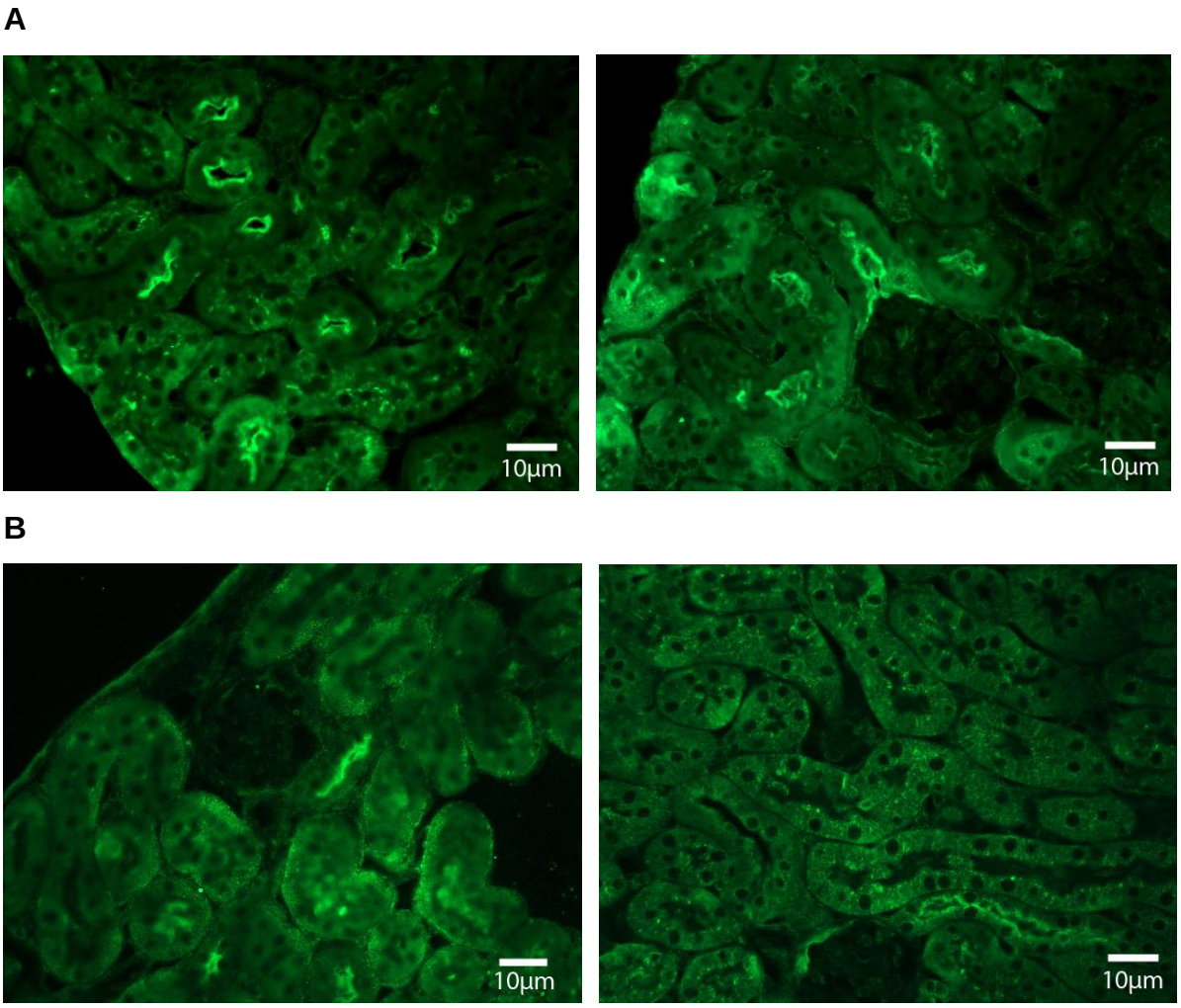

Figure 30. SLC16A14/MCT14 localization in wild type mouse kidney after 5 days "chronic" HPD and LPD. **(A)** Kidneys of HPD mice show SLC16A14/MCT14 localization in BBM of PTs **(B)** while LPD kidneys show the apical distribution of SLC16A14/MCT14 in the TALs and in the cytosol of some PT and TAL cells.

Heterologous expression of SLC16A14/MCT14 in oocytes of *Xenopus laevis* and investigations of its transport properties

Subcloning SLC16A14/MCT14 from pCMV-Sport6 to pSPOK-G

In order to study the function of SLC16A14/MCT14, *Xenopus laevis* oocytes were injected with SLC16A14/MCT14 cRNA with the purpose to express the transporter at the plasma membrane. SLC16A14/MCT14 was tagged with a myc sequence at the N-terminal end of the transporter. After obtaining SLC16A14/MCT14 in the non-expression vector pCMV-Sport6, it was consequently subcloned into pSPOK-G, a modified pSD-Easy vector containing a myc tag (see Methods). Using primers with modified ends for *Sac*I and *Xho*I, a PCR was performed using as template the SLC16A14/MCT14 in pCMV-Sport6. A terminaly modified SLC16A14/MCT14 sequence was obtained that allowed insertion into the *Sac*I and *Xho*I sites of pSPOK-G. Finally, colonies were selected that harvested the SLC16A14/MCT14 in the new vector. DNA was purified and sent for sequencing. Partial myc-tagged SLC16A14/MCT14 sequence from colony 1 is shown in Figure 31 A indicating that subloning of the transporter downstream of the myc tag was successful. This was further confirmed by restriction digestion using *Xho*I and *Sac*I (Figure 31 B).

A

GNGCTACACNNTTAGGCTTGTACATATTGTCGTTAGAACGCGGCTACAATTAATACATAACCTTATGTATCATAC
ACATACGATTTAGGTGACACTATAGAATACACGTAGGCCACCATGGAACAAAAACTCATCTCAGAAGAGGATCTG
GAATTCGAGCTCTATACGAGTCATGAAGATATCGGGTATGACCTTGAAGACGACCGAAAGGCTAAGAATAAGAAG
ACGCTGAAGCCCCACCCAGATATCGATGGCGGGTGGGCCTGGATGATGGTCCTCTCGTCCTTCTTTGTTCACATC
CTCATCATGGGCTCACAGATGGCCCTAGGAGTCCTCAACGTGGAGTGGCTTGAAGAGTTTCACCAGAGCCGCGGC
CTGACCGCCTGGGTCAGCTCCCTGAGCATGGGCATCACCTTGATCGTGGGACCTTTCATCGGCTTGTTCATTAAC
ACCTGCGGGTGCCGCCAGACAGCAATCATTGGAGGCCTGGTGAACTCCCTCGGCTGGGTGTTGAGCGCCTATGCA
GCCAATGTGCAGTCTCTCTTTATTACCTTTGGAGTGGCAGCAGGCCTTGGCAGTGGGATGGCTTACCTACCTGCA
GTGGTCATGGTGGGAAGGTACTTTCAGAAGAGACGAGCCCTGGCCCAGGGCCTCAGTACCACGGGGACAGGATTT
GGGACGTTCCTGATGACCGTGTTGCTGAAATACCTGTGCGCAGAATATGGCTGGCGGAATGCTATGTTCATCCAA
GGTGCTCTGTCCCTGAACCTGTGTGTCTGTGGGGCGCTCATGAGGCCCCTCTCTCCCGAGAAGTTAGAAAACTGC
CCAGAAGCGGAAGAGCCGTGTGCTCTCCCAGCTTACTCCACTGAATCTGTTAAGTCTGGAGGACCACTGGGCATG
GCTGAAGAACAGGACAGA

B

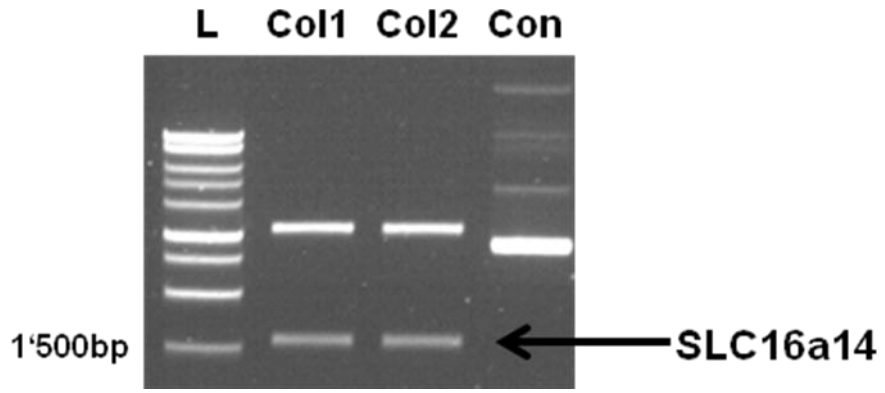

Figure 31. (A) pSPOK-G myc tagged SLC16A14/MCT14 sequenced with Sp6. Red: myc tag. Yellow: SLC16A14/MCT14 (not completely shown). Box: modified sequence with restriction site. **(B)** Agarose gel after restriction enzyme digestion with *Sac*I and *Xho*I. L: ladder, Col: Colony, Con: Control (circular plasmid without restriction cut).

Expression of the mouse SLC16A14/MCT14 gene in *Xenopus laevis* oocytes

The pSPOK-G vector containing myc-SLC16A14/MCT14 was used to 2synthesize cRNA. After injecting 25 ng (in 50 nl) of cRNA per oocytes, they were incubated for 3 days and expression was analyzed by Western blot and immunofluorescence (Figure 32). Western blots were performed using homogenates of injected and non-injected oocytes. Using anti-myc and anti-SLC16A14/MCT14 antibodies, a 57 kDa band corresponding to SLC16A14/MCT14 was detected in the injected oocytes

Furthermore, immunofluorescence indicated that SLC16A14/MCT14 was incorporated into the plasma membrane of the oocytes. These results further confirmed the specificity of the affinity purified anti-SLC16A14/MCT14 antibody used for Western blots and immunofluorescence as described before.

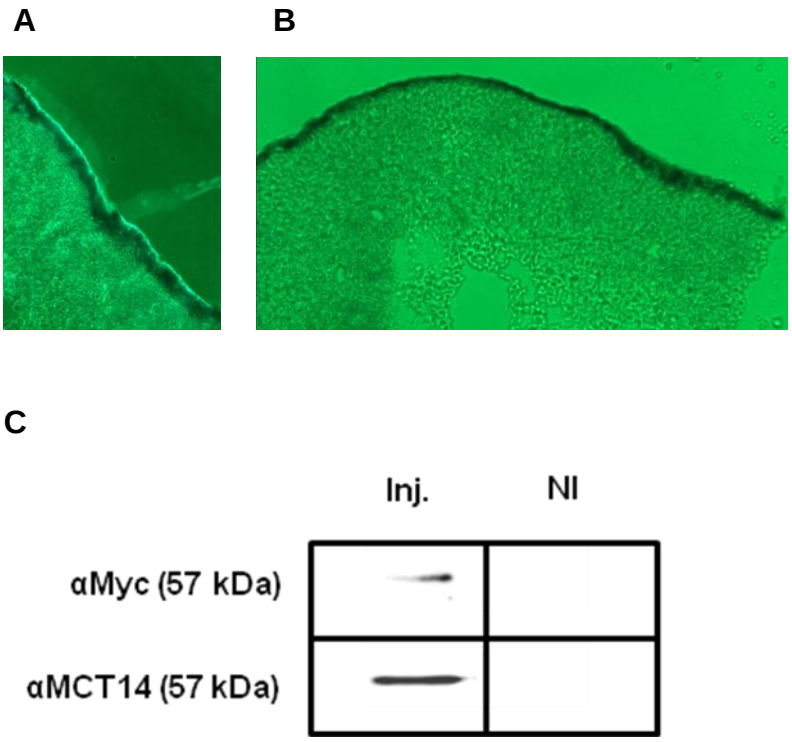

Figure 32. (A) Staining of SLC16A14/MCT14 protein in the plasma membrane of *Xenopus laevis* oocyte after third day of SLC16A14/MCT14 cRNA injection. **(B)** Control using non-injected oocytes. **(C)** Western blot analysis of injected and non injected oocytes with anti-myc and affinity purified anti-SLC16A14/MCT14 antibody. Inj.: Injected oocytes, NI: Non-Injected oocytes, αMyc: anti-myc antibody, αMCT14: anti-SLC16A14/MCT14 antibody.

Transport studies with *Xenopus laevis* oocytes expressing SLC16A14/MCT14

Based on transport data obtained from other SLC16 family members [196], it was likely that SLC16A14/MCT14 would carry monocarboxylates (i.e. lactate and pyruvate) and/or amino acids. These substrates were therefore investigated first. Initial experiments showed no differences for lactate transport between injected and non-injected oocytes (Figure 33). Some MCT members (MCT1 and MCT4) require the ancillary protein CD147 [196] for correct function and expression of their

transporter (see also discussion). An experiment was conducted to determine whether transport function could be affected by co-expressing SLC16A14/MCT14 together with CD147. However, co-injection of CD147 did not result in transport of lactate. Similarly, no evidence was obtained for pyruvate as being a substrate for SLC16A14/MCT14 (data not shown).

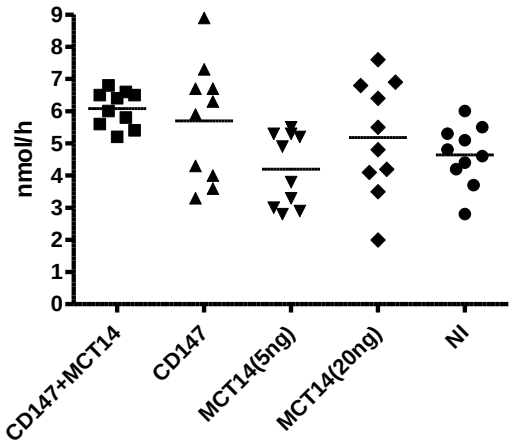

Figure 33. Transport study using radioactive labeled 10 mM lactate solution. *Xenopus laevis* eggs that have been co-injected with ancillary protein CD147 and SLC16A14/MCT14 showed no significant difference in transport rate compared to the non-injected (NI) oocytes. When injected with CD147 or SLC16A14/MCT14 alone, no difference in transport rate was observed either. No significant difference was observed in lactate uptake when injected with two different cRNA concentrations.

Further studies were conducted, in absence of CD147, using amino acids as substrates. Even though CD147 did not enhance transport function of lactate (Figure 33), it cannot be ruled out that it may enhance amino acid transport. Therefore, it would be of interest to repeat these experiments by coespressing MCT14 with CD147. Nevertheless, the following studies were conducted in the absence of CD147. Of interest, after 3 days of expression and in the presence of 100 mM sodium (ND100 solution) uptake of L-alanine was observed, but no uptake was observed for L-isoleucine or L-valine (Figure 34). The same observation was made when transport studies were performed in the absence of sodium (ND0 solution) (data not shown), indicating that SLC16A14/MCT14 transports L-alanine in a sodium-independent manner.

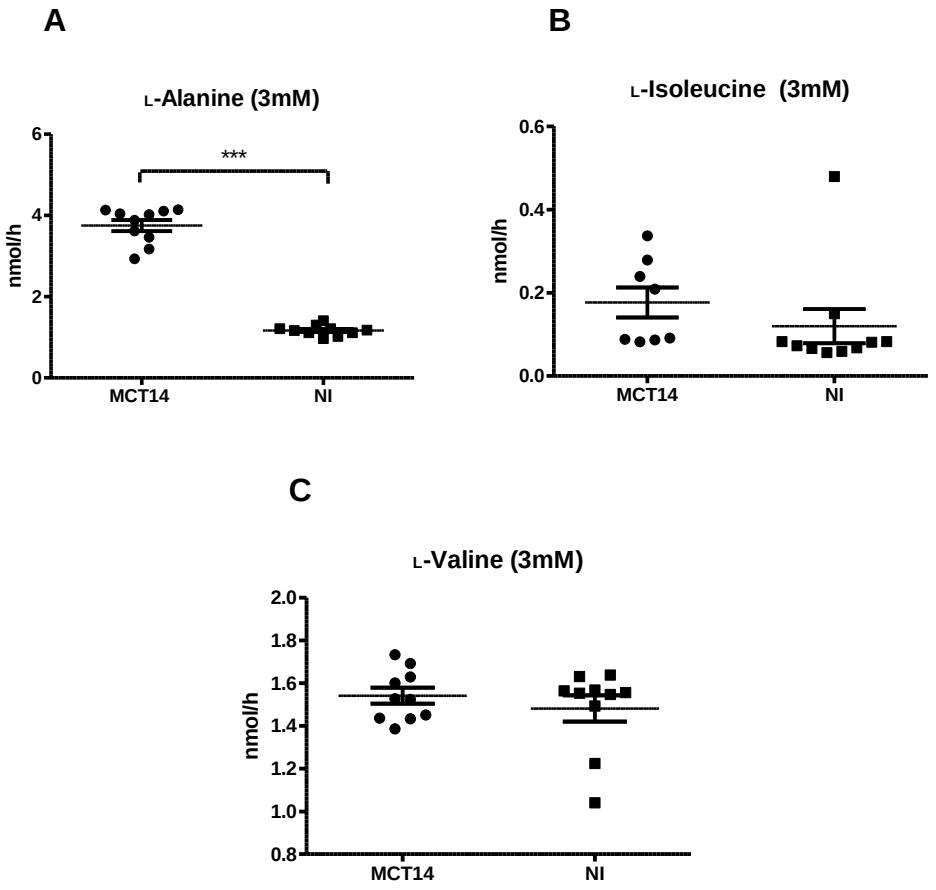

Figure 34. Uptake experiments with amino acids in *Xenopus laevis* oocytes expressing SLC16A14/MCT14 protein. **(A)** A significant transport of alanine had been determined. Transport was neither observed for **(B)** isoleucine nor for **(C)** valine. Data with ±SEM, n = 8-10, ***$p < 0.001$.

To test whether other amino acids may represent possible substrates for SLC16A14/MCT14, different amino acid cocktails were prepared for competition transport assays. All cocktails prepared included 6 mM of each amino acid. The cocktails also contained L-alanine as non radioactive (6 mM) and radioactively (^{3}H) labeled. The uptake of L-alanine in each cocktail was measured relative to the uptake of L-alanine alone. The data presented in Figure 35 indicate, that at least one of the components in cocktail C2 (L-methionine, L-tryptophane or L-phenylalanine) is competing with L-alanine transport by SLC16A14/MCT14. This competition is also shown for L-glutamate in cocktail C6b. In other words, at least two more amino acids, which are structurally very different from each other and from L-alanine may be transported by SLC16A14/MCT14 based on these transport assays.

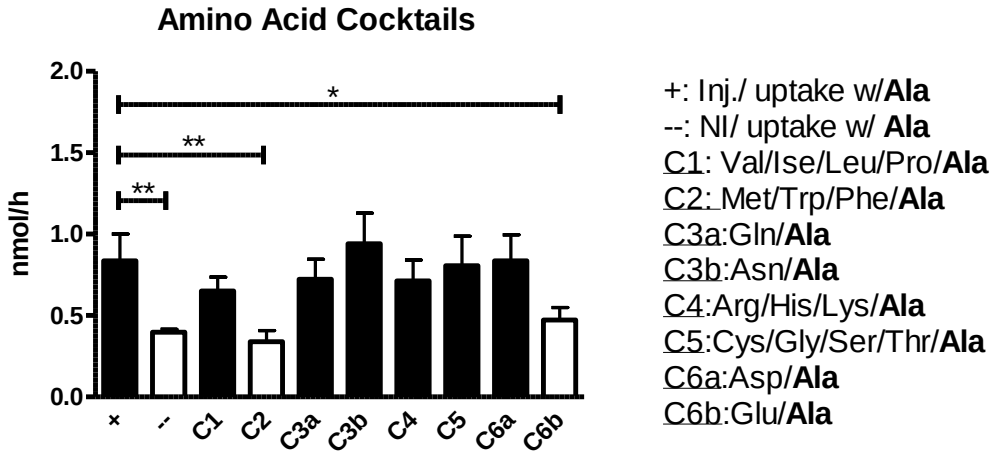

Figure 35. Different amino acids tested for transport by SLC16A14/MCT14. Each amino acid is present at 6 mM concentration in a cocktail. The goal was to determine amino acid uptake through inhibitory competition. A number of amino acid cocktails were prepared and then tested *in-vitro* for competition; (+) is the positive control using *Xenopus* oocytes injected with 25 ng cRNA of SLC16A14/MCT14 in presence of alanine whereas (–) presents the negative control, non injected oocytes, in the presence of alanine. Cocktails C2 and C6b both show an inhibition when compared to the positive control indicating a competition between alanine and another amino acids present in the cocktail. n = 6-10, $*p < 0.05$, $**p < 0.01$.

Based on competition assays shown in Figure 35, new experiments were carried out to test single amino acids (specifically amino acids contained in C2 and C6b) that reduced L-alanine uptake. These experiments indicate that L-methionine and L-glutamate indeed could be transported by SLC16A14/MCT14. Transport of L-tryptophane as well as L-phenylalanine was however not observed (Figure 36).

In summary, first results obtained characterizing transport function of SLC16A14/MCT14, indicated that it is likely that SLC16A14/MCT14 represents an amino acid transporter. However, some carboxylates (e.g. lactate, pyruvate) need to be further investigated, even though preliminary experiments suggested that SLC16A14/MCT14 does not transport them. Also, more information needs to be gathered regarding the kinetics for L-alanine, L-glutamate, and L-methionine transport.

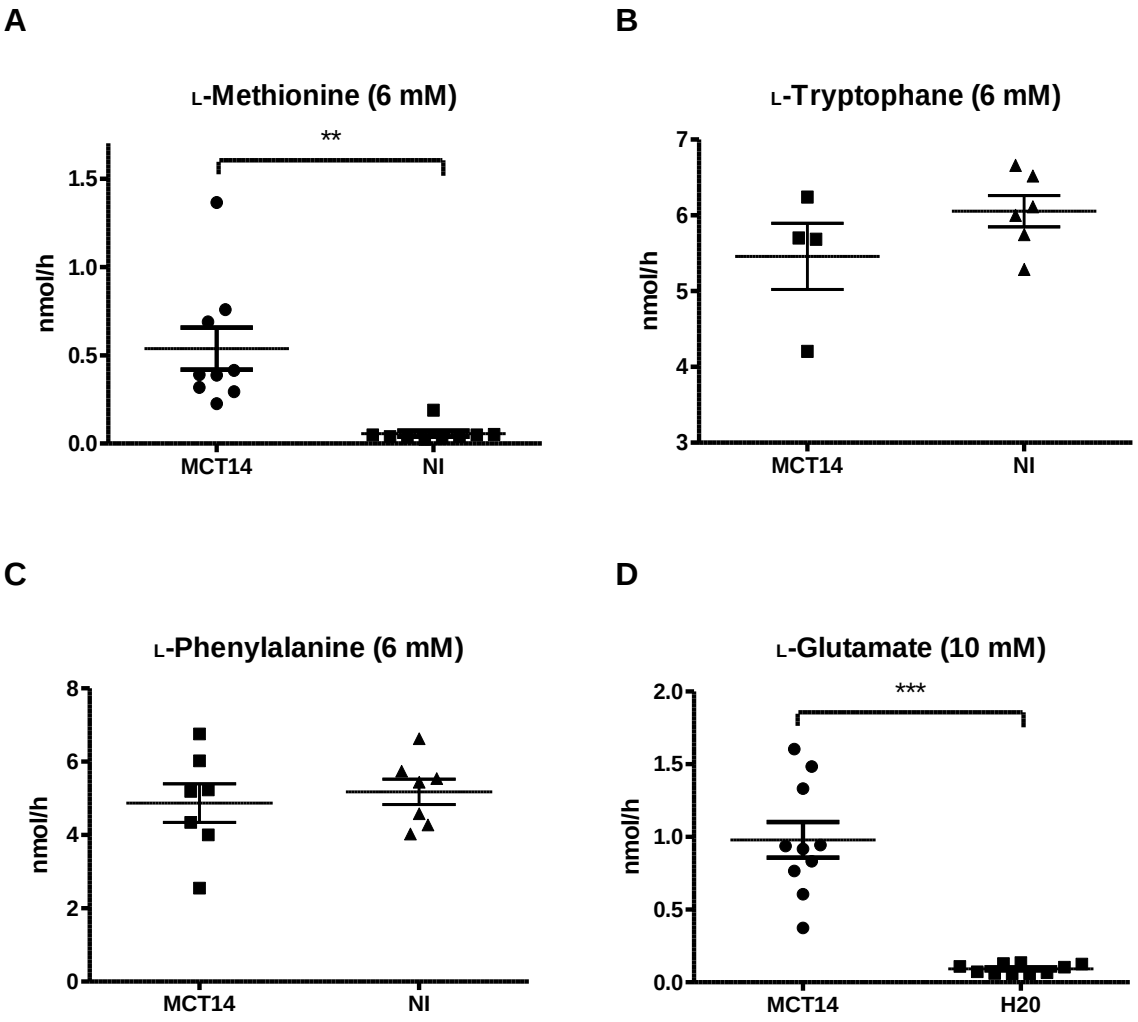

Figure 36. Experimental uptake of various amino acids. **(A)** Methionine is significantly transported in SLC16A14/MCT14 injected oocytes when compared to non-injected oocytes. **(B)** Tryptophane was not carried by SLC16A14/MCT14 and neither was **(C)** phenylalanine. **(D)** Glutamate was carried by SLC16A14/MCT14. Data collected in the absence of sodium. Data with ±SEM, n = 8-10, $^{**}p < 0.01$, $^{***}p < 0.001$.

\

DISCUSSION

Inorganic phosphate (Pi) is essential for a variety of systemic and molecular functions in the organism. Extracellular concentration of Pi is balanced mainly by the rate of renal reabsorption in the proximal tubules, and to a lesser extent by the rate of intestinal absorption of ingested Pi. Control of renal reabsorption of Pi is achieved by regulation of the abundances of Na/Pi-cotransporters that are localized at the apical membrane of proximal tubular cells. Different regulatory networks, such as an intestine-kidney axis or a bone-kidney axis are involved in the adjustment of intestinal and renal Pi-handling (see Introduction).

Deviations of extracellular concentration of Pi in either direction have severe consequences for the organism. Deficiency of Pi has been related to muscle weakness, rhabdomyolysis, impaired leukocyte function, and abnormal bone mineralization causing rickets and osteomalacia [13-15]. On the other hand, recent data has revealed that high dietary intake of Pi might promote tumor formation, as has been observed in animal models with skin cancer [197]. Another study has shown that high intake of Pi perturbs the growth of the brain in young mice [198]. Also, high Pi diets have been related to premature aging and cardiovascular diseases [199].

This study describes the effect of altered intake of dietary Pi on renal gene expression. To this end, mice were fed two different Pi-diets (LPD and HPD) for two different durations. On the one hand, mice were fed continuously with the diets for 5 days (“chronic” adaptation; “chronic” hypophosphatemic conditions) and on the other hand, mice were fed during three hours and analysis was performed 14 h after the onset of food intake (“acute” hypophosphatemic conditions). This later time point was chosen, because initial experiments demonstrated that gene expression of selected genes was not altered by LPD (compared to HPD) at earlier time points (4 and 8 h).

Obtained microarray results will be discussed first in the context of the “chronic” (5 days) dietary Pi changes. Then, the 14 h dietary Pi gene expression study will be separately analyzed and discussed. In addition, a comparison between the “acute” and “chronic” data set will be assessed. For all situations, special emphasis is given

on genes (gene products) that potentially could be involved in the control of renal handling of Pi (transporters, gene products potentially involved in trafficking, regulation).

"Chronic" (5 days) effect of LPD on renal gene expression

Dietary Pi-depletion for 5 days resulted in altered expression of genes that encode a variety of enzymes and transporters. Analysis of the microarray data set revealed, that close to one third of the genes present in the genome had been detected as transcripts in the kidney. This is in agreement with studies published on genes regulated by metabolic acidosis [189]. Expression of approximately 10% of the genes detected on the array was significantly changed ($p < 0.05$) by LPD and 80% of those were changed considerably (mFC > 50%). A number of genes were validated by RT-qPCR to confirm the data obtained from the microarray gene list, and the correlation between RT-qPCR and microarray experimental results was examined by linear regression (R^2 =0.803).

As will be discussed in more detail below, the major effect of LPD given "chronically" (5 days) was a decrease of expression of genes involved in energy metabolism. This effect was not surprising considering the role of Pi in glycolysis and oxidative phosphorylation. Therefore, expression of many genes (including transporters), may not be changed due to a Pi imbalance but rather may be changed as a result of an alteration in energy status.

The following paragraphs discuss the most relevant changes of gene expression induced by LPD given chronically. Statistics were performed on fold changes higher than 50% at a significant level of $p < 0.01$.

i) SLC Transporters

A total number of 12 transporters were found to be regulated after 5 days of “chronic” changes in dietary Pi: 3 ABC transporters and 9 SLC transporters. Interestingly, in this study, none of Na/Pi-cotransporters were detected on the microarray data set (neither at the level $p < 0.01$ nor at level $p < 0.05$). This result was not in agreement with the data obtained by RT-qPCR which demonstrated a significant increase of NaPi-2c mRNA after “chronic” low Pi-dietary conditions [1].

All ABC transporters detected were up-regulated: ABCb4 (mFC = 1.7), ABCa13 (mFC = 1.9) and ABCb1a (mFC = 4.3). These three ABC transporters have not been characterized thoroughly and therefore their implication in Pi homeostasis is not known.

Three SLC transporters were down-regulated; the monocarboxylate transporter family member SLC16A14/MCT14 (mFC = 0.2), the zinc transporter SLC39A14 (mFC = 0.5), and the glycerol/phosphate exchanger SLC37A2 (mFC = 0.6). Six other SLC members were up-regulated; L-type amino acid transporter SLC43A2 (mFC = 1.5), creatine transporter SLC6A8 (mFC = 1.6), nucleoside-sugar transporter family SLC35E3 (mFC = 1.7), aromatic amino acid transporter SLC16A10 (mFC = 2.1), mitochondrial family carrier SLC25A36 (mFC = 2.7) and cationic amino acid transporter/glycoprotein-associated family member SLC7A12 (mFC = 3.4).

ii) Electron transport chain and oxidative phosphorylation

Most of the genes affected by “chronic” low Pi belong to the electron transport chain and the mechanism of oxidative phosphorylation. 21 genes of the electron transport chain were found to be down-regulated as a consequence of LPD compared to HPD (Table 10a). As seen in Figure 37, most of the genes are grouped in Complex I (Ndufa3, Ndufa5, Ndufa7,

Ndufb7, Ndufs7, Ndufb4, Ndufb2, and Ndufc1). All of them are down-regulated between 1.5-2 fold. All other members of the electron transport chain regulated by Pi are grouped in Complex III, IV, and V. These genes are: Uqcrq, Uqcr, Cox5b, Cox7a2, Cox7c, Cox8a, Atp5e, Atp5g1, Atp5k, Atp5j2, and Atp5l. No changes of genes functioning in complex II were detected.

Table 10a. *Main processes with the highest number of down-regulated genes (p < 0.05)**

Process	Total in Pathway	Down-regulated	*p* Value
Electron transport chain	131	21	<0.001
Oxidative phosphorylation	73	13	<0.001
Adipogenesis	139	8	<0.001
Ossification	69	7	<0.001
Complement and coagulation cascades	66	5	<0.01
Complement activation, classical pathway	20	4	<0.001
Folic Acid Network	25	3	0.01
Prostaglandin Synthesis and Regulation	33	3	0.02

Table 10b. *Main processes with the highest number of up-regulated genes (p < 0.05)**

Process	Total in Pathway	Up-regulated	*P* Value
TNF-α NF-κB Signaling pathway	203	16	<0.001
Regulation of Actin Cytoskeleton	160	15	<0.001
EGFR1 Signaling pathway	188	13	<0.001
Androgen receptor signaling pathway	150	12	<0.001
Focal adhesion	199	12	0.001
Wnt signaling	135	11	<0.001
Amino acid metabolism	102	10	<0.001
G-protein signaling	111	9	<0.001
Keap1-Nrf2	14	4	<0.001

**p* value refers to the student's t-test applied to all genes with a fold change higher than 50%

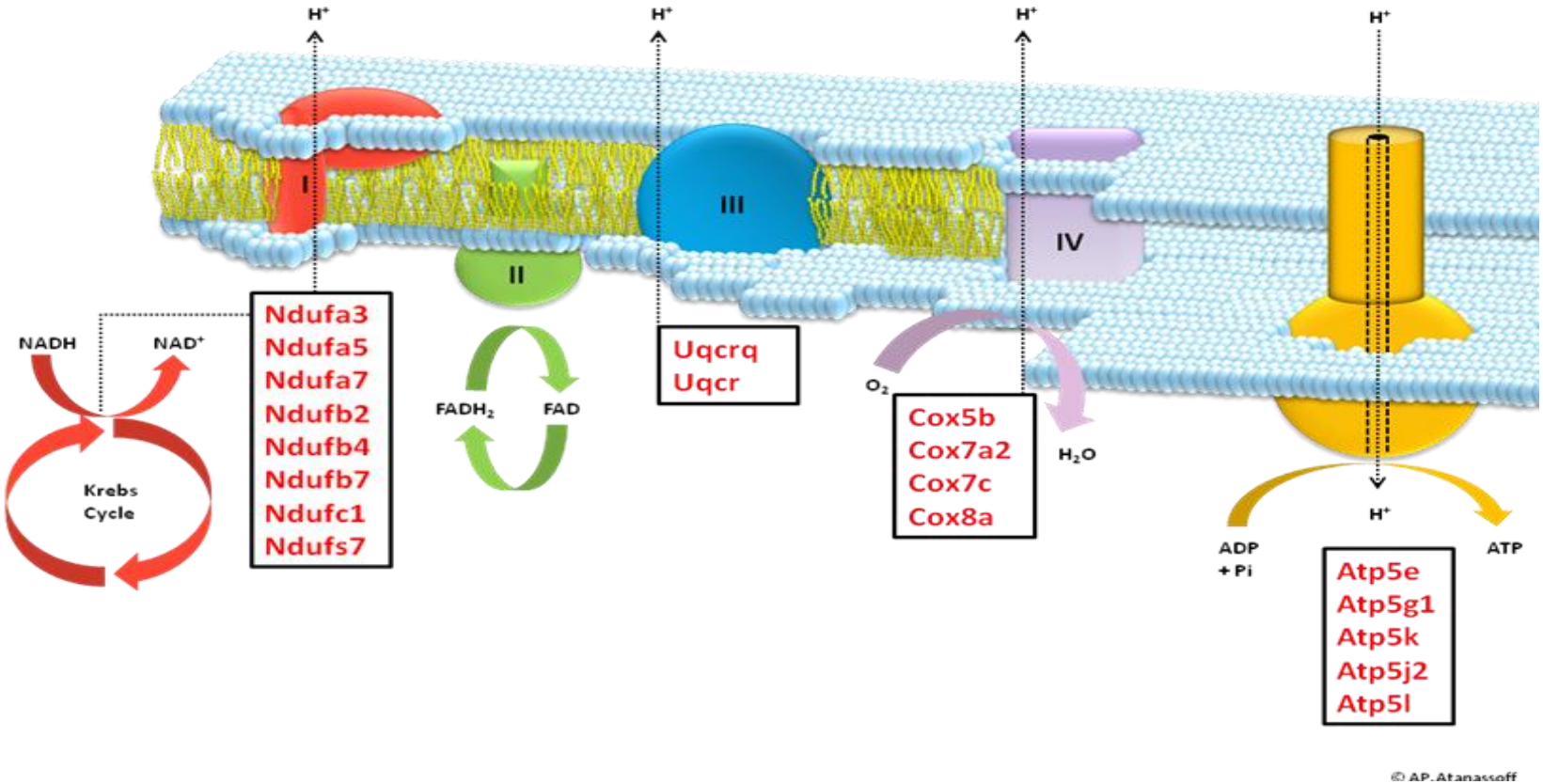

Figure 37. Electron transport chain of the mitochondria appears to be strongly targeted by dietary Pi. A low Pi diet after 5 days shuts down many genes responsible for ATP generation. Complex I contains most of the genes that are down-regulated.

iii) Glucose metabolism

Two genes have been detected that determine rate limiting steps in gluconeogenesis and glycolysis, respectively. Phosphoenolpyruvate carboxykinase, PEPCK, which is responsible for the production of oxalacetate from phosphoenolpyruvate and carbon dioxide was strongly down-regulated (mFC = 0.42). The other gene, also down-regulated (mFC = 0.64), is pyruvate kinase, Pk-1, which controls the metabolic breakdown of glucose, in particular responsible for catalyzing the transphosphorylation of phosphoenolpyruvate into pyruvate and ATP. These two genes are responsible for maintaining a balanced energy supply to all cells. In the kidney, the proximal tubular cells would be most affected since the need for oxygen and therefore glucose is very high. The strong inhibition of Pk-1 can cause a drastic decrease in ATP production and thus may affect many other processes that are dependent on this, causing a chain reaction of processes that are secondarily affected.

PEPCK is known to be crucial for gluconeogenesis in the organism and studies have shown the involvement of PEPCK in the kidney proximal tubular glucose metabolism [200]. Liver and kidney are two organs known to be involved in gluconeogenesis and glycolysis. Under certain conditions their activity can be measured in the blood plasma [200]. Early studies with hepatectomized and nephrectomized rats clearly demonstrated that the kidney is a source of plasma glucose [201-203]. Thus, the kidney is a consumer and a generator of glucose. The medulla predominates mostly in the consumption of glucose whereas the cortex (proximal tubules) functions in the reabsorption, release, and production of glucose. Since the kidney is both, a consumer and a producer of glucose, it is difficult to monitor the involvement of the kidney in glucose handling during different metabolic or pathological states. Glucose turnover is

defined by the distribution of enzymes involved in glucose metabolism along the nephron [204-206]. First studies involving glucose metabolism on isolated proximal tubuli from Pi depleted animals reported that basal gluconeogenesis was diminished [207].

Recently, a known stress responder, p53, had been determined in relation to transitory glucose or ATP depletion [208-209]. In these occasions, p53 pathway induces antioxidant defences. On the other hand, severe oxidative stress leads to p53 dependent cell death and apoptosis. However, function of p53 is very versatile and can affect a number of different pathways. The microarray data collected after 5 days of dietary Pi (also 14 h, see comparison below) reveals that transformation related protein 53 binding protein 2 (Trp53bp2) was strongly affected by dietary Pi (FC=0.42). Trp53bp related mechanisms will be discussed further below in relation to genes that were regulated by “acute” dietary Pi changes.

iv) Lipid metabolism

After 5 days of Pi-depletion, several genes involved in lipid metabolism were affected. These are: Acot12 (mFC = 0.6), Acot11 (mFC = 1.9), Acot2 (mFC = 2.6), Acot1 (mFC = 3.4), Acot 3 (mFC = 3.7). These genes encode thioesterases, a type of hydrolases responsible for catalysis (hydrolysis) of Acyl-CoA to free fatty acids and coenzyme A (CoASH). They contribute to the regulation of intracellular availability of Acyl-CoA, CoASH, and free fatty acids (see Acyl-CoA thioesterases below). The individual function of each thioesterase has not been determined in context of Pi homeostasis. Many of these thioesterases have not been characterized and therefore their role in lipid metabolism is not well understood.

v) Receptor mediated endocytosis and early endosomal trafficking

At the apical site of the proximal tubular cell, two routes for endocytosis have been described; receptor mediated- and fluid-phase endocytosis [210-211]. It was shown by colocalization of NaPi-2a and megalin, that upon PTH stimulation, NaPi-2a is likely to be internalized via receptor mediated endocytosis [212]. Shortly after PTH treatment (5 - 15 min), colocalization of NaPi-2a with clathrin has been demonstrated, and after 15 - 30 min this overlap became weaker [212]. The role of megalin, a receptor for endocytosis in the proximal tubule for multiple ligands [210-211, 213-214], seems to be essential at early stages of NaPi-2a endocytosis, since loss or reduction of megalin expression affected NaPi-2a internalization [213-214]. Further processing of NaPi-2a after endocytosis resulted in the colocalization of NaPi-2a with early endosomal antigen 1 (EEA1). Interestingly, microarray analysis data revealed an up-regulation of EEA1 (mFC = 1.6) after 5 days of low Pi-diet. EEA1 binds to phosphatidylinositol-3 phosphate (PtdIns(3)-P) and colocalizes together with Rab5 on endosomes [215-217]. Phosphatidylinositol-3 kinase (PI-(3)K) as well as Rab 5 were also up-regulated on the gene list with a 4- and 2-fold increase respectively. How these genes are involved in NaPi-2a regulation during internalization is unknown.

Other membrane proteins that have been detected on the list and that may be involved in membrane trafficking of NaPi-2a are Syntaxin 6 (mFC = 1.7), cortactin binding protein 2 (ORF4) (mFC = 5), melanoregulin (Mreg) (mFC = 5), Ankyrin repeat and BTB domain protein Abtb2 (mFC = 8), Synaptogyrin Syngr2 (mFC = 2) as well as some genes with products involved in microtubular association (e.g. microtubule-actin cross-linking factor 1 Macf1 (mFC = 1.5) and microtubule associated protein 1, Mapre1 (mFC = 1.9)).

vi) Activation Vitamin D 1α-hydroxylase (Cyp27B1)

The active form of Vitamin D (1α,25-$(OH)_2$ Vitamin D_3), is primarily formed in the kidney by 1α-hydroxylase (Cyp27B1) that is localized at the inner mitochondrial membrane. Among other factors, extracellular concentration of Pi is a well established regulator of Cyp27B1. Up-regulation by a LPD of Cyp27B1 mRNA levels and enzyme activity has been demonstrated [164, 168, 173]. Regulation of Cyp27B1 by Pi is independent of PTH and requires somatomedins as hypophysectomy blocks stimulation of Cyp27B1 by LPD [164, 168, 218]. Of interest, although hypophysectomy blocks stimulation of Cyp27B1, up-regulation of proximal tubular Na/Pi-cotransport by LPD was not affected [164, 168]. These results are also in agreement with studies performed with Cyp27B1 knock out mice, which demonstrated intact adaptation of Na/Pi-cotransport to LPD [219]. Thus, adaptation of renal Na/Pi-cotransport to LPD is independent of increases of active Vitamin D_3. In agreement with published data [173], gene expression data showed a 10-fold increase of Cyp27B1 mRNA after “chronic” intake of a LPD. This value was validated in a separate experiment by RT-qPCR. On the other hand, despite severe hypophosphatemia, no increase of Cyp27B1 mRNA content was detected after 14 h of LPD (see analysis of “acute” adaptation). Also this finding was validated by separate experiments. Taken together, results obtained with respect to regulation of Cyp27B1 were in agreement with published data [173] and suggest that the Vitamin D metabolism is not affected acutely by hypophosphatemic conditions. Active Vitamin D_3, with a half life of 4-6 hours [220], has been described as an important stimulator of the secretion of the phosphatonin FGF-23 [221]. Thus, a change in the level of FGF-23 by “acute” decreases of the extracellular concentration of Pi appears unlikely. On the other hand, FGF-23 reduces renal expression of 1α-hydroxylase and increases expression of catabolic enzyme 24-hydroxylase resulting in decreased circulating active Vitamin D_3 and thus phosphaturia [85].

"Acute" (14 hours) effect of LPD on renal gene expression

The data collected during "chronic" (5 days) Pi deprivation indicated a strong impact on energy metabolism that indirectly could have affected expression of other genes. In order to understand early adaptive mechanisms due to Pi deprivation, a shorter period, after administration of a LPD, was investigated. Based on RT-qPCR data obtained with selected genes that were regulated under "chronic" Pi depletion condition, a minimal time of 14 h after the onset of LPD has been chosen.

As shown in supplementary table S4, altered expression of 609 genes was detected with a statistical significance of $p < 0.05$. Of these, only those with a fold change higher than 50% were used for pathway analysis. These included 228 genes that were regulated (130 down- and 98 up-regulated genes). Pathway analysis grouping was not as efficient as with the data obtained after 5 days LPD and HPD. However, the pathways which mostly seemed to be affected after 14 hours of LPD vs. HPD were pointing to ammoniagenesis (and gluconeogenesis), cholesterol biosynthesis and lipid metabolism, apoptosis and the senescence pathway. Strikingly, after 14 h of LPD, no alteration of expression of genes involved in oxidative phosphorylation was detected.

i) Ammoniagenesis/Gluconeogenesis

In the PT, gluconeogenesis is closely linked to ammoniagenesis due to transformation of glutamine into glutamate and α-ketoglutarate (Figure 38). The conversion from glutamine to α-ketoglutarate releases two ammonium molecules. Animals that received a LPD, showed reduced expression of the Na^+-dependent glutamine transporter SLC38A3/SNAT3 (mFC = 0.38). This may be connected with the observation that in LPD mice ammonium excretion is reduced. In addition to reduced PEPCK (mFC = 0.16) expression, glutamate dehydrogenase Glud1 (mFC = 0.5) was also down-regulated after an "acute" LPD. Once α-ketoglutarate is converted into malate inside the mitochondria,

malate is antiported for citrate via the mitochondrial dicarboxylate transporter SLC25A10 [222-223]. SLC25A10 was also shown on the microarray list to be down-regulated (mFC = 0.58).

Down-regulation of this cascade of reactions, leading to the inhibition of gluconeogenesis, has been well known to occur during metabolic acidosis [189]. However, in association with renal Pi handling, these genes have not been put in context until now. It could be that Pi deficiency impairs malate export out of the mitochondria therefore causing a negative feedback loop on Glud and SNAT3.

A number of substrates for renal gluconeogenesis have been identified. Glycerol for example, has been shown to be unaffected in isolated proximal tubules depleted of glucose or Pi [224-225]. After 5 days of Pi depletion, a strong down-regulation ($mFC_{"chronic"}$ = 0.5) of SLC37A2 transporter was detected. SLC37A2 belongs to a sugar-phosphate/ phosphate exchanger family [226], which may indicate that this transporter may be involved during phosphate depletion. In addition, in “acute” Pi depletion glycogen synthase was found to be up-regulated ($mFC_{"acute"}$ = 1.7). Why this occurs during Pi depletion, while gluconeogenesis is impaired, is currently unknown.

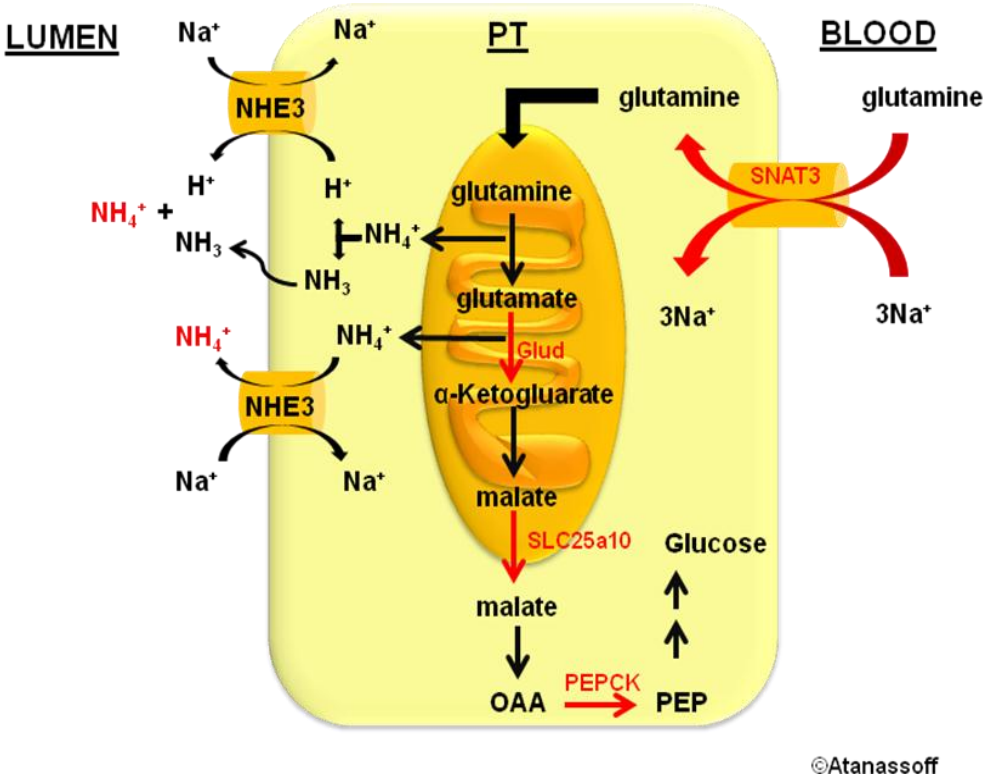

Figure 38: Down-regulation of various genes involved in gluconeogenesis and ammoniagenesis due to "acute" Pi deficiency. The strong down-regulation of the glutamine transporter SNAT3 (mFC = 0.38) may indicate less glutamine uptake into the PT cell. This leads to less substrate availability for the glutamine dehydrogenase (Glud) which is down-regulated as well.

ii) Cholesterol metabolism

After giving a LPD for 14 h, several genes involved in cholesterol metabolism were down-regulated. Previous experiments on NaPi-2a showed an inverse correlation of cotransport function with the content of cholesterol in the BBM [227-228]. In addition, modification of cholesterol content in isolated BBM *in-vitro*, selectively changed Na/Pi-cotransport activity. These studies indicated that cholesterol may have a direct effect on Na/Pi-cotransporter activity via alteration of membrane fluidity [229]. The microarray data agrees with these observations, as a series of enzymes involved in cholesterol metabolism were down-regulated after "acute" LPD ingestion (Figure 39). Reduction of 3-hydroxy-3-methyl-glutaryl-CoA synthetase (HMGCS, mFC = 0.5) and HMGC reductase

(HMGCR, mFC = 0.5) prevent the formation of mevalonate. And, the conversion of mevalonate into cholesterol is further impaired by a reduction of Cyp51 (mFC = 0.5). This suggests that the down-regulation of these genes may have a strong impact on cholesterol biosynthesis.

Earlier data obtained using dexamethasone showed inhibition of NaPi-2a cotransporter in the BBM associated with increased amount of glucosylceramide [230]. The study shows that renal BBM of rats treated with dexamethasone have a 2.5-fold decrease in NaPi-2a expression compared to control rats. This transport inhibition appeared to be selective since no transport changes of Na-dependent glucose and proline was detected after dexamethasone administration [230]. Dexamethasone did not significantly change the abundance of cholesterol in the BBM. In contrast, glucosylceramide concentration increased significantly in rats treated with dexamethasone. Interestingly, the enzyme sphingosine-1 phosphate phosphatase 1 (SPP1), which is involved in the pathway of ceramide synthesis and the production of glucosylceramide, is strongly down-regulated (mFC = 0.5) after 14 h of LPD. Taken together, it seems likely that Na/Pi-cotransport activity is not solely affected by membrane fluidity. Even though changes in membrane composition such as cholesterol and glucosylceramide may affect the NaPi-2a cotransporter through changes in membrane behaviour, the activity of glucosylceramide was also shown to specifically affect the V_{max} of the NaPi-2a cotransporter [230]. To which extent lipids play a role for NaPi-2a activity in the BBM during Pi deficiency, needs more investigation. Based on the microarray data collected, the question is raised, whether during a 14 h period of LPD an alternative mechanism is activated, since Vitamin D does not respond after this short period. By changing membrane lipid composition using cholesterol and ceramide derivatives, it seems likely that this response may act as a potential physicochemical modulator of NaPi-2a activity by affecting membrane fluidity. Eventually, it might be a combination of biochemical and physico-chemical properties that change NaPi-2a behavior at the BBM.

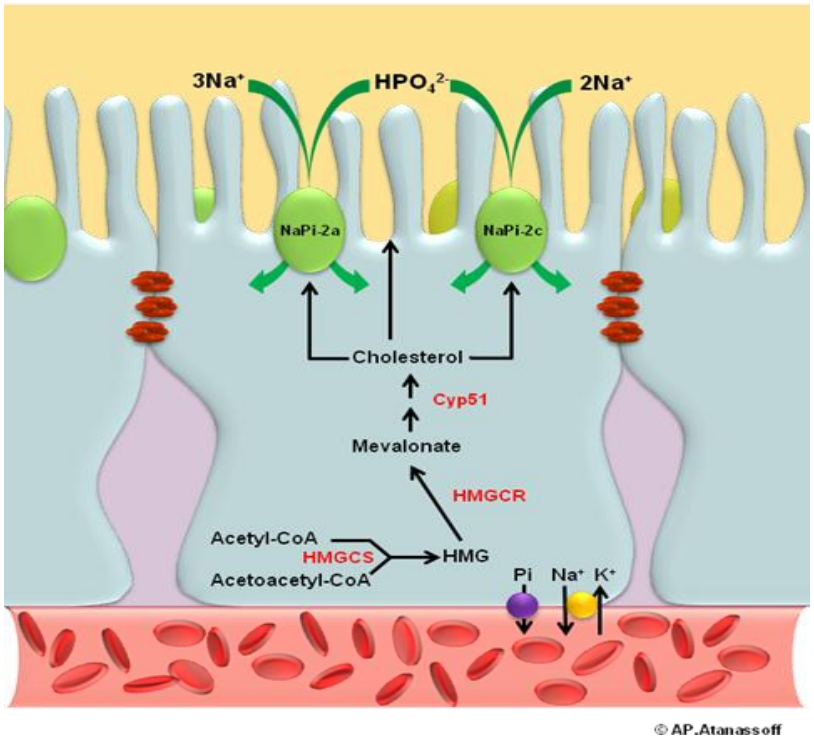

Figure 39: Impaired cholesterol synthesis causes disturbances in the membrane fluidity state of the cell. This in turn affects NaPi-2 function. In addition to that, cholesterol has been shown to directly affect NaPi-2 function.

iii) Apoptosis stimulating factor (ASPP2) and p21

Heat shock proteins (HSPs) can be activated in response to stress conditions, such as heat, alcohol, oxidative stress, heavy metals, fever, inflammation and inhibitors of energy metabolism. By increasing expression, HSPs act to promote cell survival by protecting other less stable proteins from proteolysis or disaggregation [231-233]. When HSPs are not stimulated by stress, they have other multiple “housekeeping” functions, such as assisting translocation of newly synthesized proteins into the nucleus, activating regulatory proteins (e.g. transcription factors), control protein degradation, signalling, and antigen presentation [234-235]. The overall function for HSPs was summarized as a “molecular chaperone”, a protein assisting other proteins in their process of folding or cellular maturation. As mentioned before, HSPs can modulate transcription

factors, such as p53 which is a transcriptional activator involved in tumour suppression, known to bind specifically to double stranded DNA. Hsp40 has been studied lately with immunoprecipitation methods and was found to be a key factor in recruiting other chaperones (Hsp70 and Hsp90) to p53 (Figure 40). Moreover, Hsp40 contains a J domain, responsible for regulating the ATPase activity of Hsp70 when binding to p53 [236]. While Hsp40 is able to bind p53 in absence of Hsp70 or ATP, Hsp70 is unable to form a complex with p53 in absence of Hsp40, unless a glutaraldehyde cross-linker is used [237]. This indicates that the interaction of p53 with Hsp70 is weak and its complex formation is driven by interaction with Hsp40. In this study, Hsp40 was found to be down-regulated in LPD kidney ($mFC_{"acute"} = 0.7$, $mFC_{"chronic"} = 0.6$). Under normal conditions, p53 has a low expression level but when stress signals are present (e.g. radiation, heat, hypoxia, inhibition of RNA synthesis through metabolites, heat shock, low extracellular pH, DNA damage), p53 is activated and induces cell cycle arrest. Many studies have demonstrated loss of p53 function in tumour cells due to mutations, where cells were growing indefinitely [238-240]. In 35-40% of all cancers, p53 is mutated. p53 can act either to promote cell cycle arrest or apoptosis. Which of the two pathways is finally chosen is not known. However, there are certain co-transcriptional factors that guide p53 to choose either one or the other [241-242]. p53 activity was shown to be regulated by post-translational modifications and also through post-transcriptional regulation, explaining the absence of mRNA changes [243-244] (as observed in some cases for NaPi-2a). Therefore, protein associations with p53 can modulate its activity. One of the binding proteins is the apoptosis stimulating p53 protein (ASPP2/TB53bp2), which was found on the microarray list to be down-regulated in LPD kidney ($mFC_{"acute"} = 0.6$, $mFC_{"chronic"} = 0.4$). Upon UV irradiation of MCF-7 cells, p53 association with ASPP2 was observed to increase 3.4-fold [245]. Interestingly, ASPP2 did not bind to mutated p53 and therefore apoptosis was not observed in these cells. This may explain the aggressiveness of cancers associated with p53 mutations, where ASPP2 is unable to

stimulate cell apoptosis [245]. When Saos-2 cells were transfected with p53, 17% of the cell population died through apoptosis. In contrast, when these cells were cotransfected with p53 and ASPP2 together, apoptosis was observed in 50% of the cell population [245]. Therefore, it seems that ASPP2 specifically enhances the apoptotic function of p53. The exact molecular mechanism how p53 and ASPP2 interact to stimulate apoptosis is not well established at the moment. p53 mediates transient or irreversible cell cycle arrest in the transitional phase G1 to S of cell replication, it then transcriptionally activates factors, such as the cyclin dependent kinases p16 and p21 [246]. p21/WAF1, known as the cyclin-dependent kinase inhibitor 1 or CDK-interacting protein 1, was originally found to bind and inhibit the activity of cyclin-CDK2 and –CDK4 complexes, therefore functioning as a regulator in the cell cycle progression at G_1 [247]. This regulation is tightly controlled by p53 activity [247]. In this study, p21 was up-regulated after 14 hours of LPD ($mFC_{"acute"}$ = 1.5) which may indicate that cell cycle arrest is inhibited by reduced amount of ASPP2 allowing p21 transcription by p53. Interestingly, a study involving dietary Pi demonstrated how p21 mRNA expression level increased (2-3 fold) in rat parathyroid glands 2 days after receiving a LPD (compared to HPD rats) [248]. Increased expression levels of p21 may therefore be an indicator of hypophosphatemia. Since the kidney and the parathyroid cells both increase expression of p21 after a LPD, Pi homeostasis could be linked to the regulation of p21.

In summary, Pi deficiency in mice observed in this study causes ASPP2 down-regulation, which further prevents association with p53 to cause apoptosis. Also, Hsp40 is down-regulated, not able to form a complex with p53. p53 may then bind to the p21 promoter to initiate transcription. An increased binding (2.2-fold) of p53 to p21 promoter was also observed in studies where cells where irradiated with UV light [245].

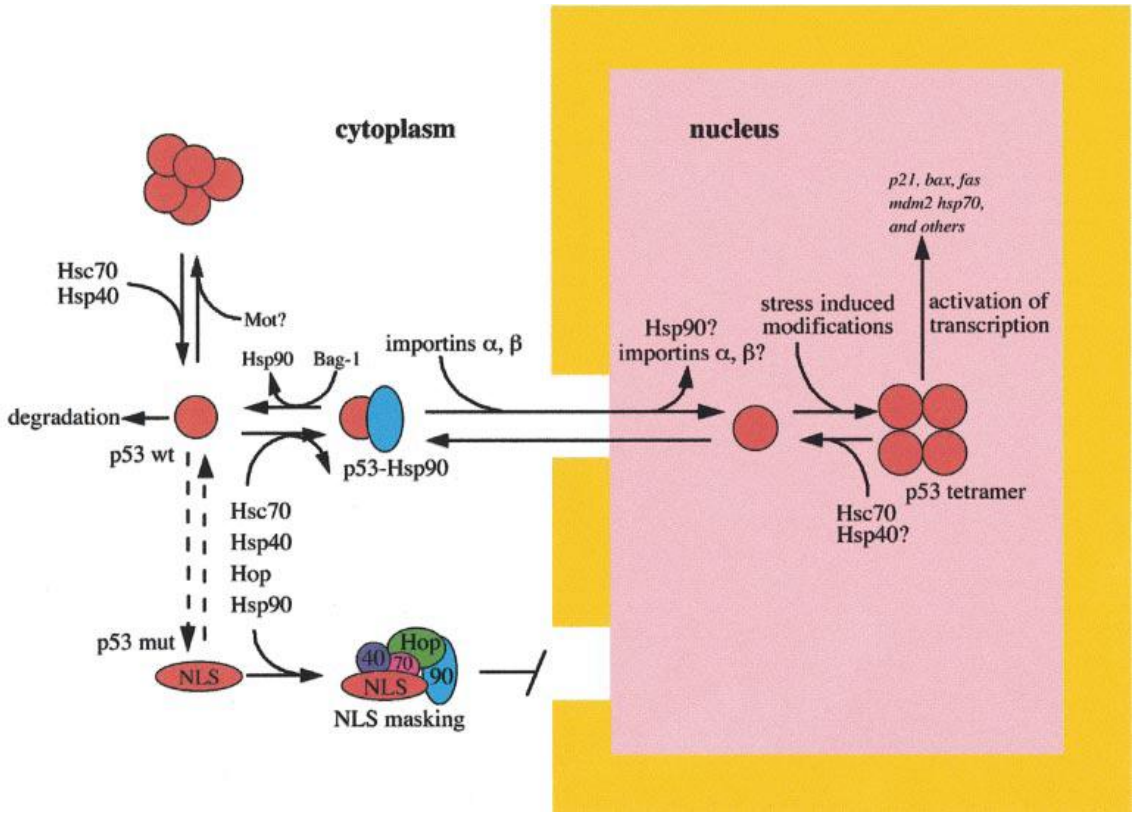

Figure 40. An overview of HSPs that participate in trafficking from and to the nucleus with p53 activity involved in p21 transcription. Image taken from [249].

iv) NaPi-2a mRNA interaction with p21 and Cyclin D1

Up-regulation of NaPi-2a cotransporter in the BBM as soon as two hours after LPD administration has suggested the existence of pre-formed NaPi-2a localized in endosomes and targeted to the apical membrane by a microtubular transport mechanism [250-251]. Even though NaPi-2a cotransporter presence is increased at the BBM [104], changes in mRNA levels have been controversial. Thus, while some observations confirm increases in mRNA levels during “chronic” hypophosphatemia [252], others, including this study, have not. The adaptive response to extracellular Pi deprivation in OK cells has shown no changes in mRNA abundance for the first two hours. This suggests a post-translational regulation of NaPi-2a that may be responsible for the presence at the BBM, independently of mRNA synthesis or regulation. However, following this

early adaptive response, a delayed effect on NaPi-2a expression was associated with an increase of mRNA abundance in these cells [253-254]. The data collected with RT-qPCR in this study shows a significant increase in NaPi-2c mRNA after “chronic” LPD and no significant change of NaPi-2a mRNA. However, in this study, no changes were observed for either NaPi-2a or NaPi-2c on the microarray list, neither after 5 days nor after 14 hours of LPD.

For correct regulation of NaPi-2a at the apical membrane of the proximal tubule, it is necessary to control the recruitment and the breakdown of the transporter in response to Pi [104, 142]. *In-vivo* studies in rats have shown post-transcriptional regulation of NaPi-2a [254-255]. NaPi-2a mRNA contains a *cis*-acting element at the junction of the coding, and the 3‘-untranslated region (UTR), that interacts with *trans*-acting proteins (e.g. p21, cyclin D). These proteins may be involved in the regulation and translation of NaPi-2a mRNA in response to dietary Pi [256]. On the other hand, a number of binding proteins have been identified that may contribute to either the apical distribution of NaPi-2a protein or its sub apical/lysosomal traffick. These are PDZ proteins such as NHERF, as well as AKAP and PEX19, the latter a protein that may be actively involved in controlling the internalization of NaPi-2a from the BBM [125, 127, 257]. Recent studies have also revealed calcineurin A*β* to be involved in renal Pi homeostasis [258]. Calcineurin inhibitor cyclosporin A (CsA) decreased NaPi-2a mRNA levels in *in-vivo* kidneys from animals fed LPD and in *in-vitro* cells that were grown in low-Pi medium. Also, calcineurin gene deletion caused decrease in NaPi-2a expression and further LPD administration did not result in increased expression of NaPi-2a [258]. This response was specific for NaPi-2a, because Vitamin D 1α- hydroxylase increased upon LPD administration [258].

It is likely that post-transcriptional regulation is mediated by proteins that can interact with target mRNA sequences. Binding of regulatory proteins to the 5’-UTR region of the mRNA is often associated with a translational role. To see whether binding proteins exist for NaPi-2a, a radioactively labelled

assay riboprobe study was conducted from rats treated with LPD and HPD [255]. Isolated 3' and 5' UTR ends were tested for binding sites of proteins. Proteins isolated from rat kidney cortex (e.g. p21, cyclin D1) were shown to compete for 5' UTR binding region of NaPi-2a mRNA suggesting possible regulation. These proteins demonstrated an increased affinity for the 5'-UTR of NaPi-2a during hypophosphatemia. As mentioned earlier, p21 ($mFC_{"acute"}$ = 1.5) had been detected in relation with p53. Interestingly, cyclin D1 was also up-regulated at a later stage ($mFC_{"chronic"}$ = 1.8) suggesting a regulatory role for the translation of NaPi-2a mRNA.

A new role of p21 and cyclin D to control translation of NaPi-2a mRNA may explain the insignificant differences observed in NaPi-2a mRNA levels after administration of LPD and HPD. When p53 is assembled as a tetramer inside the nucleus, it promotes the transcription of p21 ($mFC_{"acute"}$ = 1.5). Down-regulation of Hsp40, as observed in this study ($mFC_{"acute"}$ = 0.7, $mFC_{"chronic"}$ = 0.6), could indicate that Hsp40 cannot act with its ATPase activity on Hsc70 to disassemble the p53 tetramer and therefore prevents its export from the nucleus. This would be consistent with the up-regulation of p21 after a LPD. Down-regulation of ASPP2 ($mFC_{"acute"}$ = 0.6, $mFC_{"chronic"}$ = 0.4) would prevent the cell from apoptosis.

There is evidence that aging is affected during Pi deprivation. Aging is a fundamental process in all organisms ranging from yeast to mammals. *Klotho* was discovered nearly 15 years ago as a novel gene which has been associated with Pi, calcium and Vitamin D metabolism [259]. Mutations of *klotho,* resulting in loss of function, were associated with hyperphosphatemia, hypervitaminosis D and accelerated senescence [259]. In contrast, over-expression of *klotho* extended life span of mice and reduced damage done by oxidative stress [260-261]. The human *klotho* gene encodes a type 1 membrane protein with a putative signal sequence at its N-terminal, anchored at its C-terminal to the membrane [262]. *Klotho* has been localized to the renal distal convoluted tubule, the choroid plexus of brain epithelia, and the parathyroid gland [263]. A soluble form of *klotho* has been described [263]. Whether this soluble fraction is of the same

functional importance as its membrane bound form or not, is unknown to date. FGF-23 ablated mice are phenotypically very similar to the *klotho*$^{-/-}$ mice. This raises the question whether both share the same molecular pathways. Knock-down (RNAi) of *klotho* in human cells has shown an increase in p21. These cells were analyzed for their different cell cycle phases and determined that the klotho RNAi cells are arrested at G1/S boundary of their cell cycle. Further, early senescence has been shown to be dependent on p53 activity which results in the up-regulation of the p21 regulatory factor [264]. *Klotho* may have the ability to control senescence and apoptosis by regulating p53 action by mechanisms yet to be identified.
Taken together, elevated p21 may directly modulate translation of NaPi-2a mRNA and act to promote senescence via the klotho and p53 pathway during hyphosphatemia. Which of the two pathways is a consequence of Pi deprivation is currently unknown. Since both, NaPi-2a and *klotho* have been described in context of Pi homeostasis, it is reasonable to think that p21 has been activated to promote both NaPi-2a mRNA binding and p53-dependent senescence.

Comparison between 5 days and 14 hours Pi deprivation

Comparison of gene expression after a low Pi-diet given for 5 days to gene expression after 14 h revealed a number of common genes shared during dietary Pi deprivation. In this study, gene lists were compared on the significance level of $p < 0.01$. Most of these genes could not be identified after chronic low Pi-diet, suggesting a transient effect that is caused after an “acute” low Pi-diet period. In Table 11, genes that were affected by low Pi-diet, both after 14 h and 5 days, are listed. Two genes encode SLC transporters. These are, the unknown transporter SLC16A14/MCT14 ($mFC_{”acute”} = 0.23$ and $mFC_{”chronic”} = 0.21$) which belongs to the monocarboxylate transporter family (see below characterization of SLC16A14/MCT14), and SLC25A36 ($mFC_{”acute”} = 1.9$ and $mFC_{”chronic”} = 2.6$) also of unknown transport properties.

***Table 11**. Genes regulated by dietary Pi after 14 hours and 5 days (p < 0.01)*

Gene	Description	FC "acute"	FC "chronic"
Pepck	Phosphoenolpyruvate carboxykinase 1, cytosolic	0.16	0.43
Fkbp51	FK506 binding protein 5	0.19	0.50
SLC16A14/MCT14	Family member of the monocarboxylate transporters (see below)	0.23	0.21
Aacs	Acetoacetyl-CoA synthetase	0.45	0.56
Cckar	Cholecystokinin A receptor	0.45	0.51
Syngr2	Synaptogyrin 2	0.53	0.51
AI314027	Expressed sequence AI314027	0.56	0.53
Enpp2	ectonucleotide pyrophosphatase/phosphodiesterase 2	0.60	0.69
Trp53bp2	Transformation related protein 53 binding protein 2	0.61	0.42
Tyms	Thymidylate synthase	0.63	0.64
Spsb4	SplA/ryanodine receptor domain and SOCS box containing 4	1.6	2.5
Itgb6	Integrin beta 6	1.6	2.7
Lrat	Lecithin-retinol acyltransferase	1.6	3.4
Olfm3	Olfactomedin 3	1.7	4.2
Acot1	Acyl-CoA thioesterase 1	1.8	3.4
Jub	Ajuba	1.7	1.9
SLC25A36	Solute carrier family 25, member 36 (mitochondrial pyruvate carrier)	1.9	2.6
Tln2	Talin 2	1.9	2.1
Acot11	Acyl-CoA thioesterase 11	2.1	1.8
Gimap8	GTPase, IMAP family member 8	1.5	2.2
Omd	Osteomodulin	3.2	1.6

Some of the selected genes listed in Table 11 will be discussed in more detail below:

FK506 binding protein 51 (FKBP51)

FKBP51, has been shown to inhibit calcineurin in previous studies using *in-vitro* experiments [265]. FKBP51 was first discovered and identified in context with the progesterone receptor (PR) and shows a 60% sequence identity with FKBP52 [266-267]. In contrast to FKBP52, FKBP51 can bind to calcineurin independently from Ca^{2+} and FK506. Also, FKBP51 has the ability to be induced by heat in contrast to FKBP52 [265]. Both, FKBP51 and FKBP52, bind with their TPR domain to Hsp90 (see above Apoptosis and senescence), whereas the C-terminal end of FKBP51 enhances binding affinity to Hsp90 while the same C-terminal end of FKBP52 decreases binding affinity to Hsp90 [268-269].

Members of the FKBP family are intracellular enzymes that catalyze isomerizations of the peptidyl-proline bonds from *cis* to *trans* conformations in peptides and proteins. They have been shown to bind immunosuppressive drugs rapamycin (RAP) and FK506 [270-272]. First studies in immunology revealed, that the complex of FKBP and FK506 can bind and exhibit inhibition of calcineurin [273]. The participation of FKBP51 in phosphate homeostasis and the importance in regulation of calcineurin and NaPi-2a needs to be investigated further.

Cholecystokinin type A receptor (CCKAR)

The CCK receptors belong to the large family of GPCRs which are widely distributed in the organism [274]. The receptors for cholecystokinin (CCK) and other CCK-like peptides were first classified in acinar cells of the pancreas and named CCK type A receptors (CCKAR) [274]. Shortly thereafter, another receptor was identified in the brain with a different pharmacology, the CCK type B receptor. These two were mainly distinguished by their affinity for the agonist CCK and gastrin which share the same COOH-terminal but differ in sulphation of some amino acids in their peptide sequence. CCKAR is highly selective (500-1000 fold) for sulfated CCK analogs

whereas CCKBR has similar high affinity for sulfated and non-sulfated agonist peptides [274].

CCK release in the small intestine causes satiating effects in many species, also in humans. Even though cholecystokinin has been mostly related to pancreatic activity and intestinal bile secretion, other functions related to the kidney had been documented as well [275]. Nearly 25 years ago, a study with rabbits that were injected with CCK-8 in the renal artery presented a log-dose dependent increase in fractional sodium excretion and a log-dose dependent decrease in the fractional excretion of calcium and magnesium [275]. More detailed study of calcium distribution in the rabbit tissues showed a clear accumulation of calcium in the kidney and skeletal muscle upon CCK-8 infusion [275]. Moreover, CCK has been shown to activate calcineurin signaling, both *in-vitro* and *in-vivo* [276].

Microarray data obtained after both, “chronic” and “acute” Pi deprivation indicated a stable down-regulation of CCKAR ($mFC_{"acute"} = 0.45$, $mFC_{"chronic"} = 0.51$). It may be that the down-regulation of this G protein coupled receptor inhibits a pathway involved in Pi regulation. Whether there is a direct interaction of this receptor with dietary Pi or other factors involved in Pi homeostasis remains to be elucidated. More studies are required to see whether CCK or CCK like peptides can bind to CCKAR in the kidney and may be involved in renal regulation of Pi transport.

Acyl-CoA thioesterases (Acot1 and Acot11)

Acyl-CoA thioesterases (Acots) hydrolyze activated long- or short-chain fatty acids, saturated or poly-unsaturated, into non-esterified fatty acids and Coenzyme A (CoASH) [277]. In higher organisms, they are confined to the mitochondria, endoplasmic reticulum, peroxisomes and the cytosol. A wide range of tissues have been shown to contain these hydrolases, such as the brain, liver, heart, lung, kidney, steroidogenic and brown adipose tissue (BAT) [278]. The Acots have been grouped into two classes (type I and type II) which are determined by their molecular weight as well as by their different sequence similarity. “Acute” and “chronic” dietary Pi changes both increased gene expression of Acot1 and Acot11 (see Table 11).

Acot 1:

This thioesterase belongs to the group I and is mainly expressed in the cytosol. It has been most extensively studied in the rat liver [279-282], but its presence has also been documented in other tissues, such as the heart, kidney, brain, and testis [282-283]. Acot1 is responsible for catalyzing long-chain saturated fatty acyl-CoA esters. Usually, this enzyme is weakly expressed, but exogenous administration of peroxisome proliferating agents caused higher expression [279, 281-282]. Moreover, fasting and diabetes have both been shown to increase gene expression of Acot1 [279]. Detailed localization studies using Western blotting of Acot1 in the kidney revealed that its presence was mainly confined to the peroxisomal proximal tubular sites and other intrarenal sites involved in *β*-oxidation. *In-situ* hybridization suggested colocalization of Acot1 with Acot2 [283].

Acot11:

Acot11, a group II thioesterase, has been shown to be induced in brown adipose tissue of mice upon exposure to low temperatures. High temperatures however, have been associated with repression of Acot11 gene expression [284]. Thermogenesis involves the up-regulation of UCP1, also called thermogenin, which is involved in uncoupling oxidative phosphorylation from the proton motive force. This results in heat generation when energy is released from the oxidation of NADH instead of participating as part of the electron flow and generation of ATP. Therefore, up-regulation of Acot11 can serve various purposes; it can cause and increase in non-esterified fatty acids available to avoid UCP1 inhibition, it may serve to lower levels of esterified fatty acids therefore slowing *β*-oxidation and ATP generation, and it could modulate mitochondrial availability of CoASH [284]. Acot11 has been linked to obesity, where obesity-resistant mice have a two-fold increase of Acot11 mRNA as compared to mice that are susceptible to become obese. Nothing is known about the localization of Acot11. However, Acot11 is likely to be

present in the kidney since the microarray data collected in this study indicate an altered expression pattern after a LPD for both time periods (14 hours and 5 days).

β-oxidation is a process essential for cellular activity. Fatty acids are degraded within the mitochondria and peroxisomes to provide the energy required for cellular processes. When pristanoyl-CoA is oxidized to propionyl-CoA it can be further oxidized to succinyl-CoA in the mitochondria. Since propionyl-CoA is only slowly metabolized to succinyl-CoA, any disturbance in this reaction may result in metabolite accumulation within the cells and thereby impair metabolism [285-286] (Figure 41). An autosomal recessive metabolic disorder has been described involving the methylmalonyl-CoA mutase [287-289]. Mutation of this enzyme, responsible for succinyl-CoA synthesis, can lead to methylmalonic-aciduria [290]. This disorder is frequently diagnosed in early neonatal period, and symptoms observed are progressive encephalopathy, secondary hyperammonemia, and eventually death if left untreated [287].

Acots are involved in a variety of biological processes. Apart from *β*-oxidation, they have also been documented to regulate lipid biosynthesis (using an allosteric negative feedback of acetyl-CoA carboxylase [291] and fatty acid synthase), ion channel activity, signal transduction, fusion and budding of intracellular membranes, and gene transcription activity via nuclear receptors [286]. The energy status of the cell may be the key factor regulating the activity of Acots. Substrate inhibition had been documented for Acot1 where 5-10 µM of long chain CoA substrates in mice impaired its activity.

The increased activity of Acot1 and Acot11 after dietary Pi restrictions, as soon as 14 h and prolonging over 5 days, may be an alternative pathway to supply ATP since other ATP supplying pathways (e.g. gluconeogenesis, glycolysis) are inhibited. Whether Acots are directly influenced by Pi homeostasis or are involved in the regulation of Na/Pi-cotransport cannot be determined for now.

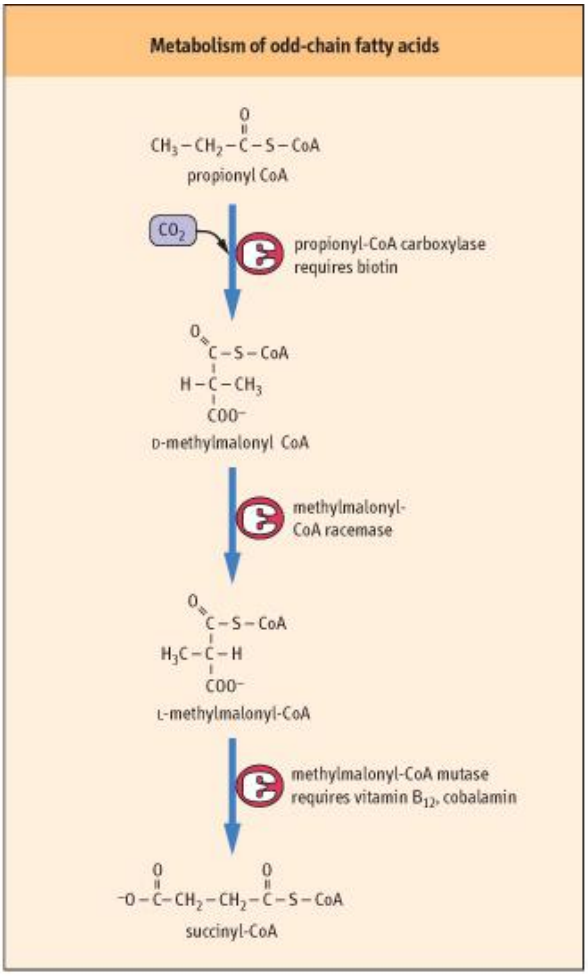

Figure 41. An alternative pathway for gluconeogenesis through *β*-oxidation of propionyl-CoA. Methylmalonyl-CoA, formed as an intermediate during the oxidation, can also be produced during catabolism of branched chained amino acids. Deficiencies in Vitamin B_{12} or mutations in methylmalonyl-CoA mutase cause methylmalonic-aciduria.

Osteomodulin/Osteoadherin (Omd)

Osteomodulin, a member of the small leucine-rich repeat (SLRP) family, has been recently described as a proteoglycan present in mineralized tissue, such as bone and teeth [292-296]. Over the past decade, new SLRP family members were found and momentarily are composed of 17 genes [297-300]. Not all of them are true proteoglycans, some of them have a glycosaminoglycan side chain and are therefore functionally related. Currently they have been further grouped into five different classes depending on their chromosome location, the presence of N-terminal Cys-

rich domains with defined spacing, and their conservation and homology at the protein and genomic levels.

Omd belongs to the class II of SLRPs and has been mostly related to mature osteoblasts where its secretion into the bone matrix is involved in mineralization [292, 294, 301-303]. Most of core protein of Omd comprises the leucine-rich repeat (LRR) sequence, while the acidic C-terminus most likely allows binding to hydroxyapatite mineral in the bone matrix [296]. Therefore, it is suggested that Omd functions partly as a bridging protein where cells bind to their extracellular matrix (ECM) of bone. Another member of the SLRP class II is decorin, which has been shown to signal via the LRR motif. This may imply that LRR motif containing proteins, such as osteomodulin, are part of signalling cascades [294].

The microarray data obtained after 14 h and 5 days low vs. high Pi diet clearly show an up-regulation of osteomodulin ($mFC_{"acute"}$ = 3.2, $mFC_{"chronic"}$ = 1.6), which was independently supported by RT-qPCR (see Results). This data may feed the idea that osteomodulin may not just be restricted to mineralized tissue after all. However, it is not possible to determine to which extent osteomodulin plays a role in maintaining Pi homeostasis. Preliminary data obtained by Western blot analysis using kidney homogenate incubated with anti-osteomodulin antibody presented a difference in protein abundance between low and high Pi-diet animals (data not shown), nevertheless this experiment was not re-validated and therefore needs to be repeated.

Integrin beta 6 and Talin

The cell maintains its shape with the help of various cytoskeletal proteins that are present at the cell membrane and in the cytosol. Moreover, a physical and dynamic connection between the cytosol and the membrane is constitutively present and regulates cell migration and adhesion besides structural properties [304]. Talin, a cytoskeletal associated protein, is composed of a globular N-terminal domain with ~200 residues that are similar to the membrane N-terminal binding domain of the ERM (ezrin-radixin-moesin) family of proteins. Unlike the ERM family members that

attach to cytoplasmic tails of membrane proteins through their N-terminal site, talin binds to integrins with its C-terminal rod-shaped-like structure, while its N-terminal site attaches to actin filaments [304]. Direct interactions between the cytoplasmic tail of β-integrin and talin have been experimentally confirmed with site directed mutations of their binding motifs [304].

Talin and β-integrin 6 were both regulated after a 14 h and 5 days of low vs. high Pi-diet. The microarray lists show a clear up-regulation of both, Integrin beta 6 ($mFC_{"acute"} = 1.6$, $mFC_{"chronic"} = 2.7$) and talin ($mFC_{"acute"} = 1.9$, $mFC_{"chronic"} = 2.1$).

SLC16A14/MCT14

The monocarboxylate transporter family SLC16A14/MCT14 is composed of 14 isoformes [196]. Initially, it was thought that lactate and pyruvate were carried by non-ionic diffusion through the plasma membrane, but when applying α-cyano-4-hydroxycinnamate (CHC) and organomercurials, the translocation in erythrocytes was inhibited [305-306]. After extensive characterization of the MCTs in erythrocytes, hepatocytes, and cardiac myocytes, it was proposed that a new family of MCTs could exist [306]. MCT1 was first characterized by specific labelling studies in rat and rabbit erythrocytes, and was therefore purified and sequenced. Further on, it was shown that the wild-type protein, catalyzed proton dependent pyruvate and lactate transport activity [307]. Garcia proceeded to clone the human MCT1 transporter [308] and after screening a rat liver cDNA library, a related protein, MCT2 was found to be highly expressed in the liver [309]. X-chromosome inactivation studies had revealed another MCT transporter, MCT8 which was originally called XPCT for X-linked, proline, glutamic acid, serine, threonine (PEST)-containing transporter [310]. MCT3 was detected in retinal pigmental epithelium of chicken and others (MCT4-7) were identified as well in the same laboratory [311-313]. Another isoform of the MCT family was very recently identified as a sodium- and proton-independent amino acid transporter called TAT1 [314]. MCT9 as well as MCT11-14 have all been identified on genetic sequence level through human genomic expressed sequence tag (EST)

database [196], but they have not been characterized in terms of their transport function.

In this study, SLC16A14/MCT14 was identified as a protein regulated by dietary Pi after 14 h and 5 days. Its distribution in the mouse was determined by screening different tissues using RT-qPCR. Results obtained, indicate the highest presence of gene expression in the kidney, 10 to 12 fold higher than in the pancreas and the testis. Expression of SLC16A14/MCT14 in the epididymis, the vesicular and the salivary glands was 40- to 50-fold less compared to the expression levels in the kidney.

Regulation of SLC16A14/MCT14 mRNA after 14 h of LPD may suggest modulation of the transporter by dietary Pi. Unfortunately, *in-situ* hybridization experiments did not reveal the presence of SLC16A14/MCT14 mRNA in the kidney. mRNA quantification of selected nephron segments indicated a low mRNA presence in the TAL, whereas no mRNA was detected in the PT. In addition to RT-qPCR, Western blot anaylsis and immunohistochemical studies show a regulation of SLC16A14/MCT14 protein by changes in dietary Pi after 14 hours and 5 days. However, no expression changes after 3 h of LPD are observed. When SLC16A14/MCT14 protein was studied by immunohistochemistry in NPD mice, it was shown to be evenly distributed along the TAL and the regions of the macula densa. However, after the administration of Pi diets, SLC16A14/MCT14 was shown to be regulated in the proximal tubule. Moreover after 14 h of LPD decreased abundance was detected in the PT when compared to the high expression of the transporter in the PT of HPD mice. Interestingly, the TAL was not targeted by changes in dietary Pi as much as the PT. Furthermore, the cellular distribution of SLC16A14/MCT14 changed in HPD mice upon receiving a LPD for 14 h or 5 days. Those mice that received a HPD presented strong expression of SLC16A14/MCT14 in the BBM of the proximal tubules. However, after a 14 h LPD period the transporter was detected no longer at the BBM, but rather in the sub apical regions of the membrane. This difference was also observed after “chronic” administration but not as pronounced as after the “acute” treatment.

Taken together, although transcriptional regulation exists for SLC16A14/MCT14, as detected by RT-qPCR and microarray analysis, immunofluorescence data for

SLC16A14/MCT14 indicates that the transporter may also be regulated on protein level (post-translational). Overall, mRNA levels for SLC16A14/MCT14 measured were low, and translocation of the transporter protein away from renal BBMs as early as 14 h after LPD was visually assessed by immunofluorescence.

SLC16A14/MCT14 was shown in this study to respond to dietary Pi as early as 14 h after a LPD administration. The mechanism of action is independent of the Vitamin D metabolism, since the 1α-hydroxylase was not regulated after 14 hours of LPD. Whether the mechanism of response of SLC16A14/MCT14 after 14 hours is the same as after 5 days, or another mechanism is involved (e.g Vitamin D) cannot be determined for now.

Transport studies obtained with oocytes expressing SLC16A14/MCT14 indicate that this carrier may be involved in renal amino acid handling. However, a link between dietary Pi changes and amino acid transport changes has not been established to date. Apparently the function for SLC16A14/MCT14 is very specific to the kidney, as its expression is rather restricted to this organ. This may be important to understand the renal adaptation of SLC16A14/MCT14 to dietary Pi changes for two reasons: first, the SLC16A14/MCT14 abundance (mRNA and protein) is regulated as early as 14 h after LPD administration, indicating that its involvement in renal Pi handling is likely. Second; the effect of LPD on the kidney, causes a sudden (14 h after LPD) decrease in SLC16A14/MCT14 abundance in the PT shown by transporter internalization. On the other hand, HPD animals present SLC16A14/MCT14 highly abundant in the BBM of the PT, suggesting that SLC16A14/MCT14 is not only regulated on the level of the kidney, but also on the level of the nephron.

Other MCT members have been previously described to interact with the chaperone CD147 in order to enhance their stability [196]. However, CD147 did not enhance lactate transport in SLC16A14/MCT14 expressing oocytes. A number of amino acids had been transported by SLC16A14/MCT14. L-Alanine, L-Methionine, and L-Glutamate all were transported by SLC16A14/MCT14. It cannot be excluded that other substrates, such as mono- di- or tricarboxylates are substrates for SLC16A14/MCT14. Also, no difference in L-Alanine uptake was observed in SLC16A14/MCT14 expressing oocytes when compared to oocytes that co-expressed the transporter with CD147 (data not shown). More experiments are required to

characterize SLC16A14/MCT14 fully and therefore understand its role in the kidney as well as its role in Pi homeostasis.

Outlook

The results obtained by microarray analysis reveal new insights related to renal gene expression during dietary Pi deprivation. However, many of these genes have not been previously associated with Pi, neither have they been identified in the kidney. Osteomodulin, as its name indicates, could eventually link dietary Pi, skeletogenesis and renal adaptation to low Pi-diet intake. Also, CCKAR had not been previously detected in the kidney, but it may play a currently unknown regulatory role in Pi reabsorption. Others, like cholesterol or calcineurin, have already been associated with changes in dietary Pi. In addition, the role of p53, p21 and klotho is not clear and could help understand senescence related to changes in dietary Pi. Future studies will shed light on this factors and their possible role in Pi homeostasis. Interestingly, different mechanisms of adaptation after 14 h and 5 days of Pi deficiency appear to exist. It would be interesting to understand the mechanisms of adaptation during dietary Pi deficiency in context of “chronic” and “acute” LPD. Also, further investigation would be necessary to identify the role of SLC16A14/MCT14 during dietary Pi changes leading to the regulation (on mRNA and protein level) of this transporter. SLC16A14/MCT14 was localized partly in the basolateral membrane of the cortical collecting ducts. This and other experimental findings need to be repeated in independent studies to characterize the transporter fully. Previous microarray experiments using isolated proximal tubular total RNA [189] shows the regulation of SLC16A14/MCT14 by metabolic acidosis. Therefore different metabolic states (i.e. metabolic acidosis and low Pi-diet) seem to affect expression level of SLC16A14/MCT14 in the proximal tubule and the TAL. It would be of great interest to find a connection between these metabolic alterations in context of SLC16A14/MCT14.

Bibliography

1. Berndt, T. and R. Kumar, *Novel mechanisms in the regulation of phosphorus homeostasis.* Physiology (Bethesda), 2009. **24**: p. 17-25.
2. Lardy, H.A. and S.M. Ferguson, *Oxidative phosphorylation in mitochondria.* Annu Rev Biochem, 1969. **38**: p. 991-1034.
3. Lehninger, A.L. and C.L. Wadkins, *Oxidative phosphorylation.* Annu Rev Biochem, 1962. **31**: p. 47-78.
4. Kornberg, A., *The enzymatic replication of DNA.* CRC Crit Rev Biochem, 1979. **7**(1): p. 23-43.
5. Krebs, E.G. and J.A. Beavo, *Phosphorylation-dephosphorylation of enzymes.* Annu Rev Biochem, 1979. **48**: p. 923-59.
6. Jencks, W.P., *From chemistry to biochemistry to catalysis to movement.* Annu Rev Biochem, 1997. **66**: p. 1-18.
7. Bessman, S.P. and C.L. Carpenter, *The creatine-creatine phosphate energy shuttle.* Annu Rev Biochem, 1985. **54**: p. 831-62.
8. Opdenkamp, J.A.F., *Lipid Asymmetry in Membranes.* Annual Review of Biochemistry, 1979. **48**: p. 47-71.
9. Stock, A.M., V.L. Robinson, and P.N. Goudreau, *Two-component signal transduction.* Annu Rev Biochem, 2000. **69**: p. 183-215.
10. Hansen, N.M., et al., *Aggregation of hydroxyapatite crystals.* Biochim Biophys Acta, 1976. **451**(2): p. 549-59.
11. Fruman, D.A., R.E. Meyers, and L.C. Cantley, *Phosphoinositide kinases.* Annu Rev Biochem, 1998. **67**: p. 481-507.
12. J.R. Geigy A.G., K. Diem, and C. Lentner, *Scientific tables*. 7th (enl.) ed. Its Documenta Geigy. 1970, Basle,: J. R. Geigy. 809 p.
13. Knochel, J.P., *The pathophysiology and clinical characteristics of severe hypophosphatemia.* Arch Intern Med, 1977. **137**(2): p. 203-20.
14. Knochel, J.P., et al., *Hypophosphatemia and rhabdomyolysis.* Trans Assoc Am Physicians, 1978. **91**: p. 156-68.
15. Shaikh, A., T. Berndt, and R. Kumar, *Regulation of phosphate homeostasis by the phosphatonins and other novel mediators.* Pediatr Nephrol, 2008. **23**(8): p. 1203-10.
16. Berndt, T. and R. Kumar, *Phosphatonins and the regulation of phosphate homeostasis.* Annu Rev Physiol, 2007. **69**: p. 341-59.
17. Chen, T.C., et al., *Role of vitamin D metabolites in phosphate transport of rat intestine.* J Nutr, 1974. **104**(8): p. 1056-60.
18. DeLuca, H.F., *Overview of general physiologic features and functions of vitamin D.* Am J Clin Nutr, 2004. **80**(6 Suppl): p. 1689S-96S.
19. Segawa, H., et al., *Intestinal Na-P(i) cotransporter adaptation to dietary P(i) content in vitamin D receptor null mice.* Am J Physiol Renal Physiol, 2004. **287**(1): p. F39-47.
20. Steele, T.H., et al., *Phosphatemic action of 1,25-dihydroxyvitamin D3.* Am J Physiol, 1975. **229**(2): p. 489-95.

21. Tanaka, Y. and H.F. Deluca, *Role of 1,25-dihydroxyvitamin D3 in maintaining serum phosphorus and curing rickets.* Proc Natl Acad Sci U S A, 1974. **71**(4): p. 1040-4.
22. Williams, K.B. and H.F. DeLuca, *Characterization of intestinal phosphate absorption using a novel in vivo method.* Am J Physiol Endocrinol Metab, 2007. **292**(6): p. E1917-21.
23. Lotscher, M., et al., *Role of microtubules in the rapid regulation of renal phosphate transport in response to acute alterations in dietary phosphate content.* J Clin Invest, 1997. **99**(6): p. 1302-12.
24. Murer, H., *Homer Smith Award. Cellular mechanisms in proximal tubular Pi reabsorption: some answers and more questions.* J Am Soc Nephrol, 1992. **2**(12): p. 1649-65.
25. Murer, H. and J. Biber, *A molecular view of proximal tubular inorganic phosphate (Pi) reabsorption and of its regulation.* Pflugers Arch, 1997. **433**(4): p. 379-89.
26. Murer, H., I. Forster, and J. Biber, *The sodium phosphate cotransporter family SLC34.* Pflugers Arch, 2004. **447**(5): p. 763-7.
27. Collins, J.F., L. Bai, and F.K. Ghishan, *The SLC20 family of proteins: dual functions as sodium-phosphate cotransporters and viral receptors.* Pflugers Arch, 2004. **447**(5): p. 647-52.
28. Fucentese, M., et al., *Functional expression of rat renal Na/Pi-cotransport (NaPi-2) in Sf9 cells by the baculovirus system.* J Membr Biol, 1995. **144**(1): p. 43-8.
29. Hartmann, C.M., et al., *Transport characteristics of a murine renal Na/Pi-cotransporter.* Pflugers Arch, 1995. **430**(5): p. 830-6.
30. Helps, C., H. Murer, and J. McGivan, *Cloning, sequence analysis and expression of the cDNA encoding a sodium-dependent phosphate transporter from the bovine renal epithelial cell line NBL-1.* Eur J Biochem, 1995. **228**(3): p. 927-30.
31. Magagnin, S., et al., *Expression cloning of human and rat renal cortex Na/Pi cotransport.* Proc Natl Acad Sci U S A, 1993. **90**(13): p. 5979-83.
32. Quabius, E.S., H. Murer, and J. Biber, *Expression of proximal tubular Na-Pi and Na-SO4 cotransporters in MDCK and LLC-PK1 cells by transfection.* Am J Physiol, 1996. **270**(1 Pt 2): p. F220-8.
33. Sorribas, V., et al., *Cloning of a Na/Pi cotransporter from opossum kidney cells.* J Biol Chem, 1994. **269**(9): p. 6615-21.
34. Verri, T., et al., *Cloning of a rabbit renal Na-Pi cotransporter, which is regulated by dietary phosphate.* Am J Physiol, 1995. **268**(4 Pt 2): p. F626-33.
35. Werner, A., H. Murer, and R.K. Kinne, *Cloning and expression of a renal Na-Pi cotransport system from flounder.* Am J Physiol, 1994. **267**(2 Pt 2): p. F311-7.
36. Busch, A., et al., *Electrophysiological analysis of Na+/Pi cotransport mediated by a transporter cloned from rat kidney and expressed in Xenopus oocytes.* Proc Natl Acad Sci U S A, 1994. **91**(17): p. 8205-8.
37. Busch, A.E., et al., *Electrophysiological insights of type I and II Na/Pi transporters.* Kidney Int, 1996. **49**(4): p. 986-7.

38. Busch, A.E., et al., *Expression of a renal type I sodium/phosphate transporter (NaPi-1) induces a conductance in Xenopus oocytes permeable for organic and inorganic anions.* Proc Natl Acad Sci U S A, 1996. **93**(11): p. 5347-51.
39. Busch, A.E., et al., *Properties of electrogenic Pi transport by a human renal brush border Na+/Pi transporter.* J Am Soc Nephrol, 1995. **6**(6): p. 1547-51.
40. Cai, Q., et al., *Brief report: inhibition of renal phosphate transport by a tumor product in a patient with oncogenic osteomalacia.* N Engl J Med, 1994. **330**(23): p. 1645-9.
41. Forster, I.C., J. Biber, and H. Murer, *Proton-sensitive transitions of renal type II Na(+)-coupled phosphate cotransporter kinetics.* Biophys J, 2000. **79**(1): p. 215-30.
42. Beck, L., et al., *Targeted inactivation of Npt2 in mice leads to severe renal phosphate wasting, hypercalciuria, and skeletal abnormalities.* Proc Natl Acad Sci U S A, 1998. **95**(9): p. 5372-7.
43. Segawa, H., et al., *Growth-related renal type II Na/Pi cotransporter.* J Biol Chem, 2002. **277**(22): p. 19665-72.
44. Tenenhouse, H.S., et al., *Differential effects of Npt2a gene ablation and X-linked Hyp mutation on renal expression of Npt2c.* Am J Physiol Renal Physiol, 2003. **285**(6): p. F1271-8.
45. Segawa, H., et al., *Type IIc sodium-dependent phosphate transporter regulates calcium metabolism.* J Am Soc Nephrol, 2009. **20**(1): p. 104-13.
46. Custer, M., et al., *Expression of Na-P(i) cotransport in rat kidney: localization by RT-PCR and immunohistochemistry.* Am J Physiol, 1994. **266**(5 Pt 2): p. F767-74.
47. Ritthaler, T., et al., *Effects of phosphate intake on distribution of type II Na/Pi cotransporter mRNA in rat kidney.* Kidney Int, 1999. **55**(3): p. 976-83.
48. Alizadeh Naderi, A.S. and R.F. Reilly, *Hereditary disorders of renal phosphate wasting.* Nat Rev Nephrol, 2010. **6**(11): p. 657-65.
49. Madjdpour, C., et al., *Segment-specific expression of sodium-phosphate cotransporters NaPi-IIa and -IIc and interacting proteins in mouse renal proximal tubules.* Pflugers Arch, 2004. **448**(4): p. 402-10.
50. Bergwitz, C., et al., *SLC34A3 mutations in patients with hereditary hypophosphatemic rickets with hypercalciuria predict a key role for the sodium-phosphate cotransporter NaPi-IIc in maintaining phosphate homeostasis.* Am J Hum Genet, 2006. **78**(2): p. 179-92.
51. Kurnik, B.R. and K.A. Hruska, *Mechanism of stimulation of renal phosphate transport by 1,25-dihydroxycholecalciferol.* Biochim Biophys Acta, 1985. **817**(1): p. 42-50.
52. Kurnik, B.R. and K.A. Hruska, *Effects of 1,25-dihydroxycholecalciferol on phosphate transport in vitamin D-deprived rats.* Am J Physiol, 1984. **247**(1 Pt 2): p. F177-84.
53. Bonjour, J.P. and J. Caverzasio, *Phosphate transport in the kidney.* Rev Physiol Biochem Pharmacol, 1984. **100**: p. 161-214.
54. Dousa, T.P., *Modulation of renal Na-Pi cotransport by hormones acting via genomic mechanism and by metabolic factors.* Kidney Int, 1996. **49**(4): p. 997-1004.

55. Hammerman, M.R., *The growth hormone-insulin-like growth factor axis in kidney.* Am J Physiol, 1989. **257**(4 Pt 2): p. F503-14.
56. Kempson, S.A., *Peptide hormone action on renal phosphate handling.* Kidney Int, 1996. **49**(4): p. 1005-9.
57. Hammerman, M.R., et al., *Insulin stimulates Pi transport in brush border vesicles from proximal tubular segments.* Am J Physiol, 1984. **247**(5 Pt 1): p. E616-24.
58. Hammerman, M.R. and S. Rogers, *Distribution of IGF receptors in the plasma membrane of proximal tubular cells.* Am J Physiol, 1987. **253**(5 Pt 2): p. F841-7.
59. Hammerman, M.R., I.E. Karl, and K.A. Hruska, *Regulation of canine renal vesicle Pi transport by growth hormone and parathyroid hormone.* Biochim Biophys Acta, 1980. **603**(2): p. 322-35.
60. Caverzasio, J., C. Montessuit, and J.P. Bonjour, *Stimulatory effect of insulin-like growth factor-1 on renal Pi transport and plasma 1,25-dihydroxyvitamin D3.* Endocrinology, 1990. **127**(1): p. 453-9.
61. Rogers, S.A. and M.R. Hammerman, *Growth hormone activates phospholipase C in proximal tubular basolateral membranes from canine kidney.* Proc Natl Acad Sci U S A, 1989. **86**(16): p. 6363-6.
62. Arar, M., et al., *Epidermal growth factor inhibits Na-Pi cotransport and mRNA in OK cells.* Am J Physiol, 1995. **268**(2 Pt 2): p. F309-14.
63. Jehle, A.W., et al., *IGF-I and vanadate stimulate Na/Pi-cotransport in OK cells by increasing type II Na/Pi-cotransporter protein stability.* Pflugers Arch, 1998. **437**(1): p. 149-54.
64. Quigley, R. and M. Baum, *Effects of epidermal growth factor and transforming growth factor-alpha on rabbit proximal tubule solute transport.* Am J Physiol, 1994. **266**(3 Pt 2): p. F459-65.
65. Boross, M., et al., *Glucocorticoids and metabolic acidosis-induced renal transports of inorganic phosphate, calcium, and NH4.* Am J Physiol, 1986. **250**(5 Pt 2): p. F827-33.
66. Freiberg, J.M., J. Kinsella, and B. Sacktor, *Glucocorticoids increase the Na+-H+ exchange and decrease the Na+ gradient-dependent phosphate-uptake systems in renal brush border membrane vesicles.* Proc Natl Acad Sci U S A, 1982. **79**(16): p. 4932-6.
67. Noronha-Blob, L. and B. Sacktor, *Inhibition by glucocorticoids of phosphate transport in primary cultured renal cells.* J Biol Chem, 1986. **261**(5): p. 2164-9.
68. Ambuhl, P.M., et al., *Regulation of renal phosphate transport by acute and chronic metabolic acidosis in the rat.* Kidney Int, 1998. **53**(5): p. 1288-98.
69. Espinosa, R.E., et al., *Effect of thyroxine administration on phosphate transport across renal cortical brush border membrane.* Am J Physiol, 1984. **246**(2 Pt 2): p. F133-9.
70. Beers, K.W. and T.P. Dousa, *Thyroid hormone stimulates the Na(+)-PO4 symporter but not the Na(+)-SO4 symporter in renal brush border.* Am J Physiol, 1993. **265**(2 Pt 2): p. F323-6.
71. Sorribas, V., et al., *Thyroid hormone stimulation of Na/P-i-cotransport in opossum kidney cells.* Pflugers Archiv-European Journal of Physiology, 1995. **431**(2): p. 266-271.

72. Beers, K.W., et al., *beta-Estradiol inhibits Na+-P(i) cotransport across renal brush border membranes from ovarectomized rats.* Biochem Biophys Res Commun, 1996. **221**(2): p. 442-5.
73. Bacic, D., et al., *Regulation of the renal type IIa Na/Pi cotransporter by cGMP.* Pflugers Arch, 2001. **443**(2): p. 306-13.
74. Nakai, M., et al., *Atrial Natriuretic Factor Inhibits Phosphate-Uptake in Opossum Kidney-Cells - as a Model of Renal Proximal Tubules.* Biochemical and Biophysical Research Communications, 1988. **152**(3): p. 1416-1420.
75. Berndt, T.J. and F.G. Knox, *Proximal tubule site of inhibition of phosphate reabsorption by calcitonin.* Am J Physiol, 1984. **246**(6 Pt 2): p. F927-30.
76. Yusufi, A.N., et al., *Calcitonin inhibits Na+ gradient-dependent phosphate uptake across renal brush-border membranes.* Am J Physiol, 1987. **252**(4 Pt 2): p. F598-604.
77. Ahloulay, M., et al., *Cyclic AMP is a hepatorenal link influencing natriuresis and contributing to glucagon-induced hyperfiltration in rats.* J Clin Invest, 1996. **98**(10): p. 2251-8.
78. Econs, M.J. and M.K. Drezner, *Tumor-induced osteomalacia--unveiling a new hormone.* N Engl J Med, 1994. **330**(23): p. 1679-81.
79. Berndt, T., et al., *Secreted frizzled-related protein 4 is a potent tumor-derived phosphaturic agent.* J Clin Invest, 2003. **112**(5): p. 785-94.
80. Berndt, T.J., S. Schiavi, and R. Kumar, *"Phosphatonins" and the regulation of phosphorus homeostasis.* Am J Physiol Renal Physiol, 2005. **289**(6): p. F1170-82.
81. Bowe, A.E., et al., *FGF-23 inhibits renal tubular phosphate transport and is a PHEX substrate.* Biochem Biophys Res Commun, 2001. **284**(4): p. 977-81.
82. De Beur, S.M., et al., *Tumors associated with oncogenic osteomalacia express genes important in bone and mineral metabolism.* J Bone Miner Res, 2002. **17**(6): p. 1102-10.
83. Rowe, P.S., et al., *MEPE, a new gene expressed in bone marrow and tumors causing osteomalacia.* Genomics, 2000. **67**(1): p. 54-68.
84. Rowe, P.S., et al., *MEPE has the properties of an osteoblastic phosphatonin and minhibin.* Bone, 2004. **34**(2): p. 303-19.
85. Shimada, T., et al., *Cloning and characterization of FGF23 as a causative factor of tumor-induced osteomalacia.* Proc Natl Acad Sci U S A, 2001. **98**(11): p. 6500-5.
86. Dominguez, J.H., et al., *Prostaglandin E2 and parathyroid hormone: comparisons of their actions on the rabbit proximal tubule.* Kidney Int, 1984. **26**(4): p. 404-10.
87. Bacic, D., et al., *Activation of dopamine D1-like receptors induces acute internalization of the renal Na+/phosphate cotransporter NaPi-IIa in mouse kidney and OK cells.* Am J Physiol Renal Physiol, 2005. **288**(4): p. F740-7.
88. Baines, A.D. and R. Drangova, *Does dopamine use several signal pathways to inhibit Na-Pi transport in OK cells?* J Am Soc Nephrol, 1998. **9**(9): p. 1604-12.
89. Cheng, L., et al., *Dopamine stimulation of cAMP production in cultured opossum kidney cells.* Am J Physiol, 1990. **258**(4 Pt 2): p. F877-82.

90. Friedlander, G. and C. Amiel, *Autocrine/paracrine control of renal phosphate transport.* Kidney Int Suppl, 1996. **57**: p. S148-53.
91. Glahn, R.P., et al., *Autocrine/paracrine regulation of renal Na(+)-phosphate cotransport by dopamine.* Am J Physiol, 1993. **264**(4 Pt 2): p. F618-22.
92. Beck, N., S.K. Webster, and H.J. Reineck, *Effect of fasting on tubular phosphorus reabsorption.* Am J Physiol, 1979. **237**(3): p. F241-6.
93. Kempson, S.A., *Effects of fasting compared to low phosphorus diet on the kinetics of phosphate transport by renal brush-border membranes.* Biochim Biophys Acta, 1985. **815**(1): p. 85-90.
94. Amiel, C., et al., *Evidence for a parathyroid hormone-independent calcium modulation of phosphate transport along the nephron.* J Clin Invest, 1976. **57**(2): p. 256-63.
95. Wong, N.L., et al., *Effects of phosphate and calcium infusion on renal phosphate transport in the dog.* Ren Physiol, 1985. **8**(1): p. 30-7.
96. Oberleithner, H., et al., *Influence of calcium and ionophore 23187 on tubular phosphate reabsorption.* Pflugers Arch, 1979. **379**(1): p. 37-41.
97. Rouse, D. and W.N. Suki, *Modulation of phosphate absorption by calcium in the rabbit proximal convoluted tubule.* J Clin Invest, 1985. **76**(2): p. 630-6.
98. Caverzasio, J. and J.P. Bonjour, *Influence of calcium on phosphate transport in cultured kidney epithelium.* Am J Physiol, 1988. **254**(2 Pt 2): p. F217-22.
99. Amstutz, M., et al., *Effect of pH on phosphate transport in rat renal brush border membrane vesicles.* Am J Physiol, 1985. **248**(5 Pt 2): p. F705-10.
100. Nowik, M., et al., *Renal phosphaturia during metabolic acidosis revisited: molecular mechanisms for decreased renal phosphate reabsorption.* Pflugers Arch, 2008. **457**(2): p. 539-49.
101. Wagner, C.A., et al., *Renal acid-base transport: old and new players.* Nephron Physiol, 2006. **103**(1): p. p1-6.
102. Chen, T.C., et al., *Volume expansion-induced changes in renal tubular membrane protein phosphorylation.* Biochem Biophys Res Commun, 1987. **143**(1): p. 74-80.
103. Silver, J., et al., *Regulation of the parathyroid hormone gene by vitamin D, calcium and phosphate.* Kidney Int Suppl, 1999. **73**: p. S2-7.
104. Kempson, S.A., et al., *Parathyroid hormone action on phosphate transporter mRNA and protein in rat renal proximal tubules.* Am J Physiol, 1995. **268**(4 Pt 2): p. F784-91.
105. Pfister, M.F., et al., *Inhibition of phosphatidylinositide 3-kinase in OK-cells reduces Na/Pi-cotransport but does not interfere with its regulation by parathyroid hormone.* Pflugers Arch, 1999. **438**(3): p. 392-6.
106. Lederer, E.D., et al., *Regulation of expression of type II sodium-phosphate cotransporters by protein kinases A and C.* Am J Physiol, 1998. **275**(2 Pt 2): p. F270-7.
107. Malmstrom, K. and H. Murer, *Parathyroid hormone regulates phosphate transport in OK cells via an irreversible inactivation of a membrane protein.* FEBS Lett, 1987. **216**(2): p. 257-60.
108. Pfister, M.F., et al., *Parathyroid hormone leads to the lysosomal degradation of the renal type II Na/Pi cotransporter.* Proc Natl Acad Sci U S A, 1998. **95**(4): p. 1909-14.

109. Biber, J., et al., *Regulation of phosphate transport in proximal tubules.* Pflugers Arch, 2009. **458**(1): p. 39-52.
110. Ohkido, I., et al., *Cloning, gene structure and dietary regulation of the type-IIc Na/Pi cotransporter in the mouse kidney.* Pflugers Arch, 2003. **446**(1): p. 106-15.
111. Segawa, H., et al., *Effect of hydrolysis-resistant FGF23-R179Q on dietary phosphate regulation of the renal type-II Na/Pi transporter.* Pflugers Arch, 2003. **446**(5): p. 585-92.
112. Segawa, H., et al., *Internalization of renal type IIc Na-Pi cotransporter in response to a high-phosphate diet.* Am J Physiol Renal Physiol, 2005. **288**(3): p. F587-96.
113. Breusegem, S.Y., et al., *Differential regulation of the renal sodium-phosphate cotransporters NaPi-IIa, NaPi-IIc, and PiT-2 in dietary potassium deficiency.* Am J Physiol Renal Physiol, 2009. **297**(2): p. F350-61.
114. Villa-Bellosta, R., et al., *The Na+-Pi cotransporter PiT-2 (SLC20A2) is expressed in the apical membrane of rat renal proximal tubules and regulated by dietary Pi.* Am J Physiol Renal Physiol, 2009. **296**(4): p. F691-9.
115. Chase, L.R. and G.D. Aurbach, *Parathyroid function and the renal excretion of 3'5'-adenylic acid.* Proc Natl Acad Sci U S A, 1967. **58**(2): p. 518-25.
116. Traebert, M., et al., *Internalization of proximal tubular type II Na-P(i) cotransporter by PTH: immunogold electron microscopy.* Am J Physiol Renal Physiol, 2000. **278**(1): p. F148-54.
117. Traebert, M., et al., *Luminal and contraluminal action of 1-34 and 3-34 PTH peptides on renal type IIa Na-P(i) cotransporter.* Am J Physiol Renal Physiol, 2000. **278**(5): p. F792-8.
118. Malmstrom, K., G. Stange, and H. Murer, *Intracellular cascades in the parathyroid-hormone-dependent regulation of Na+/phosphate cotransport in OK cells.* Biochem J, 1988. **251**(1): p. 207-13.
119. Hruska, K.A., et al., *Stimulation of inositol trisphosphate and diacylglycerol production in renal tubular cells by parathyroid hormone.* J Clin Invest, 1987. **79**(1): p. 230-9.
120. Cole, J.A., et al., *Regulation of sodium-dependent phosphate transport by parathyroid hormone in opossum kidney cells: adenosine 3',5'-monophosphate-dependent and -independent mechanisms.* Endocrinology, 1988. **122**(6): p. 2981-9.
121. Cole, J.A., et al., *A dual mechanism for regulation of kidney phosphate transport by parathyroid hormone.* Am J Physiol, 1987. **253**(2 Pt 1): p. E221-7.
122. Caverzasio, J., R. Rizzoli, and J.P. Bonjour, *Sodium-dependent phosphate transport inhibited by parathyroid hormone and cyclic AMP stimulation in an opossum kidney cell line.* J Biol Chem, 1986. **261**(7): p. 3233-7.
123. Muff, R., et al., *Parathyroid hormone receptors in control of proximal tubule function.* Annu Rev Physiol, 1992. **54**: p. 67-79.
124. Dunlay, R. and K. Hruska, *PTH receptor coupling to phospholipase C is an alternate pathway of signal transduction in bone and kidney.* Am J Physiol, 1990. **258**(2 Pt 2): p. F223-31.
125. Gisler, S.M., et al., *Interaction of the type IIa Na/Pi cotransporter with PDZ proteins.* J Biol Chem, 2001. **276**(12): p. 9206-13.

126. Biber, J., *Emerging roles of transporter-PDZ complexes in renal proximal tubular reabsorption.* Pflugers Arch, 2001. **443**(1): p. 3-5.
127. Murer, H., et al., *Regulation of Na/Pi transporter in the proximal tubule.* Annu Rev Physiol, 2003. **65**: p. 531-42.
128. Weinman, E.J., et al., *NHERF-1 is required for renal adaptation to a low-phosphate diet.* Am J Physiol Renal Physiol, 2003. **285**(6): p. F1225-32.
129. Weinman, E.J., et al., *The role of NHERF-1 in the regulation of renal proximal tubule sodium-hydrogen exchanger 3 and sodium-dependent phosphate cotransporter 2a.* J Physiol, 2005. **567**(Pt 1): p. 27-32.
130. Cunningham, R., et al., *Signaling pathways utilized by PTH and dopamine to inhibit phosphate transport in mouse renal proximal tubule cells.* Am J Physiol Renal Physiol, 2009. **296**(2): p. F355-61.
131. Cunningham, R., et al., *Defective parathyroid hormone regulation of NHE3 activity and phosphate adaptation in cultured NHERF-1-/- renal proximal tubule cells.* J Biol Chem, 2004. **279**(36): p. 37815-21.
132. Weinman, E.J., et al., *Sodium-hydrogen exchanger regulatory factor 1 (NHERF-1) transduces signals that mediate dopamine inhibition of sodium-phosphate co-transport in mouse kidney.* J Biol Chem, 2010. **285**(18): p. 13454-60.
133. Deliot, N., et al., *Parathyroid hormone treatment induces dissociation of type IIa Na+-P(i) cotransporter-Na+/H+ exchanger regulatory factor-1 complexes.* Am J Physiol Cell Physiol, 2005. **289**(1): p. C159-67.
134. Weinman, E.J., et al., *Parathyroid hormone inhibits renal phosphate transport by phosphorylation of serine 77 of sodium-hydrogen exchanger regulatory factor-1.* J Clin Invest, 2007. **117**(11): p. 3412-20.
135. Reczek, D. and A. Bretscher, *The carboxyl-terminal region of EBP50 binds to a site in the amino-terminal domain of ezrin that is masked in the dormant molecule.* J Biol Chem, 1998. **273**(29): p. 18452-8.
136. Reczek, D., M. Berryman, and A. Bretscher, *Identification of EBP50: A PDZ-containing phosphoprotein that associates with members of the ezrin-radixin-moesin family.* J Cell Biol, 1997. **139**(1): p. 169-79.
137. Murthy, A., et al., *NHE-RF, a regulatory cofactor for Na(+)-H+ exchange, is a common interactor for merlin and ERM (MERM) proteins.* J Biol Chem, 1998. **273**(3): p. 1273-6.
138. Weinman, E.J., et al., *PTH transiently increases the percent mobile fraction of Npt2a in OK cells as determined by FRAP.* Am J Physiol Renal Physiol, 2009. **297**(6): p. F1560-5.
139. Keusch, I., et al., *Parathyroid hormone and dietary phosphate provoke a lysosomal routing of the proximal tubular Na/Pi-cotransporter type II.* Kidney Int, 1998. **54**(4): p. 1224-32.
140. Fleisch, H., J.P. Bonjour, and U. Troehler, *Homeostasis of inorganic phosphate: an introductory review.* Calcif Tissue Res, 1976. **21 Suppl**: p. 327-31.
141. Wen, S.F., J.W. Boynar, Jr., and R.W. Stoll, *Effect of phosphate deprivation on renal phosphate transport in the dog.* Am J Physiol, 1978. **234**(3): p. F199-206.

142. Levi, M., et al., *Cellular mechanisms of acute and chronic adaptation of rat renal P(i) transporter to alterations in dietary P(i).* Am J Physiol, 1994. **267**(5 Pt 2): p. F900-8.
143. Lotscher, M., et al., *Rapid downregulation of rat renal Na/P(i) cotransporter in response to parathyroid hormone involves microtubule rearrangement.* J Clin Invest, 1999. **104**(4): p. 483-94.
144. Bonjour, J.P., et al., *Regulation of the tubular transport of phosphate in the rat: role of parathyroid hormone and 1,25-dihydroxyvitamin D3.* Adv Exp Med Biol, 1978. **103**: p. 97-103.
145. Gloor, H.J., et al., *Resistance to the phosphaturic and calcemic actions of parathyroid hormone during phosphate depletion. Prevention by 1,25-dihydroxyvitamin D3.* J Clin Invest, 1979. **63**(3): p. 371-7.
146. Knox, F.G., J.A. Haas, and A. Haramati, *Nephron sites of adaptation to changes in dietary phosphate.* Adv Exp Med Biol, 1982. **151**: p. 13-9.
147. Isaac, J., et al., *Dopamine enhances the phosphaturic response to parathyroid hormone in phosphate-deprived rats.* J Am Soc Nephrol, 1992. **2**(9): p. 1423-9.
148. Haramati, A., J.A. Haas, and F.G. Knox, *Adaptation of deep and superficial nephrons to changes in dietary phosphate intake.* Am J Physiol, 1983. **244**(3): p. F265-9.
149. Caverzasio, J. and J.P. Bonjour, *Mechanism of rapid phosphate (Pi) transport adaptation to a single low Pi meal in rat renal brush border membrane.* Pflugers Arch, 1985. **404**(3): p. 227-31.
150. Levine, B.S., et al., *Renal adaptation to phosphorus deprivation: characterization of early events.* J Bone Miner Res, 1986. **1**(1): p. 33-40.
151. Lotscher, M., et al., *New aspects of adaptation of rat renal Na-Pi cotransporter to alterations in dietary phosphate.* Kidney Int, 1996. **49**(4): p. 1012-8.
152. Murer, H. and J. Biber, *Molecular mechanisms in renal phosphate reabsorption.* Nephrol Dial Transplant, 1995. **10**(9): p. 1501-4.
153. Levi, M., et al., *Low-Pi diet increases the abundance of an apical protein in rat proximal-tubular S3 segments.* Pflugers Arch, 1994. **426**(1-2): p. 5-11.
154. Cheng, L., et al., *Renal adaptation to phosphate load in the acutely thyroparathyroidectomized rat: rapid alteration in brush border membrane phosphate transport.* Am J Physiol, 1984. **246**(4 Pt 2): p. F488-94.
155. Villa-Bellosta, R. and V. Sorribas, *Different effects of arsenate and phosphonoformate on P(i) transport adaptation in opossum kidney cells.* Am J Physiol Cell Physiol, 2009. **297**(3): p. C516-25.
156. Cheng, L., C.T. Liang, and B. Sacktor, *Phosphate uptake by renal membrane vesicles of rabbits adapted to high and low phosphorus diets.* Am J Physiol, 1983. **245**(2): p. F175-80.
157. Dousa, T.P. and S.A. Kempson, *Regulation of renal brush border membrane transport of phosphate.* Miner Electrolyte Metab, 1982. **7**(3): p. 113-21.
158. Jahan, M. and P.J. Butterworth, *Study of the mechanism by which the Na+-Pi co-transporter of mouse kidney proximal-tubule cells adjusts to phosphate depletion.* Biochem J, 1988. **252**(1): p. 105-9.
159. Shah, S.V., et al., *Renal adaptation to a low phosphate diet in rats.* J Clin Invest, 1979. **64**(4): p. 955-66.

160. Kempson, S.A., et al., *Renal brush border membrane adaptation to phosphorus deprivation: effects of fasting versus low-phosphorus diet.* Kidney Int, 1980. **18**(1): p. 36-47.
161. Sigler, M.H., *The mechanism of the natriuresis of fasting.* J Clin Invest, 1975. **55**(2): p. 377-87.
162. Van Liew, J.B., et al., *Renal sodium conservation during starvation in the rat.* J Lab Clin Med, 1978. **91**(4): p. 650-9.
163. Jones, G., S.A. Strugnell, and H.F. DeLuca, *Current understanding of the molecular actions of vitamin D.* Physiol Rev, 1998. **78**(4): p. 1193-231.
164. Hughes, M.R., et al., *Regulation of serum 1alpha,25-dihydroxyvitamin D3 by calcium and phosphate in the rat.* Science, 1975. **190**(4214): p. 578-80.
165. Tanaka, Y. and H.F. Deluca, *The control of 25-hydroxyvitamin D metabolism by inorganic phosphorus.* Arch Biochem Biophys, 1973. **154**(2): p. 566-74.
166. Portale, A.A., B.P. Halloran, and R.C. Morris, Jr., *Physiologic regulation of the serum concentration of 1,25-dihydroxyvitamin D by phosphorus in normal men.* J Clin Invest, 1989. **83**(5): p. 1494-9.
167. Portale, A.A., et al., *Oral intake of phosphorus can determine the serum concentration of 1,25-dihydroxyvitamin D by determining its production rate in humans.* J Clin Invest, 1986. **77**(1): p. 7-12.
168. Tenenhouse, H.S., et al., *Pituitary involvement in renal adaptation to phosphate deprivation.* Am J Physiol, 1988. **255**(3 Pt 2): p. R373-8.
169. Gray, R.W., *Evidence that somatomedins mediate the effect of hypophosphatemia to increase serum 1,25-dihydroxyvitamin D3 levels in rats.* Endocrinology, 1987. **121**(2): p. 504-12.
170. Gray, R.W. and T.L. Garthwaite, *Activation of renal 1,25-dihydroxyvitamin D3 synthesis by phosphate deprivation: evidence for a role for growth hormone.* Endocrinology, 1985. **116**(1): p. 189-93.
171. Halloran, B.P. and E.M. Spencer, *Dietary phosphorus and 1,25-dihydroxyvitamin D metabolism: influence of insulin-like growth factor I.* Endocrinology, 1988. **123**(3): p. 1225-9.
172. Spanos, E., et al., *Effect of growth hormone on vitamin D metabolism.* Nature, 1978. **273**(5659): p. 246-7.
173. Zhang, M.Y., et al., *Dietary phosphorus transcriptionally regulates 25-hydroxyvitamin D-1alpha-hydroxylase gene expression in the proximal renal tubule.* Endocrinology, 2002. **143**(2): p. 587-95.
174. Lamarche, M.G., et al., *The phosphate regulon and bacterial virulence: a regulatory network connecting phosphate homeostasis and pathogenesis.* FEMS Microbiol Rev, 2008. **32**(3): p. 461-73.
175. Mouillon, J.M. and B.L. Persson, *New aspects on phosphate sensing and signalling in Saccharomyces cerevisiae.* FEMS Yeast Res, 2006. **6**(2): p. 171-6.
176. Suzuki, S., et al., *The SphS-SphR two component system is the exclusive sensor for the induction of gene expression in response to phosphate limitation in synechocystis.* J Biol Chem, 2004. **279**(13): p. 13234-40.
177. Martin, D.R., et al., *Acute regulation of parathyroid hormone by dietary phosphate.* Am J Physiol Endocrinol Metab, 2005. **289**(4): p. E729-34.

178. Berndt, T., et al., *Evidence for a signaling axis by which intestinal phosphate rapidly modulates renal phosphate reabsorption.* Proc Natl Acad Sci U S A, 2007. **104**(26): p. 11085-90.
179. Hubbell, E., W.M. Liu, and R. Mei, *Robust estimators for expression analysis.* Bioinformatics, 2002. **18**(12): p. 1585-92.
180. Liu, W.M., et al., *Analysis of high density expression microarrays with signed-rank call algorithms.* Bioinformatics, 2002. **18**(12): p. 1593-9.
181. Butte, A., *The use and analysis of microarray data.* Nat Rev Drug Discov, 2002. **1**(12): p. 951-60.
182. Biber, J., et al., *Isolation of renal proximal tubular brush-border membranes.* Nat Protoc, 2007. **2**(6): p. 1356-9.
183. Slot, C., *Plasma creatinine determination. A new and specific Jaffe reaction method.* Scand J Clin Lab Invest, 1965. **17**(4): p. 381-7.
184. Seaton, B. and A. Ali, *Simplified manual high performance clinical chemistry methods for developing countries.* Med Lab Sci, 1984. **41**(4): p. 327-36.
185. Fiske, C.H. and Y. Subbarow, *The Nature of the "Inorganic Phosphate" in Voluntary Muscle.* Science, 1927. **65**(1686): p. 401-3.
186. Berthelot, M., *Chimie organique fondée sur la synthèse*. 1860, Paris: Mallet-Bachelier.
187. Wagner, C.A., et al., *Mouse model of type II Bartter's syndrome. II. Altered expression of renal sodium- and water-transporting proteins.* Am J Physiol Renal Physiol, 2008. **294**(6): p. F1373-80.
188. Wagner, C.A., J. Biber, and H. Murer, *Of men and mice: who is in control of renal phosphate reabsorption?* J Am Soc Nephrol, 2008. **19**(9): p. 1625-6.
189. Nowik, M., et al., *Genome-wide gene expression profiling reveals renal genes regulated during metabolic acidosis.* Physiol Genomics, 2008. **32**(3): p. 322-34.
190. Loughlin, J., et al., *Functional variants within the secreted frizzled-related protein 3 gene are associated with hip osteoarthritis in females.* Proc Natl Acad Sci U S A, 2004. **101**(26): p. 9757-62.
191. Guo, Y., et al., *Frzb, a secreted Wnt antagonist, decreases growth and invasiveness of fibrosarcoma cells associated with inhibition of Met signaling.* Cancer Res, 2008. **68**(9): p. 3350-60.
192. Schumann, H., et al., *Expression of secreted frizzled related proteins 3 and 4 in human ventricular myocardium correlates with apoptosis related gene expression.* Cardiovasc Res, 2000. **45**(3): p. 720-8.
193. Ninomiya, K., et al., *Osteoclastic activity induces osteomodulin expression in osteoblasts.* Biochem Biophys Res Commun, 2007. **362**(2): p. 460-6.
194. Inoue, H., et al., *Human cholecystokinin type A receptor gene: cytogenetic localization, physical mapping, and identification of two missense variants in patients with obesity and non-insulin-dependent diabetes mellitus (NIDDM).* Genomics, 1997. **42**(2): p. 331-5.
195. Okubo, T. and S. Harada, *Polymorphisms of the CCK, CCKAR and CCKBR genes: an association with alcoholism study.* J Stud Alcohol, 2001. **62**(4): p. 413-21.

196. Halestrap, A.P. and N.T. Price, *The proton-linked monocarboxylate transporter (MCT) family: structure, function and regulation.* Biochem J, 1999. **343 Pt 2**: p. 281-99.
197. Camalier, C.E., et al., *Elevated phosphate activates N-ras and promotes cell transformation and skin tumorigenesis.* Cancer Prev Res (Phila), 2010. **3**(3): p. 359-70.
198. Jin, H., et al., *A high inorganic phosphate diet perturbs brain growth, alters Akt-ERK signaling, and results in changes in cap-dependent translation.* Toxicol Sci, 2006. **90**(1): p. 221-9.
199. Ohnishi, M. and M.S. Razzaque, *Dietary and genetic evidence for phosphate toxicity accelerating mammalian aging.* FASEB J, 2010. **24**(9): p. 3562-71.
200. Meyer, C., J.M. Dostou, and J.E. Gerich, *Role of the human kidney in glucose counterregulation.* Diabetes, 1999. **48**(5): p. 943-8.
201. Reinecke, R.M., *The kidney as a source of glucose in the eviscerated rat.* American Journal of Physiology, 1943. **140**(2): p. 0276-0285.
202. Drury, D.R., A.N. Wick, and E.M. Mackay, *Formation of Glucose by the Kidney.* American Journal of Physiology, 1950. **163**(3): p. 655-661.
203. Bergman, H. and D.R. Drury, *The relationship of kidney function to the glucose utilization of the extra abdominal tissues.* American Journal of Physiology, 1938. **124**(2): p. 279-284.
204. Guder, W.G. and B.D. Ross, *Enzyme distribution along the nephron.* Kidney Int, 1984. **26**(2): p. 101-11.
205. Schoolwerth, A.C., B.C. Smith, and R.M. Culpepper, *Renal gluconeogenesis.* Miner Electrolyte Metab, 1988. **14**(6): p. 347-61.
206. Wirthensohn, G. and W.G. Guder, *Renal substrate metabolism.* Physiol Rev, 1986. **66**(2): p. 469-97.
207. Kreusser, W.J., et al., *Effect of Phosphate-Depletion on Renal Gluconeogenesis.* Mineral and Electrolyte Metabolism, 1980. **3**(6): p. 312-322.
208. Ventura, N., et al., *p53/CEP-1 increases or decreases lifespan, depending on level of mitochondrial bioenergetic stress.* Aging Cell, 2009. **8**(4): p. 380-93.
209. Torgovnick, A., et al., *A role for p53 in mitochondrial stress response control of longevity in C. elegans.* Exp Gerontol, 2010. **45**(7-8): p. 550-7.
210. Christensen, E.I. and H. Birn, *Megalin and cubilin: multifunctional endocytic receptors.* Nat Rev Mol Cell Biol, 2002. **3**(4): p. 256-66.
211. Christensen, E.I. and H. Birn, *Megalin and cubilin: synergistic endocytic receptors in renal proximal tubule.* Am J Physiol Renal Physiol, 2001. **280**(4): p. F562-73.
212. Bacic, D., et al., *The renal Na+/phosphate cotransporter NaPi-IIa is internalized via the receptor-mediated endocytic route in response to parathyroid hormone.* Kidney Int, 2006. **69**(3): p. 495-503.
213. Bachmann, S., et al., *Kidney-specific inactivation of the megalin gene impairs trafficking of renal inorganic sodium phosphate cotransporter (NaPi-IIa).* J Am Soc Nephrol, 2004. **15**(4): p. 892-900.
214. Bacic, D., et al., *Impaired PTH-induced endocytotic down-regulation of the renal type IIa Na+/Pi-cotransporter in RAP-deficient mice with reduced megalin expression.* Pflugers Arch, 2003. **446**(4): p. 475-84.

215. Gaullier, J.M., et al., *FYVE fingers bind PtdIns(3)P.* Nature, 1998. **394**(6692): p. 432-3.
216. Mu, F.T., et al., *EEA1, an early endosome-associated protein. EEA1 is a conserved alpha-helical peripheral membrane protein flanked by cysteine "fingers" and contains a calmodulin-binding IQ motif.* J Biol Chem, 1995. **270**(22): p. 13503-11.
217. Stenmark, H., et al., *Endosomal localization of the autoantigen EEA1 is mediated by a zinc-binding FYVE finger.* J Biol Chem, 1996. **271**(39): p. 24048-54.
218. Grieff, M., et al., *Renal calcitriol synthesis and serum phosphorus in response to dietary phosphorus restriction and anabolic agents.* Am J Kidney Dis, 1996. **28**(4): p. 589-95.
219. Capuano, P., et al., *Intestinal and renal adaptation to a low-Pi diet of type II NaPi cotransporters in vitamin D receptor- and 1alphaOHase-deficient mice.* Am J Physiol Cell Physiol, 2005. **288**(2): p. C429-34.
220. Hollis, B.W. and C.L. Wagner, *Normal serum vitamin D levels.* N Engl J Med, 2005. **352**(5): p. 515-6; author reply 515-6.
221. Tang, W.J., et al., *Autocrine/paracrine action of vitamin D on FGF23 expression in cultured rat osteoblasts.* Calcif Tissue Int, 2010. **86**(5): p. 404-10.
222. Fiermonte, G., et al., *The sequence, bacterial expression, and functional reconstitution of the rat mitochondrial dicarboxylate transporter cloned via distant homologs in yeast and Caenorhabditis elegans.* J Biol Chem, 1998. **273**(38): p. 24754-9.
223. Robinson, B.H., et al., *The effects of 2-ethylcitrate and tricarballylate on citrate transport in rat liver mitochondria and fatty acid synthesis in rat white adipose tissue.* Eur J Biochem, 1970. **15**(2): p. 263-72.
224. Guder, W.G. and A. Rupprecht, *Metabolism of Isolated Kidney-Tubules - Independent Actions of Catecholamines on Renal Cyclic Adenosine 3'-5'-Monophosphate Levels and Gluconeogenesis.* European Journal of Biochemistry, 1975. **52**(2): p. 283-290.
225. Wirthensohn, G., A. Vandewalle, and W.G. Guder, *Renal glycerol metabolism and the distribution of glycerol kinase in rabbit nephron.* Biochem J, 1981. **198**(3): p. 543-9.
226. Bartoloni, L. and S.E. Antonarakis, *The human sugar-phosphate/phosphate exchanger family SLC37.* Pflugers Arch, 2004. **447**(5): p. 780-3.
227. Levi, M., D.M. Jameson, and B.W. van der Meer, *Role of BBM lipid composition and fluidity in impaired renal Pi transport in aged rat.* Am J Physiol, 1989. **256**(1 Pt 2): p. F85-94.
228. Molitoris, B.A., et al., *Renal apical membrane cholesterol and fluidity in regulation of phosphate transport.* Am J Physiol, 1985. **249**(1 Pt 2): p. F12-9.
229. Levi, M., B.M. Baird, and P.V. Wilson, *Cholesterol modulates rat renal brush border membrane phosphate transport.* J Clin Invest, 1990. **85**(1): p. 231-7.
230. Levi, M., et al., *Dexamethasone modulates rat renal brush border membrane phosphate transporter mRNA and protein abundance and glycosphingolipid composition.* J Clin Invest, 1995. **96**(1): p. 207-16.

231. Skowyra, D., C. Georgopoulos, and M. Zylicz, *The E. coli dnaK gene product, the hsp70 homolog, can reactivate heat-inactivated RNA polymerase in an ATP hydrolysis-dependent manner.* Cell, 1990. **62**(5): p. 939-44.
232. Skowyra, D. and M. Zylicz, *[Heat-shock proteins].* Postepy Biochem, 1987. **33**(2-3): p. 259-76.
233. Wickner, S., M.R. Maurizi, and S. Gottesman, *Posttranslational quality control: folding, refolding, and degrading proteins.* Science, 1999. **286**(5446): p. 1888-93.
234. Helmbrecht, K., E. Zeise, and L. Rensing, *Chaperones in cell cycle regulation and mitogenic signal transduction: a review.* Cell Prolif, 2000. **33**(6): p. 341-65.
235. Jolly, C. and R.I. Morimoto, *Role of the heat shock response and molecular chaperones in oncogenesis and cell death.* J Natl Cancer Inst, 2000. **92**(19): p. 1564-72.
236. Wall, D., M. Zylicz, and C. Georgopoulos, *The NH2-terminal 108 amino acids of the Escherichia coli DnaJ protein stimulate the ATPase activity of DnaK and are sufficient for lambda replication.* J Biol Chem, 1994. **269**(7): p. 5446-51.
237. King, F.W., et al., *Co-chaperones Bag-1, Hop and Hsp40 regulate Hsc70 and Hsp90 interactions with wild-type or mutant p53.* EMBO J, 2001. **20**(22): p. 6297-305.
238. Zhao, R., et al., *Analysis of p53-regulated gene expression patterns using oligonucleotide arrays.* Genes Dev, 2000. **14**(8): p. 981-93.
239. Hupp, T.R., D.P. Lane, and K.L. Ball, *Strategies for manipulating the p53 pathway in the treatment of human cancer.* Biochem J, 2000. **352 Pt 1**: p. 1-17.
240. Evan, G.I. and K.H. Vousden, *Proliferation, cell cycle and apoptosis in cancer.* Nature, 2001. **411**(6835): p. 342-8.
241. Espinosa, J.M., *Mechanisms of regulatory diversity within the p53 transcriptional network.* Oncogene, 2008. **27**(29): p. 4013-23.
242. Benchimol, S., *p53--an examination of sibling support in apoptosis control.* Cancer Cell, 2004. **6**(1): p. 3-4.
243. Bode, A.M. and Z. Dong, *Post-translational modification of p53 in tumorigenesis.* Nat Rev Cancer, 2004. **4**(10): p. 793-805.
244. Zhang, J. and X. Chen, *Posttranscriptional regulation of p53 and its targets by RNA-binding proteins.* Curr Mol Med, 2008. **8**(8): p. 845-9.
245. Samuels-Lev, Y., et al., *ASPP proteins specifically stimulate the apoptotic function of p53.* Mol Cell, 2001. **8**(4): p. 781-94.
246. Campisi, J., *Senescent cells, tumor suppression, and organismal aging: good citizens, bad neighbors.* Cell, 2005. **120**(4): p. 513-22.
247. Harper, J.W., et al., *The p21 Cdk-interacting protein Cip1 is a potent inhibitor of G1 cyclin-dependent kinases.* Cell, 1993. **75**(4): p. 805-16.
248. Dusso, A.S., et al., *p21(WAF1) and transforming growth factor-alpha mediate dietary phosphate regulation of parathyroid cell growth.* Kidney Int, 2001. **59**(3): p. 855-65.
249. Zylicz, M., F.W. King, and A. Wawrzynow, *Hsp70 interactions with the p53 tumour suppressor protein.* EMBO J, 2001. **20**(17): p. 4634-8.
250. Loghman-Adham, M., *Adaptation to changes in dietary phosphorus intake in health and in renal failure.* J Lab Clin Med, 1997. **129**(2): p. 176-88.

251. Prabhu, S., et al., *Effect of glucocorticoids on neonatal rabbit renal cortical sodium-inorganic phosphate messenger RNA and protein abundance.* Pediatr Res, 1997. **41**(1): p. 20-4.
252. Kilav, R., et al., *Coordinate regulation of rat renal parathyroid hormone receptor mRNA and Na-Pi cotransporter mRNA and protein.* Am J Physiol, 1995. **268**(6 Pt 2): p. F1017-22.
253. Biber, J., J. Forgo, and H. Murer, *Modulation of Na+-Pi cotransport in opossum kidney cells by extracellular phosphate.* Am J Physiol, 1988. **255**(2 Pt 1): p. C155-61.
254. Markovich, D., et al., *Regulation of opossum kidney (OK) cell Na/Pi cotransport by Pi deprivation involves mRNA stability.* Pflugers Arch, 1995. **430**(4): p. 459-63.
255. Moz, Y., J. Silver, and T. Naveh-Many, *Protein-RNA interactions determine the stability of the renal NaPi-2 cotransporter mRNA and its translation in hypophosphatemic rats.* J Biol Chem, 1999. **274**(36): p. 25266-72.
256. Moz, Y., J. Silver, and T. Naveh-Many, *Characterization of cis-acting element in renal NaPi-2 cotransporter mRNA that determines mRNA stability.* Am J Physiol Renal Physiol, 2003. **284**(4): p. F663-70.
257. Ito, M., et al., *Interaction of a farnesylated protein with renal type IIa Na/Pi co-transporter in response to parathyroid hormone and dietary phosphate.* Biochem J, 2004. **377**(Pt 3): p. 607-16.
258. Moz, Y., et al., *Calcineurin Abeta is central to the expression of the renal type II Na/Pi co-transporter gene and to the regulation of renal phosphate transport.* J Am Soc Nephrol, 2004. **15**(12): p. 2972-80.
259. Kuroo, M., et al., *Mutation of the mouse klotho gene leads to a syndrome resembling ageing.* Nature, 1997. **390**(6655): p. 45-51.
260. Kurosu, H., et al., *Suppression of aging in mice by the hormone Klotho.* Science, 2005. **309**(5742): p. 1829-1833.
261. Yamamoto, M., et al., *Regulation of oxidative stress by the anti-aging hormone Klotho.* Journal of Biological Chemistry, 2005. **280**(45): p. 38029-38034.
262. Nabeshima, Y. and H. Imura, *alpha-klotho: A regulator that integrates calcium homeostasis.* American Journal of Nephrology, 2008. **28**(3): p. 455-464.
263. Matsumura, Y., et al., *Identification of the human klotho gene and its two transcripts encoding membrane and secreted klotho protein.* Biochemical and Biophysical Research Communications, 1998. **242**(3): p. 626-630.
264. de Oliveira, R.M., *Klotho RNAi induces premature senescence of human cells via a p53/p21 dependent pathway.* FEBS Lett, 2006. **580**(24): p. 5753-8.
265. Li, T.K., et al., *Calcium- and FK506-independent interaction between the immunophilin FKBP51 and calcineurin.* J Cell Biochem, 2002. **84**(3): p. 460-71.
266. Smith, D.F., L.E. Faber, and D.O. Toft, *Purification of unactivated progesterone receptor and identification of novel receptor-associated proteins.* J Biol Chem, 1990. **265**(7): p. 3996-4003.
267. Smith, D.F., et al., *Reconstitution of progesterone receptor with heat shock proteins.* Mol Endocrinol, 1990. **4**(11): p. 1704-11.

268. Barent, R.L., et al., *Analysis of FKBP51/FKBP52 chimeras and mutants for Hsp90 binding and association with progesterone receptor complexes.* Mol Endocrinol, 1998. **12**(3): p. 342-54.
269. Cheung-Flynn, J., et al., *C-terminal sequences outside the tetratricopeptide repeat domain of FKBP51 and FKBP52 cause differential binding to Hsp90.* J Biol Chem, 2003. **278**(19): p. 17388-94.
270. Sigal, N.H. and F.J. Dumont, *Cyclosporine-a, Fk-506, and Rapamycin - Pharmacological Probes of Lymphocyte Signal Transduction.* Annual Review of Immunology, 1992. **10**: p. 519-560.
271. Schreiber, S.L. and G.L. Verdine, *Protein Overproduction for Organic Chemists.* Tetrahedron, 1991. **47**(14-15): p. 2543-2562.
272. Bierer, B.E., et al., *Cyclosporin A and FK506: molecular mechanisms of immunosuppression and probes for transplantation biology.* Curr Opin Immunol, 1993. **5**(5): p. 763-73.
273. Baughman, G., et al., *Tissue distribution and abundance of human FKBP51, and FK506-binding protein that can mediate calcineurin inhibition.* Biochem Biophys Res Commun, 1997. **232**(2): p. 437-43.
274. Wank, S.A., *Cholecystokinin receptors.* Am J Physiol, 1995. **269**(5 Pt 1): p. G628-46.
275. Duggan, K.A., G. Hams, and G.J. MacDonald, *Modification of renal and tissue cation transport by cholecystokinin octapeptide in the rabbit.* J Physiol, 1988. **397**: p. 527-38.
276. Gurda, G.T., et al., *Cholecystokinin activates pancreatic calcineurin-NFAT signaling in vitro and in vivo.* Mol Biol Cell, 2008. **19**(1): p. 198-206.
277. Hunt, M.C. and S.E. Alexson, *Novel functions of acyl-CoA thioesterases and acyltransferases as auxiliary enzymes in peroxisomal lipid metabolism.* Prog Lipid Res, 2008. **47**(6): p. 405-21.
278. Yamada, J., *Long-chain acyl-CoA hydrolase in the brain.* Amino Acids, 2005. **28**(3): p. 273-8.
279. Dongol, B., et al., *The acyl-CoA thioesterase I is regulated by PPARalpha and HNF4alpha via a distal response element in the promoter.* J Lipid Res, 2007. **48**(8): p. 1781-91.
280. Huhtinen, K., et al., *The peroxisome proliferator-induced cytosolic type I acyl-CoA thioesterase (CTE-I) is a serine-histidine-aspartic acid alpha /beta hydrolase.* J Biol Chem, 2002. **277**(5): p. 3424-32.
281. Svensson, L.T., M. Wilcke, and S.E. Alexson, *Peroxisome proliferators differentially regulate long-chain acyl-CoA thioesterases in rat liver.* Eur J Biochem, 1995. **230**(2): p. 813-20.
282. Yamada, J., et al., *Purification and properties of long-chain acyl-CoA hydrolases from the liver cytosol of rats treated with peroxisome proliferator.* Arch Biochem Biophys, 1994. **308**(1): p. 118-25.
283. Kuramochi, Y., et al., *Immunohistochemical localization of acyl-CoA hydrolase/thioesterase multigene family members to rat epithelia.* Histochem Cell Biol, 2002. **117**(3): p. 211-7.
284. Adams, S.H., et al., *BFIT, a unique acyl-CoA thioesterase induced in thermogenic brown adipose tissue: cloning, organization of the human gene*

and assessment of a potential link to obesity. Biochem J, 2001. **360**(Pt 1): p. 135-42.
285. Hunt, M.C., et al., *Characterization of an acyl-coA thioesterase that functions as a major regulator of peroxisomal lipid metabolism.* J Biol Chem, 2002. **277**(2): p. 1128-38.
286. Hunt, M.C. and S.E. Alexson, *The role Acyl-CoA thioesterases play in mediating intracellular lipid metabolism.* Prog Lipid Res, 2002. **41**(2): p. 99-130.
287. Matsui, S.M., M.J. Mahoney, and L.E. Rosenberg, *The natural history of the inherited methylmalonic acidemias.* N Engl J Med, 1983. **308**(15): p. 857-61.
288. Radmanesh, A., et al., *Methylmalonic acidemia: brain imaging findings in 52 children and a review of the literature.* Pediatr Radiol, 2008. **38**(10): p. 1054-61.
289. Sakamoto, O., et al., *Mutation and haplotype analyses of the MUT gene in Japanese patients with methylmalonic acidemia.* J Hum Genet, 2007. **52**(1): p. 48-55.
290. Dionisi-Vici, C., et al., *'Classical' organic acidurias, propionic aciduria, methylmalonic aciduria and isovaleric aciduria: long-term outcome and effects of expanded newborn screening using tandem mass spectrometry.* J Inherit Metab Dis, 2006. **29**(2-3): p. 383-9.
291. Cheng, Z., et al., *Human thioesterase superfamily member 2 (hTHEM2) is co-localized with beta-tubulin onto the microtubule.* Biochem Biophys Res Commun, 2006. **350**(4): p. 850-3.
292. Buchaille, R., et al., *Expression of the small leucine-rich proteoglycan osteoadherin/osteomodulin in human dental pulp and developing rat teeth.* Bone, 2000. **27**(2): p. 265-70.
293. Buchaille, R., et al., *A substractive PCR-based cDNA library from human odontoblast cells: identification of novel genes expressed in tooth forming cells.* Matrix Biol, 2000. **19**(5): p. 421-30.
294. Ramstad, V.E., et al., *Ultrastructural distribution of osteoadherin in rat bone shows a pattern similar to that of bone sialoprotein.* Calcif Tissue Int, 2003. **72**(1): p. 57-64.
295. Sommarin, Y., et al., *Osteoadherin, a cell-binding keratan sulfate proteoglycan in bone, belongs to the family of leucine-rich repeat proteins of the extracellular matrix.* J Biol Chem, 1998. **273**(27): p. 16723-9.
296. Wendel, M., Y. Sommarin, and D. Heinegard, *Bone matrix proteins: isolation and characterization of a novel cell-binding keratan sulfate proteoglycan (osteoadherin) from bovine bone.* J Cell Biol, 1998. **141**(3): p. 839-47.
297. Hocking, A.M., T. Shinomura, and D.J. McQuillan, *Leucine-rich repeat glycoproteins of the extracellular matrix.* Matrix Biol, 1998. **17**(1): p. 1-19.
298. Iozzo, R.V., *The family of the small leucine-rich proteoglycans: key regulators of matrix assembly and cellular growth.* Crit Rev Biochem Mol Biol, 1997. **32**(2): p. 141-74.
299. Iozzo, R.V., *The biology of the small leucine-rich proteoglycans. Functional network of interactive proteins.* J Biol Chem, 1999. **274**(27): p. 18843-6.
300. Iozzo, R.V., et al., *Structural and functional characterization of the human perlecan gene promoter. Transcriptional activation by transforming growth*

factor-beta via a nuclear factor 1-binding element. J Biol Chem, 1997. **272**(8): p. 5219-28.
301. Rehn, A.P., A.M. Chalk, and M. Wendel, *Differential regulation of osteoadherin (OSAD) by TGF-beta1 and BMP-2.* Biochem Biophys Res Commun, 2006. **349**(3): p. 1057-64.
302. Lucchini, M., et al., *TGF beta 1 signaling and stimulation of osteoadherin in human odontoblasts in vitro.* Connect Tissue Res, 2002. **43**(2-3): p. 345-53.
303. Couble, M.L., et al., *Immunodetection of osteoadherin in murine tooth extracellular matrices.* Histochem Cell Biol, 2004. **121**(1): p. 47-53.
304. Calderwood, D.A., et al., *The Talin head domain binds to integrin beta subunit cytoplasmic tails and regulates integrin activation.* J Biol Chem, 1999. **274**(40): p. 28071-4.
305. Deuticke, B., *Monocarboxylate transport in erythrocytes.* J Membr Biol, 1982. **70**(2): p. 89-103.
306. Poole, R.C. and A.P. Halestrap, *Transport of lactate and other monocarboxylates across mammalian plasma membranes.* Am J Physiol, 1993. **264**(4 Pt 1): p. C761-82.
307. Garcia, C.K., et al., *Molecular characterization of a membrane transporter for lactate, pyruvate, and other monocarboxylates: implications for the Cori cycle.* Cell, 1994. **76**(5): p. 865-73.
308. Garcia, C.K., et al., *cDNA cloning of the human monocarboxylate transporter 1 and chromosomal localization of the SLC16A1 locus to 1p13.2-p12.* Genomics, 1994. **23**(2): p. 500-3.
309. Garcia, C.K., et al., *cDNA cloning of MCT2, a second monocarboxylate transporter expressed in different cells than MCT1.* J Biol Chem, 1995. **270**(4): p. 1843-9.
310. Lafreniere, R.G., L. Carrel, and H.F. Willard, *A novel transmembrane transporter encoded by the XPCT gene in Xq13.2.* Hum Mol Genet, 1994. **3**(7): p. 1133-9.
311. Grollman, E.F., et al., *Determination of transport kinetics of chick MCT3 monocarboxylate transporter from retinal pigment epithelium by expression in genetically modified yeast.* Biochemistry, 2000. **39**(31): p. 9351-7.
312. Price, N.T., V.N. Jackson, and A.P. Halestrap, *Cloning and sequencing of four new mammalian monocarboxylate transporter (MCT) homologues confirms the existence of a transporter family with an ancient past.* Biochem J, 1998. **329 (Pt 2)**: p. 321-8.
313. Yoon, H., et al., *Identification of a unique monocarboxylate transporter (MCT3) in retinal pigment epithelium.* Biochem Biophys Res Commun, 1997. **234**(1): p. 90-4.
314. Kim, D.K., et al., *Expression cloning of a Na+-independent aromatic amino acid transporter with structural similarity to H+/monocarboxylate transporters.* J Biol Chem, 2001. **276**(20): p. 17221-8.

Acknowledgements

Many thanks to the following people that made it possible for me to conduct my research at the University of Zürich:

Prof. Dr. Jürg Biber, my thesis supervisor, to whom I specially thank for his strong support and advice that contributed to the project.

Prof. Dr. Carsten Wagner, responsible faculty member and committee member, **Dr. Natividad Hernando,** committee member, for their help during these years and their great support.

Dr. Joseph Caverzasio, committee member, for his helpful discussions during the meetings.

Functional Genomics Center in Zürich (FGCZ) and their members, for conducting the microarray experiments and their time helping me understand the software.

Insitute of Physiology and Anatomy, Universität Zürich for creating a comfortable working environment and with the possibility to exchange knowledge with other faculty members.